Chair of Thermal Processing Technology

Master's Thesis

Improvement of the Utilization Versatility of High Chromium, Manganese and Phosphorus Basic Oxygen Furnace Slags by Carbo-thermal Reduction

Felix Robert Breuer, BSc

February 2021

MONTANUNIVERSITÄT LEOBEN
www.unileoben.ac.at

EIDESSTATTLICHE ERKLÄRUNG

Ich erkläre an Eides statt, dass ich diese Arbeit selbständig verfasst, andere als die angegebenen Quellen und Hilfsmittel nicht benutzt, und mich auch sonst keiner unerlaubten Hilfsmittel bedient habe.

Ich erkläre, dass ich die Richtlinien des Senats der Montanuniversität Leoben zu "Gute wissenschaftliche Praxis" gelesen, verstanden und befolgt habe.

Weiters erkläre ich, dass die elektronische und gedruckte Version der eingereichten wissenschaftlichen Abschlussarbeit formal und inhaltlich identisch sind.

Datum 16.02.2021

Unterschrift Verfasser/in
Felix Robert Breuer

Acknowledgement

First and foremost I would like to thank my supervisor and friend Dr.mont. Christoph Ponak for his excellent support and supervision of my master`s thesis. Without your input, the manifold discussions that we had and your commitment on both a professional and a friendly level, this work would have never been possible in this quality. Special thanks also goes to my fiancée Avni, who was always by my side and motivated me all the time. Thank you for your patience, your helpfulness and for your understanding even in stressful situations.

Moreover, I would like to thank Professor Harald Raupenstrauch and my colleagues and friends at the Chair of Thermal Processing Technology for their constant willingness to help. In particular, I am thanking my friend Valentin Mally for his continuous support since I started working at this chair. Thank you for your help during all the trial operations as well as for your encouraging input.

In addition, I would also like to thank my brother Niki and my parents for their continuous support and for their backing during the last five years of studying. Thank you for giving me such an educational and memorable time.

Danksagung

An erster Stelle möchte ich mich bei meinem Betreuer, Dr.mont. Christoph Ponak für seine ausgezeichnete Unterstützung und Begleitung meiner Masterarbeit bedanken. Ohne deinen gelieferten Input, den gemeinsamen wiederkehrenden Austausch, als auch deinen Einsatz auf professioneller und freundschaftlicher Ebene wäre diese Arbeit nicht in dieser Qualität möglich gewesen. Besonderer Dank gilt auch meiner Verlobten Avni, die immer an meiner Seite war und mich immerfort motiviert hat. Danke für deine Geduld, deine Hilfsbereitschaft und für dein Verständnis auch in jeder stressigen Situation.

Auch möchte ich mich bei Professor Harald Raupenstrauch und meinen Kolleginnen und Kollegen bzw. Freunde am Lehrstuhl für Thermoprozesstechnik für Ihre ständige Hilfsbereitschaft bedanken. Insbesondere bedanke ich mich bei Valentin Mally für die durchgehende Unterstützung seitdem ich am Lehrstuhl arbeite. Danke für deine Hilfe während des Versuchsbetriebes, als auch für deinen fördernden Input.

Danken möchte ich auch meinem Bruder Niki und meinen Eltern für ihre andauernde Unterstützung und ihren Rückhalt während der letzten Fünf Studienjahre. Danke, dass ihr mir eine so lehrreiche und unvergessliche Zeit ermöglicht habt.

Funding

The author gratefully acknowledges the funding support of K1-MET GmbH, metallurgical competence center. The research programme of the K1-MET competence center is supported by COMET (Competence Center for Excellent Technologies), the Austrian programme for competence centers. COMET is funded by the Federal Ministry for Climate Action, Environment, Energy, Mobility, Innovation and Technology, the Federal Ministry for Digital and Economic Affairs, the Federal States of Upper Austria, Tyrol and Styria as well as the Styrian Business Promotion Agency (SFG) and the Standortagentur Tyrol. Furthermore, we thank Upper Austrian Research GmbH for the continuous support. Beside the public funding from COMET, this research project is partially financed by the scientific partner Montanuniversität Leoben and the industrial partners SCHOLZ Austria GmbH, Primetals Technologies Austria GmbH, voestalpine Stahl GmbH, and voestalpine Stahl Donawitz GmbH.

Förderung

Das Forschungsprogramm des Competence Center for Excellent Technologies in “Advanced Metalurgical and Environmental Process Development” (K1-MET) wird im Rahmen des österreichischen Kompetenzzentren-Programms COMET (Competence Center for Excellent Technologies) mit Mitteln des Bundesministeriums für Klimaschutz, Umwelt, Energie, Mobilität, Innovation und Technologie, des Bundesministeriums für Digitalisierung und Wirtschaftsstandort, der Länder Oberösterreich, Steiermark und Tirol sowie der steirischen Wirtschaftsförderungsgesellschaft m.b.H. und der Standortagentur Tirol gefördert. Außerdem danken wir der Upper Austrian Research GmbH für die Unterstützung. Neben der Finanzierung durch das COMET Programm kommen die weiteren finanziellen Mittel des gegenständlichen Projektes vom wissenschaftlichen Partner Montanuniversität Leoben und den Industriepartnern SCHOLZ Austria GmbH, Primetals Technologies Austria GmbH, voestalpine Stahl GmbH und voestalpine Stahl Donawitz GmbH.

Abstract

Steel is an indispensable material used in manifold industries, like construction, transportation or engineering. The global steel production is steadily rising and reached a new record with 1.869 million tons in the year 2019. More than 70% of the worldwide steel production is based on the blast furnace – basic oxygen furnace process route, whereof the steelmaking technique using the basic oxygen furnace converter has been developed in great parts in cooperation of the University of Leoben and the Austrian-based steel producer voestalpine Stahl GmbH. During this treatment method high amounts of basic oxygen furnace slag are generated, which consist of valuable elements like iron, phosphorus, chromium or manganese in addition to the calcium and silicon oxides. In Austria, regulations regarding the chromium amount in this slag system allow only limited use of basic oxygen furnace slags.

To increase the recovery of this residual product and to access the containing valuable elements, a novel treatment approach called InduRed was developed at the Chair of Thermal Processing Technology at the University of Leoben in cooperation with the companies voestalpine Stahl GmbH and SCHOLZ Austria GmbH. By using this treatment method, an inductively heated plant called InduMelt was built and its specific characteristics during operation have been analyzed. By reducing the input slag mixture with carbon powder, this treatment method separates the phosphorus from the initial slag mixture via a gas phase and produces an iron-rich alloy and an additional product slag mixture. The gaseous phosphorus therefore can possibly be used as an input stream in the fertilizer production industry and the emerging liquid iron alloy has a potential to be used again as a recycled steel product.

Previous research regarding the efficient integration of the InduRed plant into the industrial steelmaking process state that, during a novel process sequence, especially a chromium- and manganese-rich slag system can be produced, which can potentially be treated in the InduRed plant. By reducing this novel slag, low phosphorus gasification degrees were identified resulting in a low efficiency of this treatment method compared to treating slags, which contain only low amounts of manganese and chromium. In this master's thesis the influence of both chromium and manganese on the phosphorus reduction degree and the phosphorus activity in the occurring liquid metal phase is analyzed by conducting simulations using the thermochemical simulation software FactSage™.

By analyzing the temperature influence, the basicity and the amounts of chromium and manganese of the input slag mixture, optimizations of the carbo-thermal treatment of this initial slag system were derived. Especially a strong dependency of the maximum treatment temperature and the input amounts of chromium and manganese on the phosphorus

distribution between the emerging metal and gas phase is identified. Further benchmarks with results from other researchers underline the findings and trends, which are generated based on the conducted simulations.

Kurzfassung

Stahl ist ein unverzichtbarer Werkstoff, welcher in diversen Branchen, wie in der Bauindustrie, im Transportwesen oder im Engineering eingesetzt wird. Die weltweite Stahlproduktion steigt stetig an und erreichte mit 1,869 Millionen Tonnen produzierten Stahl im Jahr 2019 einen neuen Höchstwert. Hierbei basiert über 70 % der globalen Stahlproduktion auf der Hochofen – Sauerstoffkonverter Route, wobei das Prozessverfahren im Sauerstoffkonverter maßgeblich in Zusammenarbeit mit der Montanuniversität Leoben und dem österreichischen Stahlunternehmen voestalpine Stahl GmbH entwickelt wurde. Im Zuge dieses sogenannten LD-Verfahrens fallen große Mengen an LD-Schlacke an, welche unter anderem auch wertvolle Elemente, wie Eisen, Phosphor, Chrom und Mangan, neben den Kalzium- und Siliziumoxiden enthält. Aufgrund gesetzlicher Rahmenbedingungen im Hinblick auf den Chromgehalt in der LD-Schlacke darf diese Schlacke in Österreich nur eingeschränkt weiterverwendet werden.

Um diesen anfallenden Reststoff zu verwerten und die darin enthaltenen Wertstoffe zu recyclen, wurde am Lehrstuhl für Thermoprozesstechnik an der Montanuniversität Leoben in Kooperation mit den Firmen voestalpine Stahl GmbH und SCHOLZ Austria GmbH ein neuartiger Behandlungsprozess namens InduRed entwickelt. Durch Nutzung dieses Prozesses wurde eine neue induktiv beheizte Anlage namens InduMelt konstruiert und deren spezifisches Verhalten im Betrieb analysiert. Bei diesem Verfahren wird durch Reduktion des ursprünglichen Schlackengemisches mit Kohlenstoffpulver der Phosphor gasförmig abgetrennt und zudem eine eisenreiche Legierung erzeugt. Dadurch kann der gasförmige Phosphor im Bereich der Düngemittelproduktion genutzt werden. Die entstehende flüssige Eisenlegierung hat das Potential wiederum als recyceltes Stahlprodukt Verwendung zu finden.

Bisherige Untersuchungen im Hinblick auf eine mögliche effiziente Integration der InduRed-Anlage in den Prozess der industriellen Stahlherstellung zeigen, dass im Zuge einer neuen, angepassten Prozessabfolge eine chrom- und manganreiche Schlacke anfällt, welche in der InduRed-Anlage behandelt werden kann. Durchgeführte Reduktionsexperimente dieser anfallenden Schlacke führten jedoch zu einer geringen Abtrennung vom Phosphor in die Gasphase, wodurch die Effizienz des gesamten Behandlungsprozesses, im Vergleich zur Behandlung von chrom- und manganarmen Schlacken, herabgesetzt wird. Daher zielt diese Masterarbeit darauf ab den Einfluss von Chrom und Mangan auf den Reduktionsgrad und auf

die Aktivität von Phosphor in der entstehenden flüssigen Metallphase durch Simulationen zu untersuchen. Hierfür wurde die thermochemische Simulationssoftware FactSage™ verwendet.

Durch Analysen der Temperaturabhängigkeit, eine Änderung der Basizität und der Chrom- und Mangangehalte konnten Optimierungen dieser carbo-thermischen Behandlung von LD-Schlacken abgeleitet werden. Insbesondere kann eine starke Abhängigkeit der Maximaltemperatur und der enthaltenen Mengen an Chrom und Mangan auf die Phosphorverteilung zwischen der entstehenden Metall- und Gasphase erkannt werden. Zusätzliche Vergleiche mit Ergebnissen anderer Forscher unterstreichen die Erkenntnisse und Trends, die auf Basis der durchgeführten Simulationen abgeleitet werden konnten.

Table of Contents

List of Abbreviations, Formulae and Symbols

General Abbreviations

BF	Blast Furnace
BOF	Basic Oxygen Furnace
BFS	Blast Furnace Slag
BOFS	Basic Oxygen Furnace Slag
CTPT	Chair of Thermal Processing Technology
EAF	Electric Arc Furnace
LD	Linz-Donawitz
P	Phosphorus
Cr	Chromium
Si	Silicon
C	Carbon
Fe	Iron
Mn	Manganese
m.%	Mass Percent
PGD	Phosphorus Gasification Degree
PRD	Phosphorus Reduction Degree

Chemical Formulae

S	Slag
M	Metal
G	Gas
Ca_2SiO_4	C_2S (also known as $Ca_4Si_2O_8$ in FactSage™) – Dicalcium Silicate (Berlite)
$Ca_3(PO_4)_2$	C_3P – Tricalcium Phosphate
$Ca_4(PO_4)_2O$	Tetracalcium Diphosphate Monoxide
$Ca_3Mg(SiO_4)_2$	Merwinite (also known as $O_8Ca_3Si_2Mg$ in FactSage™)

Formula Symbols

T	Temperature	[K]
p	Pressure	[atm]
$B_{2/3/4}$	Basicity	[-]
ΔG	Change in Gibbs Free Energy	$[\frac{J}{mol}]$
ΔH	Change in Enthalpy	$[\frac{J}{mol}]$
ΔS	Change in Entropy	$[\frac{J}{mol*K}]$

Aggregation State

(s)	Solid State
(l)	Liquid State
(g)	Gaseous State

List of Illustrations

List of Tables

1 Challenge Outline

The global steel production is continually growing, especially because of its application in the construction of railways, roads and building due to its high strength and toughness. In only 9 years, from 2010 to 2019, the global crude steel production increased from 850 million tonnes to 1866 million tonnes. More than 70 % of the total global steel is produced via the blast furnace (BF) and basic oxygen furnace (BOF) route. [1-2]

In this most common steel production route roughly 125 to 150 kilograms of basic oxygen furnace slag (BOFS) per tonne crude steel are produced. The slag, amongst other tasks or functions, binds the unwanted accompanying elements from the pig iron (Fe), which would reduce the steel quality. BOFS consists of high amounts of valuable elements like Fe, chromium (Cr), manganese (Mn) and phosphorus (P), which are bound in the form of oxides and phosphates. Due to different recycling and reusing regulations of BOFS, the major amount of BOFS worldwide is disposed. [3-4]

In Austria, over 90 % of the crude steel is produced via the BF and the BOF production route. 2019 roughly 7.4 million tonnes of crude steel and more than 800.000 tonnes of BOFS were generated. Due to the challenging regulations in Austria in terms of the recycling of building materials the produced BOFS itself can only be partially utilized. [6]

Reusing and recycling of the by-products, especially of the steelmaking slags, is a key factor to increase resource efficiency, prevent landfill waste and reduce CO_2 emissions and energy consumption in the steel sector. [3]

To increase the resource efficiency of the steelmaking process and reduce the amount of disposed BOFS, a treatment method is developed at the CTPT at the University of Leoben which separates the valuable elements of BOFS and makes the co-products usable. During

this novel treatment process, BOFS, which is particularly high in Cr, Mn and P, is produced. In this treatment method P incubates into the metal phase and therefore reduces the quality of the final metal product. The key area of this master thesis is the analyzation of the slag composition on the efficiency of the proposed treatment process in order to improve its utilization versatility, increase its recycling capability and reduce the quantity of disposed BOFS. A special focus of this thesis is to understand the dependency of Cr and Mn on the P activity in the hot melt.

1.1 Motivation and Research Relevance

In 2019, the crude steel production reached an all time high with 1866 million tonnes. During the main production route via the BF and the BOF more than 183 million tonnes of BOF slag is generated per year. The produced slag consists of high amounts of valuable elements like Fe, Cr, Mn or P which are bound in the form of oxides and phosphates and which could potentially be used in various industries for example as feedstocks or additives. The treatment of this valuable by-product of the steelmaking process depends on the legislation and the profitability of BOFS recovery of each country. Therefore, the major amount of BOFS worldwide is stored or placed on disposal sites. China produces more than 53 % of the worldwide steel and over 71 % of the generated BOFS in China is put on landfill disposal. [2-4]

In Austria, regulations allow only strictly limited use of BOFS since 2015 and, as a consequence, a storage facility for a later utilization with a volume of over 7 million m^3 is intended to be constructed. [6]

The utilization and recycling of BOFS has a high potential to reduce the amounts of steelmaking waste products and could lead to a more environmentally sustainable and resource efficient steelmaking production process.

1.2 Objectives

This chapter aims at giving an overview of the specific challenges that are addressed in the course of this master thesis. Therefore, relevant research questions are presented as well as the methodology that is used to answer them.

1.2.1 Relevant Research Questions

1. How does the activity coefficient of P depend on the amount of Cr and Mn in Fe-P-Mn-Cr alloys?
2. How does the amount of Cr and Mn in BOFS affect the inclusion of P in the metal phase?
3. Which composition of BOFS could lead to high P gasification rates and simultaneously low P accumulation in the metal phase?

1.2.2 Methodology

In the beginning of this master thesis the theoretical fundamentals about crude steel production and BOFS, especially its formation, composition and challenges in its utilization are explained. Additionally, currently existing recycling methods of BOFS are stated and their different approaches and results are benchmarked.

Furthermore, the proposed BOFS treatment process to improve the utilization of BOFS is elucidated and the results of previous research are exemplified. Therefore, the carbo-thermal treatment of BOFS is described in detail.

Moreover, the dependency of the slag composition on the efficiency of the proposed treatment process is analyzed. The state of knowledge in the P inclusion in metal alloys with varying Cr and Mn amounts and current research findings are illustrated. The effect of different amounts of Cr and Mn in the slag on the P inclusion in the metal phase as well as the P gasification rate are explained in detail.

Based on that knowledge, the thermodynamic behaviour of BOFS with a focus on the P accumulation in Fe-P-Cr-Mn alloys during the proposed treatment process is simulated using FactSage™. The results of the conducted simulations are compared to the findings from the literature research and to outcomes of previously conducted experiments using a similar slag composition.

2 Theoretical Fundamentals

This chapter contains the theoretical fundamentals about BOFS, the proposed treatment approach to access its valuable elements and current research findings to increase the efficiency of the utilization process that are needed to model the thermodynamic simulation.

In the beginning, the major steelmaking production routes, as well as the formation and utilization of BF and BOF slags are described. BOFS is the co-product of interest in this thesis and therefore the difficulties in the reuse and worldwide utilization approaches are presented.

Further, the carbothermic treatment approach of BOFS with simultaneous P gasification and the thermodynamic fundamentals of this process are discussed. Due to the high potential of BOFS recycling with simultaneous P gasification, extensive research worldwide has been conducted. The Chair of Thermal Processing Technology (CTPT) at the University of Leoben has developed a very efficient and highly promising BOFS treatment approach using an inductively heated bed of graphite pieces. Current research findings of this proposed treatment approach are presented.

Finally, the interaction behaviour of P with Cr and Mn in liquid Fe is analyzed. Therefore, current theoretical and practical descriptions of this inclusion process are benchmarked, and its similarities and differences are discussed.

At the end of this chapter the research findings and theoretical assumptions that are needed for modeling the thermodynamic simulation will be summarized.

2.1 Crude Steel Production

Almost everything that we are using is made from or manufactured with steel. Due to its high strength and toughness, low manufacturing costs and high versatility steel is one of the main engineering materials in the world. Additionally, steel has the lowest strength-to-weight ratio of any construction material, which makes it an essential material in the building, construction and manufacturing industry. [1]

Crude steel and its production process are highly studied and optimized. As can be seen in Figure 1 below, steel can be produced mainly via two different production routes.

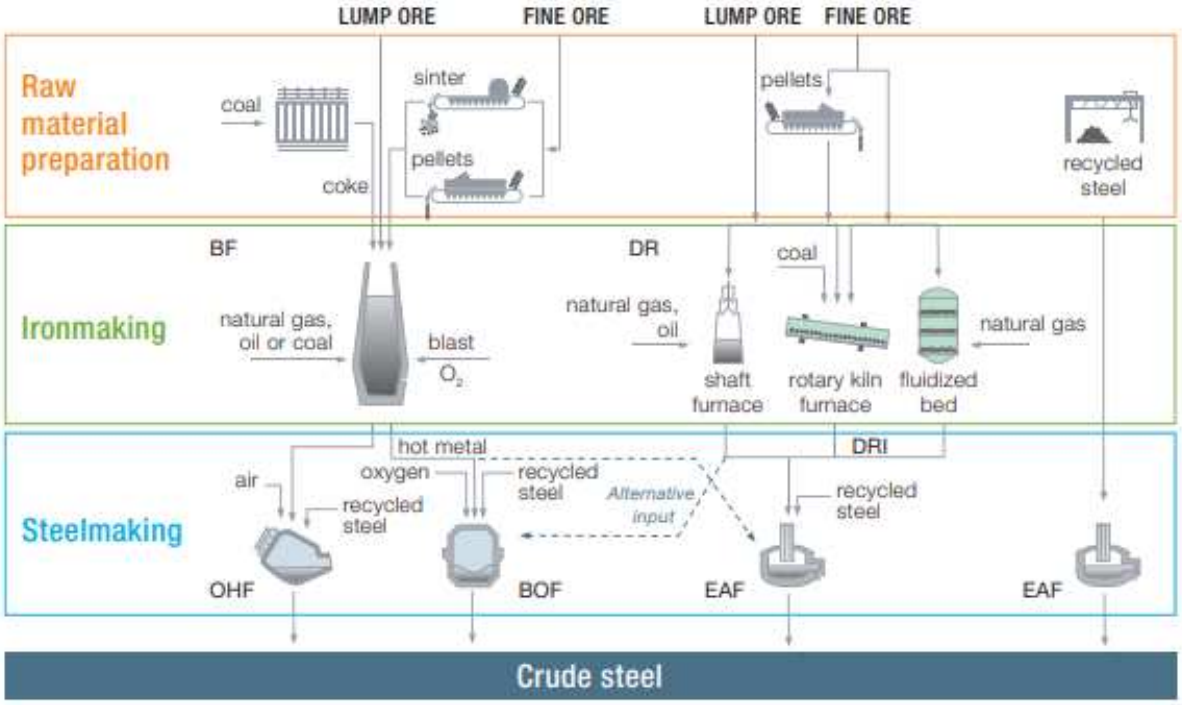

Figure 1: Steelmaking routes [1]

The most common production route is the integrated steelmaking route via the BF and BOF. More than 70 % of the total global crude steel is produced via this route. The input materials are mainly Fe ore, coal, limestone and recycled steel. To produce one tonne of crude steel, about 1.37 tonnes of Fe ore, 0.78 tonnes of metallurgical coal, 0.27 tonnes of limestone and 0.125 tonnes of recycled steel are needed. [1, 7]

The remaining 30 % of the total global crude steel is produced via the EAF route, which uses mainly recycled steel and Fe ore as its input materials. Additionally, small amounts of coal and limestone are needed. To produce one tonne of crude steel via the EAF about 0.71 tonnes of recycled steel, 0.586 tonnes of Fe ore, 0.15 tonnes of coal and 88 kilograms of limestone are

needed. In an EAF, scrap and Fe ore are molten using an electric arc. The electric current passes through steel and thereby heats it. This process is known as joule heating. To produce one tonne of crude steel via the EAF enormous amounts of energy are used. Approximately 600 kWh electrical energy per tonne crude steel are needed and to make this possible, large-scale EAFs are often built near power stations. [1, 7]

In the steel industry numerous process steps are needed to manufacture high quality steel products. As can be seen in Figure 2 below, the BF-BOF and the electric arc production route differ only by the kind and the amount of input materials that are used and by the casting method during the steel making process.

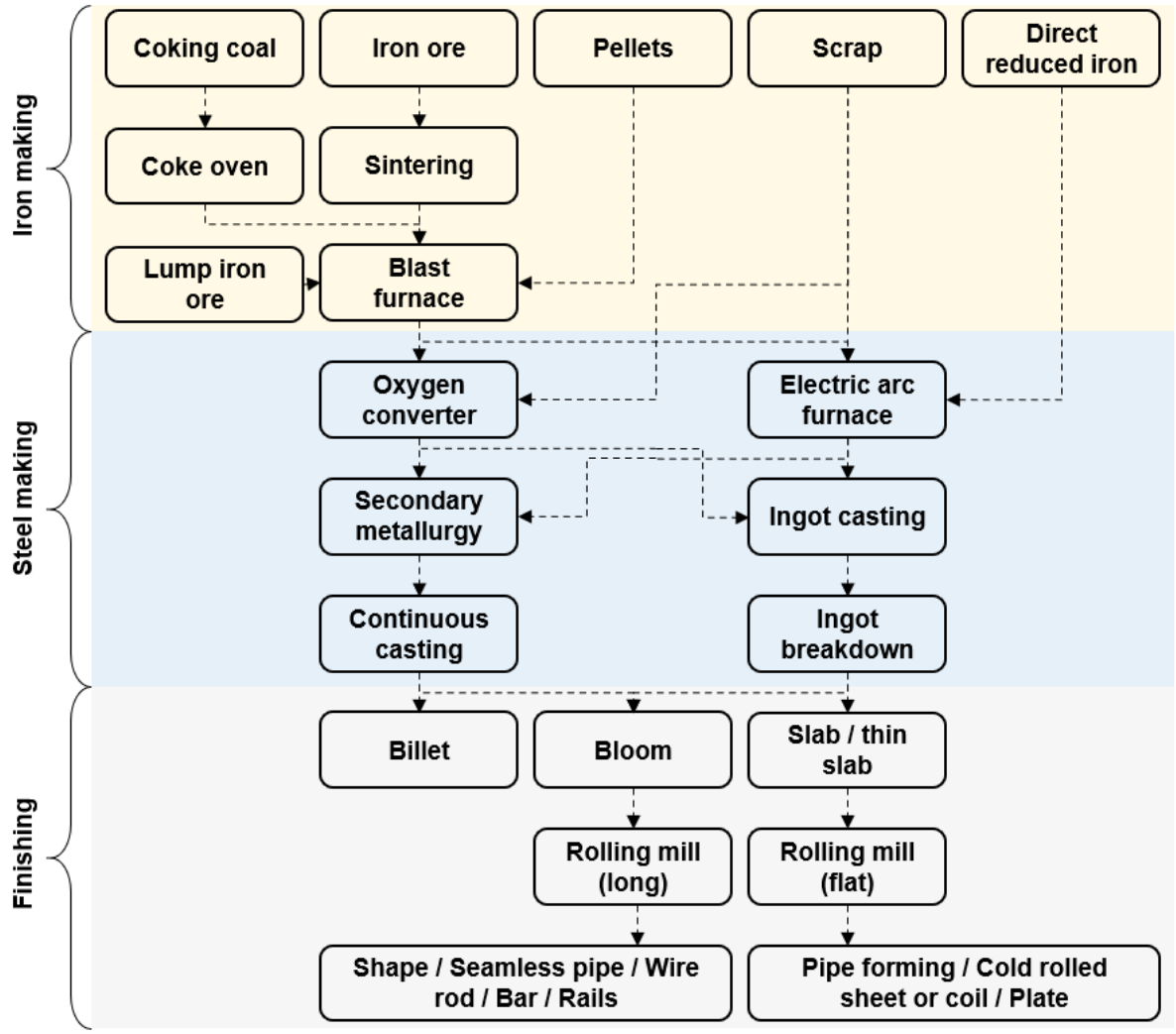

Figure 2: Steelmaking production steps (data gathered from [8])

In the BF-BOF production route Fe ore is sintered and reduced with coke, pellets and lump Fe ore to Fe using a BF. The Fe is a main input material for the following oxygen converter, also called BOF, where Fe and steel scrap are converted into steel. The BOF uses an oxygen lance,

which blows pure oxygen on the Fe and scrap mixture and, due to the oxidizing action, the impurities of the Fe are bound as oxides and phosphates and the C content is reduced. The produced fractions are steel, BOFS and BOF dusts. Then, the produced steel is cast and in the finishing process different shapes of steel are generated using special kinds of mills and barrels. [2, 8]

This thesis focuses on the utilization of BOFS. Therefore, in the following chapter the formation of BOFS, challenges in its reuse as well as current utilizing approaches are outlined and discussed.

2.2 Basic Oxygen Furnace Slag

As described above, more than 70 % of the global steel is produced via the BF-BOF route. In this route, 275 kilograms BF slag (BFS), 125 to 150 kilograms BOFS, 20 kilograms of BF dust and sludge as well as 2.9 kilograms BOF dust and sludge are generated. [2]

BFS can easily be separated from Fe during the tapping process because it has a lower density than the metal product and both products are immiscible. Up to 100 % of the global BFS can be utilized, therefore BFS is mainly available in three categories:

1. Air-cooled slag, which can be used as a construction aggregate, as addition to concrete, road bases and surfaces.
2. Granulated slag, which can be used to make cementitious material due to its hydration behaviour, which stabilizes the cement.
3. Pelletised or expanded slag, which is commonly used as a lightweight aggregate. [2]

The reuse of BOFS differs from that of BFS due to its different composition and formation as well as regulatory restrictions and currently uneconomic recycling methods. For example, China is the major steel producer worldwide and, due to the cost-intensive recycling process and regulatory restrictions, more than 71 % of the generated BOFS are placed on landfill disposal nowadays. [5, 10]

In Austria the situation is even more critical because, due to challenging regulations in terms of the recycling of building materials, the accumulated BOFS is not utilized at all. As a result, more than 800.000 tonnes of BOFS in Austria are put on an intermediate storage facility, which was constructed exclusively for this application. [5-6]

2.2.1 Formation of Basic Oxygen Furnace Slag

The end products of the BF are a molten metal alloy as well as BFS. An excessive C content in the metal could result in inclusions or blowholes during solidification, which makes the metal product unstable. The metal product of the BF is fed into the BOF, which has the aim to lower the C content. The BOF is a converter in which the heat for melting scrap is internally generated by the oxidation of impurities of the metal alloy and the scrap. These impurities are bound as oxides and phosphates and form BOFS. The BOF process steps can be seen in Figure 3. [11-12]

Figure 3: BOF process steps (data gathered from [11])

After charging both the Fe and hot metal, a water-cooled oxygen lance blows ultrapure oxygen on the slag-metal mixture, which leads to the oxidation of the impurities. During this process also limestone is added as a flux agent to remove sulfur and P from the slag. Oxygen reacts with Si, C, Fe, Mn and P in the scrap and hot metal mixture and the BOFS is formed. After the blowing process, a sample of the metal product is taken to check if the C content is less than 1 %. Next, the high-quality low C steel is tapped through a lateral hole by turning the converter by 90 degrees. The remaining BOFS in the converter can be poured out into a slag pot. The largest converter can make up to 360-ton heats every 45 minutes. In every heat, the temperatures, chemical composition and quantities vary due to different quantities and compositions of the input materials and the type of the steel produced. In Table 1 the diverse compositions of BOFS, which occur at various steelmaking sites throughout the world are benchmarked. [11]

Table 1: Chemical composition of different BOFS

Nr.	Chemical Composition [m.-%]											Reference
	CaO	SiO_2	Al_2O_3	MgO	FeO	Fe_2O_3	MnO	P_2O_5	TiO_2	Cr_2O_3	MnS	
1	39.40	11.97	2.16	9.69	30.23	n/a	2.74	1.00	0.40	0.20	n/a	[13]
2	47.71	13.25	3.04	6.37	n/a	24.36	2.64	1.47	0.67	0.19	n/a	[14]
3	45-60	10-15	1-5	3-13	7-20	3-9	2-6	1-4	n/a	n/a	n/a	[15]
4	42-55	12-18	≤3	≤8	n/a	n/a	≤5	≤2	n/a	≤10	n/a	[16]
5	47.90	12.20	1.20	0.80	26.30	n/a	0.30	3.30	n/a	n/a	n/a	[17]
6	30-55	8-20	1-6	5-15	10-35	n/a	2-8	≤2	0.40	≤0.73	n/a	[18]

7	40.21	12.77	2.17	6.66	27.23	n/a	6.25	1.22	0.38	0.39	0.11	[19]

In Table 1 sample 1 is from Texas, USA, sample 2 is from France, sample 3 is from Wuhan, China, sample 4 is from Montreal, Canada, sample 5 is from India, sample 6 is from Hunan, China and sample 7 is from Linz, Austria. CaO, SiO_2, FeO and MnO are the main chemical compounds in the BOFS. Especially the notable FeO content leads to the concept of utilizing Fe from steelmaking slag. Different compositions in regard to MnO, CaO and SiO_2 influence the pH value of solutions. CaO hydrates with water molecules from the solution and forms calcium hydroxide, which dissolves to Ca^{2+} and OH^- ions. The basic OH^- ions are the driver for an increasing pH value. The chemical reactions can be seen in Equation (2.1) and Equation (2.2). [12]

$$CaO + H_2O \rightarrow Ca(OH)_2 \quad (2.1)$$

$$Ca(OH)_2 \rightarrow Ca^{2+} + 2\,OH^- \quad (2.2)$$

To describe the acidic or basic behavior of substances, two common definitions are existent. According to the Bronsted-Lowry definition a base accepts, and an acid donates H^+ ions and according to the Lewis definition a base donates an electron pair and an acid accepts an electron pair. Both definitions are not mutually exclusive, but the Lewis theory is most used nowadays. The basic behavior of CaO in BOFS leads to the emergence of an important parameter in the research of steelmaking slags, the so-called basicity. Generally, all BOFS have a high basicity ratio due to the impurities from the Fe ore and the limestone, which is a parameter to describe the flowability and stability of slags during contact with other oxides. The basicity is characterized as the ratio between the CaO and SiO_2 contents in the BOFS. CaO has the tendency to form basic OH^- ions when dissolved in water and is therefore considered as a basic oxide. SiO_2 on the other hand does not show that specific behavior and is called an acidic oxide. The basicity is a parameter that describes the tendency of donating or accepting electron pairs. The transport of electrons therefore runs via the acceptance or donation of O^{2-} ions. As can be seen in Equation (2.3), Equation (2.4) and Equation (2.5) three types of basicity are currently used. Depending on the regarded compounds in the equations, the basic or acidic behavior of more oxides is considered. Due to the amphoteric characteristics of Al_2O_3, the

basicity B_4 is debatable in terms of accurately describing the pH characteristics of slags. [12-13, 19]

$$B_2 = \frac{m.-\%\ CaO}{m.-\%\ SiO_2} \quad (2.3)$$

$$B_3 = \frac{m.-\%\ CaO + m.-\%\ MgO}{m.-\%\ SiO_2} \quad (2.4)$$

$$B_4 = \frac{m.-\%\ CaO + m.-\%\ MgO}{m.-\%\ SiO_2 + m.-\%Al_2O_3} \quad (2.5)$$

The basicity B_2 is the most common kind of basicity used in the field of BOFS research and therefore B_2 is considered for further investigations in the course of this master thesis.

2.2.2 Challenges in the Reuse of Basic Oxygen Furnace Slag

Increasing stringent regulations as well as high disposal costs affect the treatment of BOFS at steelmaking sites worldwide. Extensive research about different recycling and reusing processes of BOFS is undertaken. The concept of circular economy leads to the cooperation and collaboration of various industrial sectors with the aim to increase the reuse and recycling of by-products op to a 100 % recycling rate. This ambitious zero-waste goal has led to the emergence of significant effort regarding the recovery of industrial by-products in general. Especially the treatment of BOFS has raised attention in the past years because of its high amounts of valuable components, such as FeO, MnO or P_2O_5. [20-21]

However, various restrictions make the recycling of BOFS challenging nowadays:

- Reuse in a BF would result in high P contents in the hot metal due to the high P amounts of the BOFS and make the dephosphorization treatment challenging. [22]
- BOFS surpasses the boundary values for the Cr content in the eluate, as well as the total Cr content for its application as a building material in Austria and therefore the reuse of BOFS from Austrian steel sites is considered to be illegal. [23]
- Current recycling processes of BOFS are inefficient and cost-intensive making the utilization of BOFS an unattractive investment for steelmaking companies. [24]
- State of the art recycling processes do not meet all requirements of the desired products, for example in terms of product purity and product quality. [20, 24]

2.2.3 Basic Oxygen Furnace Slag Utilization Worldwide

In order to access the valuable elements in BOFS and to reach the zero-waste goal especially in Europe lots of research regarding BOFS utilization techniques is conducted. From a global perspective outdated treatment approaches lead to low reusing activities. In China the situation

has become more critical in the past years due to the increasing steel production on the one hand and low utilization rates on the other hand. To analyze this movement, in the following Figure 4 and Figure 5 the conflicting trend between increasing global steel and BOFS production and low BOFS utilizing ratios of the major steel producers is pictured.

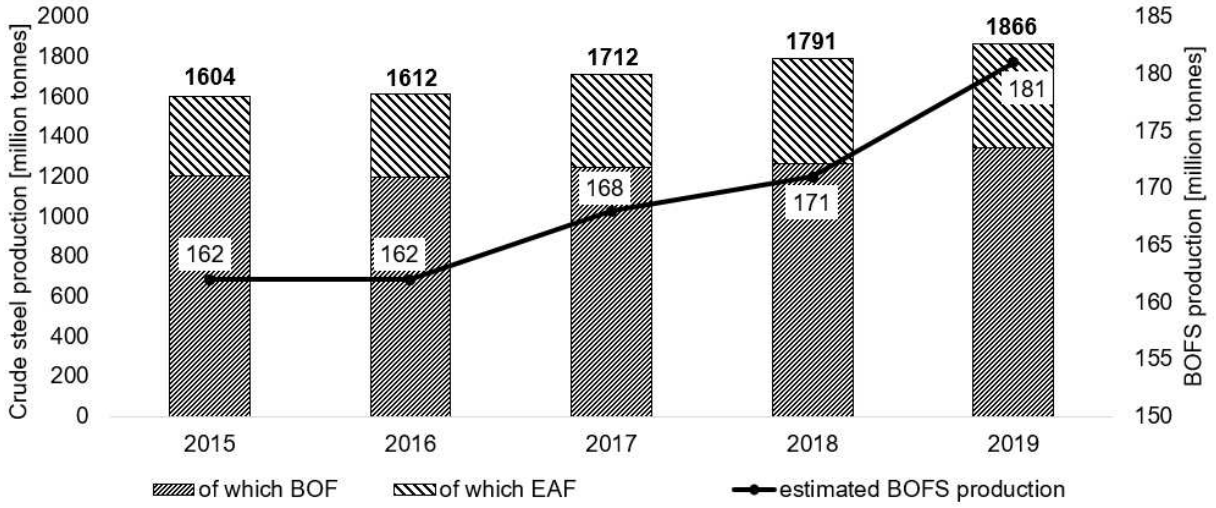

Figure 4: World crude steel production by process route and estimated global BOFS production (data gathered from [2] and [25])

The global crude steel production is at an all-time high with 1866 tons in the year 2019. More than 71 % of crude steel is produced via the BF-BOF process route and therefore the production of BOFS is continuously increasing. The major crude steel producing countries are China with 996 million tons, India with 111 million tons, Japan with 99 million tons and the United States with 87 million tons 2019. In Europe, 158 million tons of crude steel were produced in 2019. Germany, Italy, Spain and France are the leading steelmakers, whereas Germany and France commonly use the BF-BOF route. In Austria, 7.4 million tons of crude steel were produced in 2019 and 90 % of that has gone through the BF-BOF process route. [4]

Massive amounts of BOFS are produced every year but the recycling potential of this co-product is not exploited, as shown in Figure 5. China, Europe, Japan and USA are the top four regions in the world`s crude steel production. Together these four regions produce more than 72 % of the global steel. In these regions the treatment of BOFS differs strongly. BOFS is largely used in road construction, interim storage and internal recycling in Europe whereas in Japan civil engineering, road construction and internal recycling are the most common reusing fields. The USA use more than half of the produced BOFS in road construction, but about 16 % of the produced BOFS is put on landfill disposal. China put enormous amounts of BOFS on

disposal sites, the remaining 30 % are commonly used in civil engineering, internal recycling or cement production. [24]

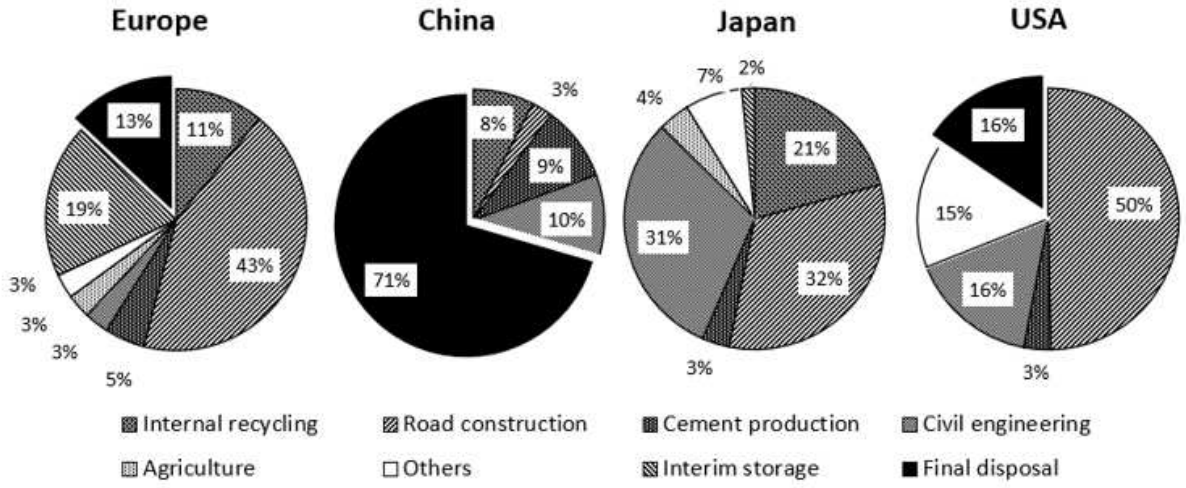

Figure 5: BOFS utilization of the top regions in the world`s crude steel production (data gathered from [24])

Comparing these four regions, the major use cases for BOFS are in the fields of civil engineering, internal recycling and road construction. China stands out with its massive 71 % disposal rate. The application of utilizing techniques could potentially have the highest environmental impact in China, therefore the emergence of this extraordinary treatment of BOFS in China is described below.

In China, utilizing BOFS as an industrial by-product has a short history and can be divided into three stages:

1. Disposal stage (1950-1980): In 1980 the steel production in China was relatively low with approximately 37 million tons. Only minimal amounts of BOFS were reused, mostly for the production of cement, the remaining slag was discharged into the environment. During that stage most steel plants had so-called slag mountains where more than 99 % of the produced BOFS was stored. These slag agglomerations led to serious pollution in these steel production regions. Especially due to the low production rates and missing financial feasibility for utilizing by-products the recycling of BOFS has been given only low attention. [24]
2. Extensive development stage (1980-2005): In these 25 years the steel production in China climbed from 37 million tons to 355 million tons making China the leader in the global crude steel production. At this time, due to the huge amounts of the produced BOFS, various BOFS treatment technologies occurred. Most common treatments were the manual or mechanical magnetic separation. Because of the missing knowledge of

BOFS treatment technology some serious failures resulted in the reused BOFS. For example, Baosteel Group Corp. Ltd. used BOFS for the construction of an indoor stadium in 1980, which cracked as a result of the changing temperature. Due to these failed treatment attempts the utilization rate was roughly 10 %. [24, 26]

3. Comprehensive utilization stage (2005-today): With 996 million tons of crude steel production China is by far still the major steel producer. The large amounts of emissions caused by BOFS attracted the attention of the government and various environmental groups. Increasing social pressure and established laws, policies, standards and regulations are the main driving force for BOFS utilization rising the recycling rate of BOFS up to 29 % nowadays. Tsinghua University, Chongqing Jaiotong University and the University of Science and Technology Beijing conduct a lot of research in the field of BOFS recycling. Stringent regulatory restrictions as well as cost intensive utilization techniques limit the reuse of BOFS and most technologies are still in the research and development stage. Especially the treatment of P in BOFS is a big challenge in the current BOFS utilization. [24]

The massive production of BOFS worldwide and low utilization rates in the major BOFS production regions show that steelmaking sites are in the need of an efficient, technical feasible and cost-effective recycling process. At the CTPT at the University of Leoben, extensive research in the development of such a BOFS treatment process has been conducted. The following chapter describes this novel treatment approach and summarizes current research outcomes.

2.3 InduRed Reactor and Basic Oxygen Furnace Slag Treatment Process

As described in Chapter 2.2.1, BOFS contains valuable metallic elements, which exist in oxidic form. In order to access these valuable elements, the BOFS needs to be reduced again so that the oxygen is removed. Treating BOFS in a reduction apparatus like, for example, an EAF, leads to the reduction of Fe, Mn and Cr oxides but also to the simultaneous reduction of P compounds. As a result, the reduced pure P appears in its elementary and gaseous form and hence reacts with the reduced liquid Fe in the mixture and the P inclusion in the Fe increases. Reusing this Fe could lead to an enrichment of P in steel. The novel InduRed process offers a potential solution for the treatment of steelmaking slags because this process reduces the input materials and simultaneously removes the P via the gas phase. The output streams are a

metal product, which is low in P, and pure gaseous P. The core part of this process is the InduRed reactor, which is pictured in Figure 6. [27]

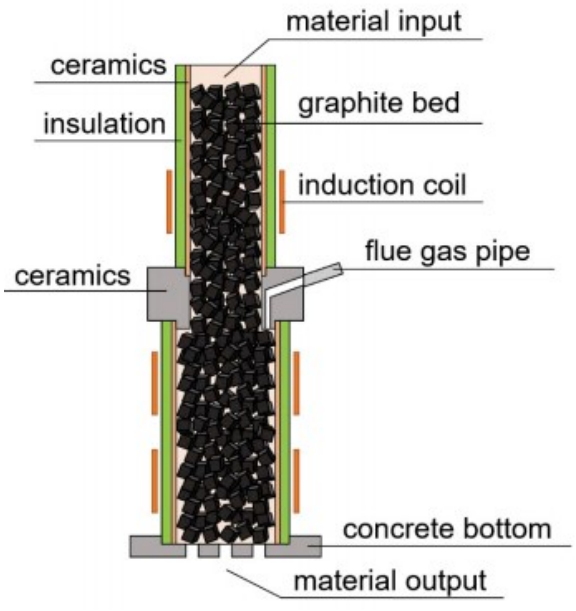

Figure 6: InduRed reactor [19]

The InduRed reactor consists of a cylindrical ceramics tube, which is filled with graphite cubes. The cubes are inductively heated with water-cooled coils. This special heating technique achieves a horizontally and radially homogeneous temperature distribution in the whole reactor. A flue gas pipe in the middle of the reactor removes the vaporized P and the reduced Fe flows through holes of the concrete bottom and can be recovered. After the input material is fed into the reactor, it almost immediately melts due to the high operating temperature of around 1900 K. The thin film of the molten input materials flows to the bottom of the reactor and, due to the large surface area, the reduction reactions occur simultaneously. To support the transport of fine particles to the graphite surface, an Argon gas stream is led into the reactor from the top and bottom. The pilot reactor is around 1 m in height and has an inner diameter of 20 cm. The products generated are liquid Fe and slag as well as gaseous P. Ultrapure C powder is added as a reduction source. The whole pilot plant consists of the described reactor, a combustion chamber and a gas scrubber. The entire plant can be seen below in Figure 7. [19, 27]

Figure 7: InduRed plant with its main components (1-reactor, 2- combustion chamber, 3-gas scrubber) [19]

A flow chart of the InduRed process is diagramed in Figure 8.

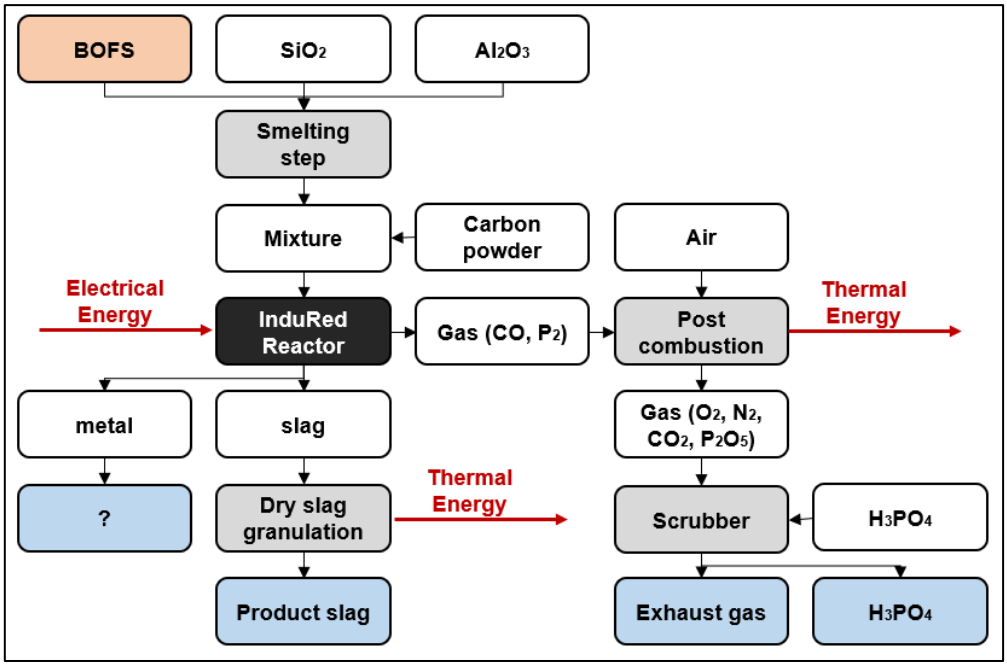

Figure 8: InduRed process flow chart (made with data from [19])

To provide an appropriate B_2, SiO_2 and, optionally, Al_2O_3 are added to the BOFS and the mixture is then fed in the InduRed reactor. The liquid products generated through this process are a slag and metal phase. The slag phase can be used for the production of electrical energy by heat recovery via dry slag granulation. The gaseous product is P, which could potentially be used for the production of phosphoric acid. Producing high quality H_3PO_4 is currently investigated at the CTPT at the University of Leoben. The treatment of the produced metal product is one of the core areas of this thesis. [19]

The InduRed process is personnel- and cost-intensive during operation, which is why the site can only be run unfrequently during trial operation. To enable more frequent experiments of treating BOFS in the InduRed reactor a laboratory scale plant called InduMelt was constructed. The InduMelt plant consists of an oscillating circuit, a cooling circuit, a power supply unit, a royer converter and a microcontroller, as visualized in Figure 9.

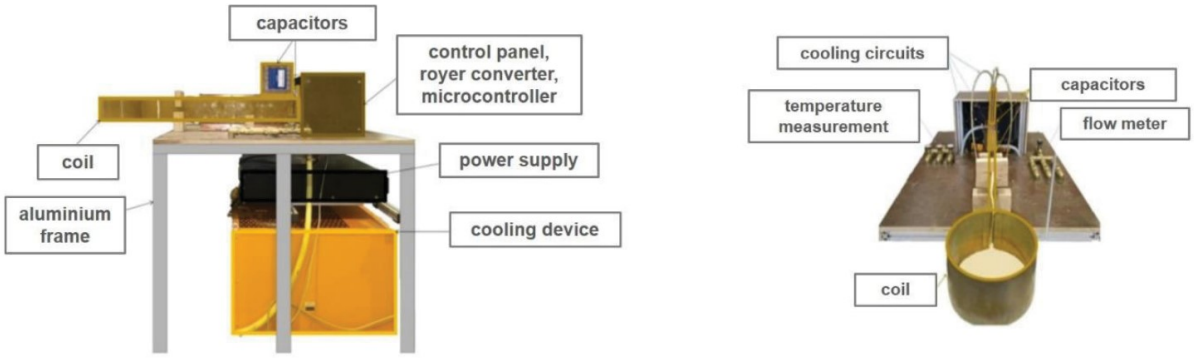

Figure 9: InduMelt plant [19]

The InduMelt plant operates with a frequency of around 50 kHz and via the oscillating circuit eddy-currents are induced into the susceptor, whereby the susceptor gets heated regarding to the Joule's law. To guarantee a secure operation, the capacitors, the power electronics as well as the coil have different cooling circuits. In order to simulate the InduRed plant the smelting and reduction processes are analyzed separately. The experimental setup can be adjusted so that by the smelting experiment the input material is heated through heat transfer via a ceramic wall and a graphite susceptor and by the reduction experiment the input material is directly heated via graphite cubes and reduced by previously added C powder. [19]

To further understand the thermodynamic processes that appear during the reduction of steelmaking slags with simultaneous P gasification, this treatment approach is described in the following chapter in detail.

2.4 Carbothermic Treatment of Basic Oxygen Furnace Slags

In order to understand the behaviour of BOFS during the InduRed process, its underlying fundamental thermodynamic and kinetic principles are described in this chapter. The metal oxides in BOFS are reduced by using C powder as a reduction agent at high temperatures, which is why this process is called carbothermic. First, the process of reducing BOFS and simultaneously vaporizing P is explained. Then, the challenges of this treatment approach are outlined and finally, an extended treatment concept to solve the raised problems is presented and illustrated.

2.4.1 Thermodynamics of Basic Oxygen Furnace Slag Reduction with Simultaneous P Gasification

Thermodynamics play a significant role in the reduction processes and therefore this Chapter describes the most important thermodynamic processes during the carbothermic reduction of BOFS.

The thermodynamic driving force for the occurrence of a reaction can be measured by the Gibbs free energy ΔG of this reaction. A negative value of ΔG indicates that the reaction can proceed under the specific conditions spontaneously and without external forces, while a positive value of ΔG indicates that the reaction under these conditions does not. The Gibbs free energy can be described as in Equation (2.6).

$$\Delta G = \Delta H - T * \Delta S \tag{2.6}$$

The liberated energy during a reaction can be described with the enthalpy ΔH. Exothermic reactions give off energy and have a negative value of ΔH while endothermic reactions require energy for its occurrence and therefore have a positive value of ΔH. The entropy ΔS indicates the change of possibilities for disorders in the products in relation to the reactants. For example, ΔS increases if a solid and a liquid, which are both ordered states react to a gas, which is in disordered state. The driving force of a reaction depends on the temperature and since ΔH and ΔS are essentially constant with temperature, unless a phase change occurs, the dependency of ΔG on the temperature is significant to describe the behavior of oxides in the InduRed reactor. In the Ellingham diagram ΔG for the oxidation of metals is plotted against the temperature. All reactions are normalized to consume one mole O_2 and the oxygen partial pressure is one atmosphere in order to easily benchmark the reactions. The position of the reaction line shows the stability of the oxide as a function of the temperature. The majority of

lines have a positive incline due to a negative entropy change of the specific reactions, except for the oxidization of C. The Ellingham diagram can be used to describe multiple features of the reduction process: [28]

1. To determine the reduction behavior of oxides to metals: The position of the lines is significant for describing the reduction behavior. A metal can reduce the oxides of all metals whose lines are above. Since the oxidation of C to CO decreases with increasing temperature it overlaps with many metals, which makes C useful as a reduction agent. As mentioned in Chapter 2.3 the InduRed process also uses C as a reduction agent because it can reduce most of the containing oxides in BOFS and therefore makes its valuable elements accessible. [28]
2. To estimate the partial oxygen pressure, which is in equilibrium with a metal oxide at a specific temperature: The additional scale of P_{O_2} indicates what partial oxygen pressure is in the equilibrium reaction at a specific temperature. Therefore, if P_{O_2} in the analyzed process is higher than the equilibrium value the metal will be oxidized and if it is lower the metal will be reduced. To estimate the partial oxygen pressure of a reaction at a specific temperature the point on the oxidation line needs to be connected with the zero point at the upper left corner of the diagram and this line needs to be extended so that it crosses the P_{O_2} scale. The crossing point on the P_{O_2} scale is the equilibrium partial oxygen potential. [28]
3. Identifying the ration of $\frac{CO}{CO_2}$, which will reduce the oxide at a specific temperature by using the same procedure as for determining the equilibrium partial oxygen value except the start point is marked with an C in the center of the left axis at the diagram. [28]

In Figure 10 the Ellingham diagram is shown and the reduction, or oxidation behavior, of the oxides, which are found in BOFS are highlighted at 1900 K, which is the operating temperature of the InduMelt plant.

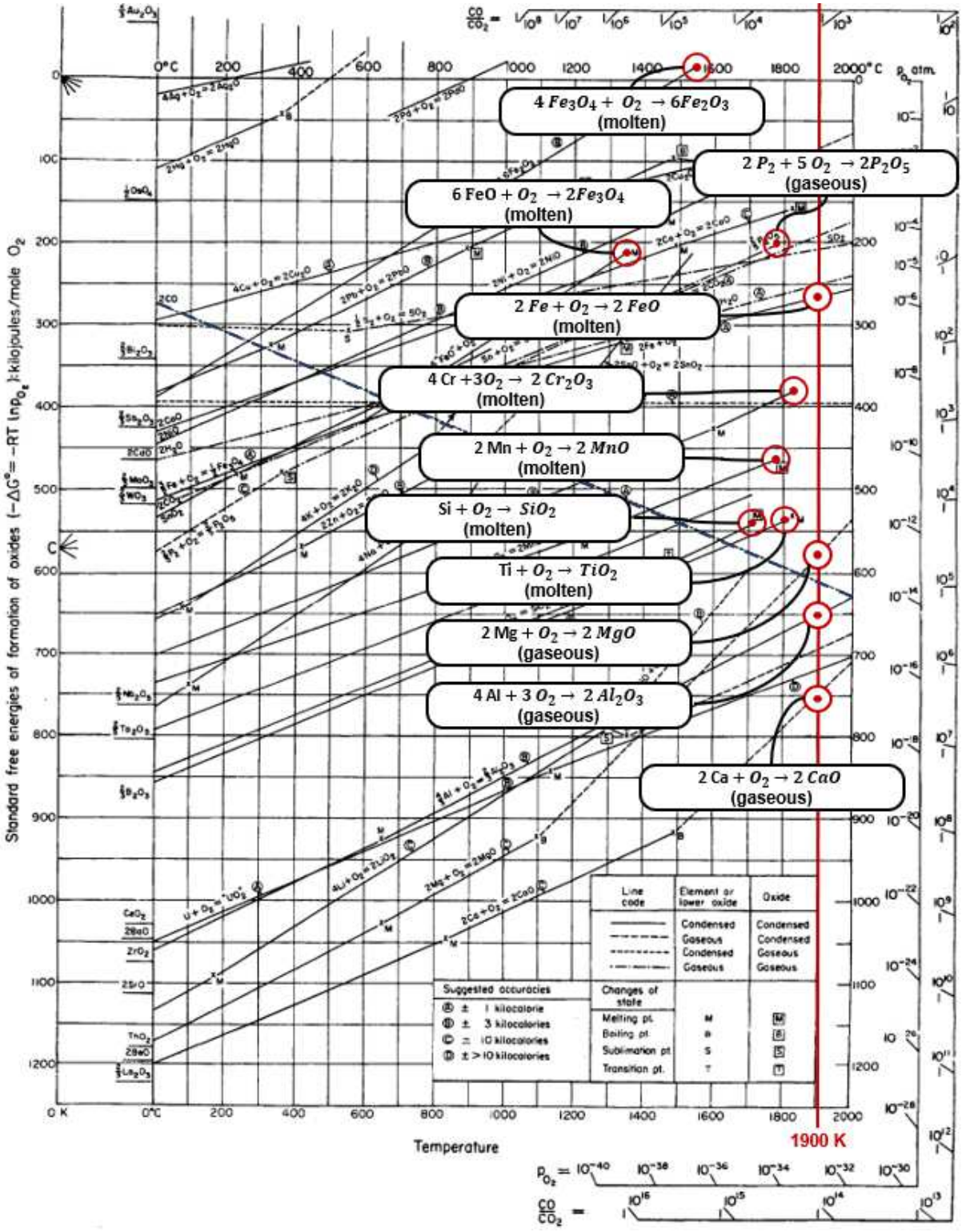

Figure 10: Ellingham diagram with highlighted oxides from the BOFS

With the help of the Ellingham diagram the reduction, or oxidation, behaviour of the oxides of BOFS can be understood. The dashed line indicates the oxidization of C: $2\,C + O_2 \rightarrow 2\,CO$ and as a result all reactions above this line occur as reductions and reactions

below this line occur as oxidations. At 1900 K the following reduction reactions preferably occur:

Reduction of FeO	$FeO \rightarrow 2\,Fe + O_2$	(2.7)
Reduction of MnO	$2\,MnO \rightarrow 2\,Mn + O_2$	(2.8)
Reduction of Cr_2O_3	$2\,Cr_2O_3 \rightarrow 4\,Cr + 3\,O_2$	(2.9)
Reduction of SiO_2	$SiO_2 \rightarrow Si + O_2$	(2.10)
Reduction of TiO_2	$TiO_2 \rightarrow Ti + O_2$	(2.11)
Reduction of MgO	$2\,MgO \rightarrow 2\,Mg + O_2$	(2.12)
Reduction of P_2O_5	$2\,P_2O_5 \rightarrow 2\,P_2 + 5\,O_2$	(2.13)

Al_2O_3 and CaO are not reduced because their line is below the CO line. The carbothermic treatment of P leads to the accumulation of P in liquid Fe, which lowers the Fe quality. Previous research show that P makes different compounds with other elements during the reduction process. Gaseous P and CaO react to a calcium phosphate, which is reduced with SiO_2 again to gaseous P during previous trial operations at the InduMelt plant. Simultaneously P_2O_5 is reduced regarding Equation (2.13). In Equation (2.14) and (2.15) the formation and reduction of the calcium phosphate is described. [19]

Formation of calcium phosphate [19]	$\frac{6}{5}CaO + \frac{2}{5}P_2 + O_2 \rightarrow \frac{2}{5}(3\,CaO \cdot P_2O_5)$	(2.14)
Reduction of calcium phosphate [19]	$3\,CaO \cdot P_2O_5 + 3 * SiO_2 + 5\,C \rightarrow 3\,CaSiO_3 + P_2 + 5\,CO$	(2.15)

The behaviour especially of P during BOFS reduction needs to be understood in detail to further optimize the Fe quality and increase the P vaporization degree. These subjects and related P treatment approaches are discussed in detail in chapter 2.5.

2.4.2 Proposed Treatment Approach of Basic Oxygen Furnace Slags [19]

As explained in Chapter 2.3 and 2.4, reducing BOFS by C powder in an inductively heated reactor is a novel and highly effective way to access valuable elements like P or Fe. Results from previous research projects at the CTPT at the University of Leoben are promising in terms of the phosphorus gasification degree (PGD) as well as the Fe reduction degree. Based on the successful operation of the InduMelt plant so far, further implementations of this treatment method are investigated by Ponak et. al. By conducting preliminary experiments, an alteration of this treatment process has been investigated, which aimed for the separation of a P-rich phase from an Fe- and Mn-rich phase. The goal of this altered process is to implement an internal recycling route along the industrial BF-BOF route of steelmaking. Recent literature also states that the FeO content is a key factor regarding the PGD during the reduction process of slags. Hence, an internal recycling route needs further process steps to be industrially feasible, which are listed below: [19]

1. Reducing BOFS in a reduction unit like an EAF. The products of this process step are a P-rich metal product and a slag phase. [19]
2. Refining the generated metal product using a lime, magnesia and an Fe source. The refining product shall be bound into another slag system and the metal product shall consist of mainly Fe and Mn. The aggregated slag potentially will be high in Cr, Mn, P and as low in Fe as possible compared to BOFS. [19]
3. This slag will be treated in the InduRed plant and reduced by using a bed of inductively heated graphic cubes and added C powder. The products of this process are gaseous P, a liquid metal phase, which is especially high in Cr as well as a slag phase. [19]

The sequence of this proposed process is shown in Figure 11. In total, the output BOFS from the initial BOF will be treated in three diverse aggregates, an EAF, an additional BOF and the InduRed plant.

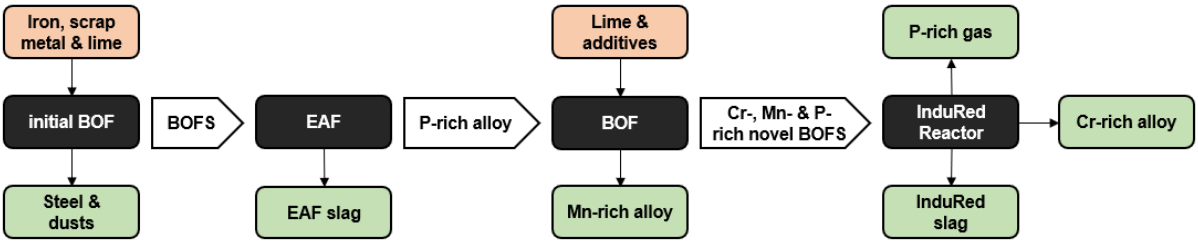

Figure 11: Process flow chart of the novel internal BOFS recycling route (made with data from [19])

By including this internal BOFS recycling process into integrated steelworks three potentially usable product phases can be generated: A Mn-rich metal product from the refining process,

a Cr-rich alloy product from the InduMelt plant as well as a gaseous P product stream again from the InduMelt plant. To further understand the particular process steps in the following chapter 2.4.2.1 the compositions of the slag and metal products after the EAF and the refining step are estimated. [18]

2.4.2.1 Determination of the Slag and Metal Composition [19]

Under the assumption that BOFS is completely reduced in an EAF and all P accumulates in the metal phase, the composition of this metal product can be estimated. In the following refining step, the P from the metal product is oxidised and bound into a novel slag system. The species after the refining step can be estimated by the amount of the metal phase that is oxidised. The amount of Cr_2O_3 can be estimated by assuming that 70 % of the metal phase is oxidised. In terms of MnO 60 % of the metal phase is assumed to be oxidised and regarding SiO_2 100% of the metal phase is supposed to be oxidised. The quantity of CaO can be determined by the assumption that 100 % of Si generate dicalcium silicate or so called Belite $(CaO)_2 \cdot SiO_2$ (C_2S) and 90 % of P generate tricalcium phosphate, $Ca_3(PO_4)_2$ (C_3P). Out of that, also the amount of P_2O_5 can be determined. After the refining step the basicity of the emerged slag is set to 1.5 by adding SiO_2 and small amounts of MgO and Al_2O_3 are added to assimilate an industrial BOFS composition. Table 2 below shows the estimated elements in the metal phase after reducing BOFS in an EAF as well as the slag composition after refining this metal product and the finally desired slag composition with a basicity of 1.5. [19]

Table 2: Estimated compositions during the proposed internal BOFS recycling route [19]

Metal composition after reducing BOFS in an EAF			**Slag composition after refining the metal phase from the EAF**			**Slag composition after adjusting the basicity to a value of 1.5**	
element	**m.%**		**species**	**Mass in [g] after refining 100 g of metal**		**species**	**m.%**
Fe	87.00		FeO	3.85		FeO	11.56
Cr	1.00		Cr_2O_3	1.02		Cr_2O_3	3.07
Mn	5.00		MnO	3.87		MnO	11.63
P	2.00		P_2O_5	4.12		P_2O_5	12.38
Si	1.00		SiO_2	2.14		SiO_2	21.38
C	4.00		CaO	10.65		CaO	31.98
total	100.00		total	25.66		Al_2O_3	3.00
						MgO	5.00

				total	100.00

It can be seen that the desired slag composition of this altered process route, which will be reduced in the InduMelt plant, is high in P, Cr and Mn. Results of previous experiments using this slag composition are described in the next chapter. [19]

2.4.2.2 Results of Previous Experiments [19]

By heating synthetically mixed slag samples of roughly 35 g in an MgO crucible up to 1793.15 K in the smelting experiments and up to 1893.15 K in the reduction experiments show promising first results. On the one hand, smelting and standard carbo-thermal reduction experiments were undertaken with a furnace, which is heated by heating elements from the outside. On the other hand, reference reduction experiments in the InduMelt plant were conducted with the previously molten slag product. As can be seen in Figure 12, substantial reduction degrees (RD) of Fe, Mn, Cr and especially P were achieved by Ponak et. al. [19]

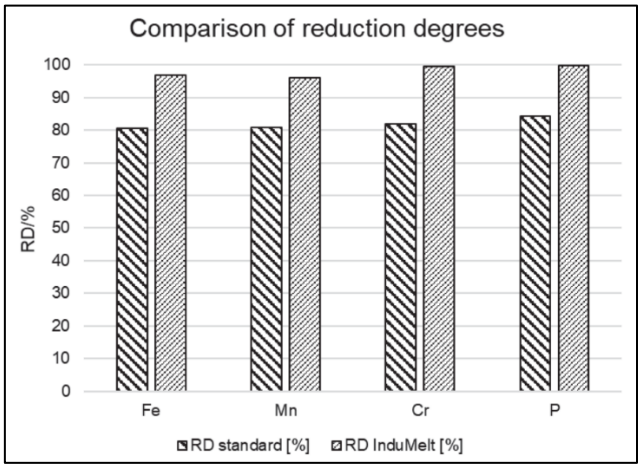

Figure 12: Reduction degrees (RD) achieved by standard reduction and by reduction in the InduMelt plant [19]

By comparing the P distribution in the slag, metal and gas phase, the reduction experiments conducted at the InduMelt plant show a higher PGD, as pictured in Figure 13 below.

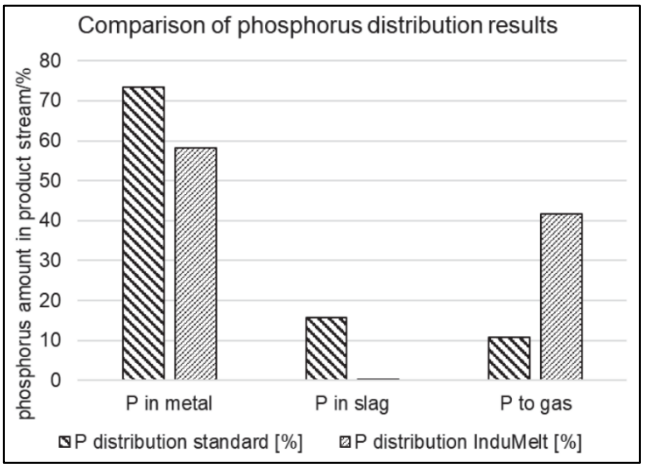

Figure 13: P distribution achieved by standard reduction and by reduction in the InduMelt plant [19]

High Cr and Mn amounts in the slag might be a reason for achieving lower gasification degrees than by reducing standard BOFS. The formation of phosphides might be one of the key parameters that affects the PGD, which is why this formation process will be further analyzed in the course of this thesis. Especially the influence of elements like Cr and Mn on the P gasification will be discussed. In the following chapter 2.5, these parameters are analyzed and findings of previous researchers are summarized.

2.5 Dependency of the Slag Composition on the Efficiency of the Proposed Treatment Process

In the previously illustrated InduMelt plant, the Fe oxide from the slag is reduced by C powder. The produced liquid Fe flows to the bottom of the reactor through interspaces between the graphite cubes, whereby the contact between gaseous P and liquid Fe is minimal. However, as soon as liquid Fe and gaseous P get in contact, Fe phosphides are formed. This accumulation of P in the metal product is a limitation for treating BOFS in the InduMelt plant, but previous experiments depict that higher temperatures limit the formation of Fe phosphides. The formation of phosphides is a major limitation of the illustrated BOFS treatment process because it hinders the P gasification. [19, 29]

Therefore, slags which are high in FeO have a higher tendency to form Fe phosphides, respectively. As mentioned in chapter 2.4.2.2, recent experiments in treating synthetically produced high-Fe as well as high-Cr and Mn slags show a dependency of the slag composition on the PGD. In addition to the formation of Fe phosphides, also the formation of Cr and Mn phosphides could be a parameter, which reduced the PGD. This formation process needs to

be further investigated since the influence of Mn and Cr on the solubility of P in liquid Fe is supposed to play a significant role on the efficiency of the gasification degree of P. [19]

2.5.1 Effect of Phosphide Formation on the Phosphorus Gasification Degree

During the carbo-thermal reduction of BOFS, the formation of Fe phosphides occurs as soon as the liquid Fe and the reduced gaseous P get in contact. The generated high P containing Fe alloy does not reach the quality requirements to be reused in integrated steelworks. Reducing the enclosure of P in liquid Fe is a key factor to increase the efficiency of the proposed treatment process and to generate a utilizable Fe-alloy with a low P content. The formation process is favored by high activities of P and Fe and inhibited by increasing temperature. [19]

Current research describes that increasing Cr and P contents in the melt lead to an increasing P activity. Additionally, P enrichment at the surface area of reduced Fe particles was monitored, but the inclusion behavior needs further research to be fully understood. [30]

Further phosphide formations like Cr or Mn phosphides seem to be uncommon in the considered system and temperature range, especially due to the high Cr and Mn amounts that are needed for its formation. Moreover, the driving force of these reactions decreases with increasing temperature, which is an indicator that Cr and Mn phosphides are unlikely to be formed during the proposed treatment process. Although, previous experiments show that Cr and Mn phosphides occurred during carbo-thermal reduction of slags and therefore this formation process needs to be further investigated. [29, 31]

In order to increase the P gasification rate and analyze the influence of the occurring phosphide formations during reduction of high Cr and P slags, both, the interactions between P and Cr or Mn, are analyzed separately.

2.5.2 Interaction Between Chromium and Phosphorus in Liquid Iron

To control the P gasification reaction and the Fe phosphide formation in the proposed BOFS treatment process it is crucial to understand the behavior of the Fe-C_{sat}-Cr-P system over various Cr contents and a wide temperature range. While the influence of Fe on the activity of P in a liquid melt is consistent in current research, the effect of Cr on the P activity differs widely in several publications, as pictured in Figure 14. [32]

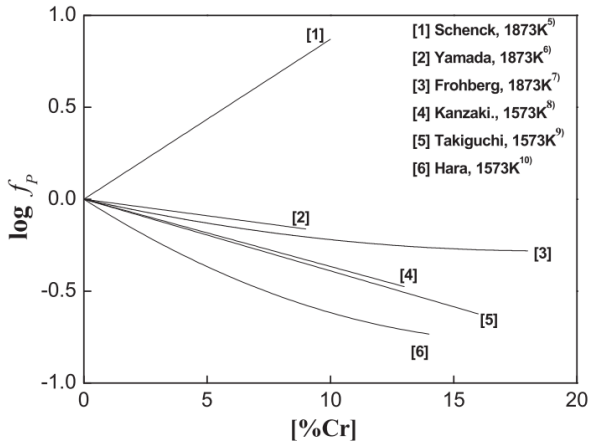

Figure 14: Dependency of the Cr content on the P activity in liquid Fe [32]

Several research groups have a different understanding due to various experimental outcomes when it comes to the effect of Cr on the P activity in a liquid melt. While Schenck et.al state a rise in the P activity with increasing Cr amounts, other researchers detected a reduction in the P activity with an increase in Cr. At a temperature of 1573 K the decreasing trend of the P activity with increasing Cr amounts is consistent by various publications. However, current experiments conducted by Do et. al. in an electric resistance furnace report that increasing the Cr content leads to rising C content but has no noticeable influence on the P activity. The temperature variation between 1623 K and 1723 K has neither significant influence on the C solubility nor on the P activity in the Fe-C_{sat}-Cr-P melt. Results of these conducted experiments are shown in Figure 15 and Figure 16. [32]

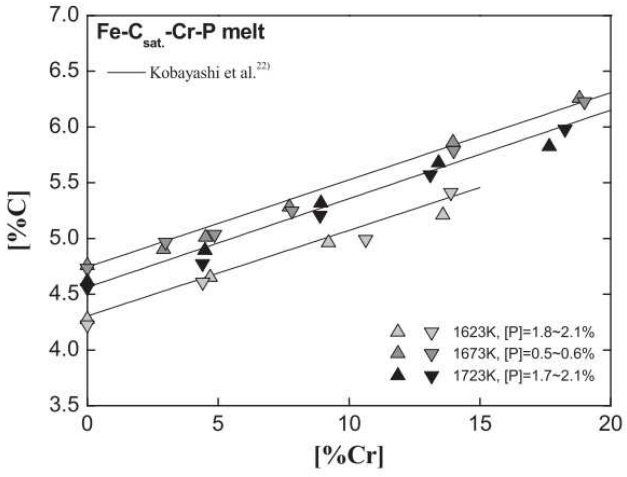

Figure 15: Influence of the Cr content on the C content in a Fe-C_{sat}-Cr-P melt in the temperature range from 1623 K to 1723 K [32]

As pictured in Figure 15, higher temperature does not necessarily lead to a higher C solubility. In Figure 16 the P activity remains constant over a temperature range from 1623 K to 1723 K and a Cr content from 0 % up to 20 %.

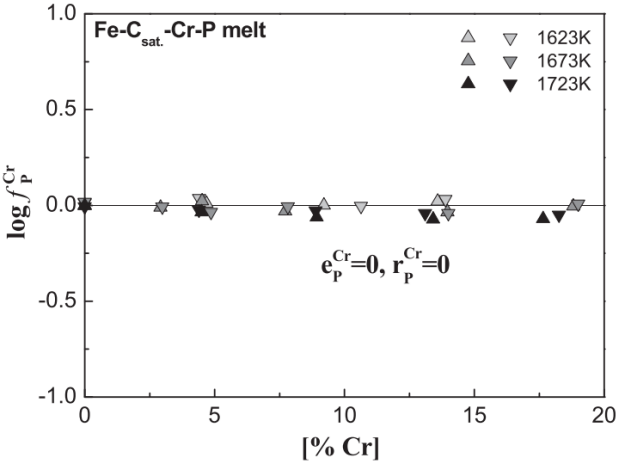

Figure 16: Influence of the Cr content on the P activity in a Fe-C_{sat}-Cr-P melt in the temperature range from 1623 K to 1723 K [32]

Increasing the Cr content has no recognizable effect on the P activity in a liquid Fe melt. The first and second order Wagner interaction parameter were determined to be zero, respectively. These parameters describe the influence of specific elements on various activity coefficients in multi-component Fe melts. Equation (2.16) expresses the relation of the first and second order interaction parameters on the P activity in a Fe-C_{sat}-Cr-P melt. [32-33]

Effect of the Cr content on the P activity [32]

$$log\left(f_P^{Cr}\right) = e_P^{Cr} * [\%Cr] + r_P^{Cr} * [\%Cr]^2 \qquad (2.16)$$

While Cr has no detected effect on the P activity in a liquid melt, the research group around Shim et. al. has identified a decreasing P activity with an increasing mass fraction of Mn, which will be discussed in chapter 2.5.3.

2.5.3 Interaction between Manganese and Phosphorus in Liquid Iron

By heating a 2 g sample of a Fe-Mn-C_{sat} alloy in a graphite crucible in a SiC resistance furnace for 24 hours at 1573 K and 1673 K, a dependency of both the P activity and the C content in the alloy on the Mn content was identified. A slight decrease in the activity coefficient of P with increasing Mn contents in the Fe-Mn-C_{sat} alloy was observed, as figured in Figure 17 below.

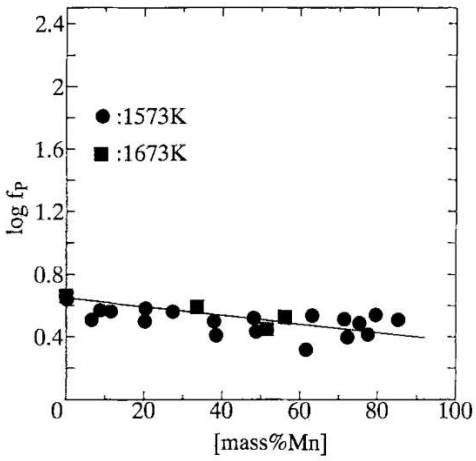

Figure 17: Influence of the Mn content on the P activity in a Fe-Mn-C_{sat} system at 1573 K and 1673 K [34]

The decreasing P activity reflects a stronger interaction between Mn and P than between Fe and P. This interaction behavior was also noticed during previously carried out reduction experiments of high Cr and high Mn slags in the InduMelt plant on the one hand and standard reduction experiments on the other hand, as mentioned in chapter 2.4.2.2. [19, 34]

An increase in temperature from 1573 K to 1673 K led to no significant impact on the P activity. The activity coefficient of P in the Fe-Mn-C_{sat} alloy from 1573 K to 1673 K can be depicted based on Figure 17 and is expressed in Equation (2.17).

Activity coefficient of P as a function of the Mn content and the temperature [34]

$$log(f_P^{Mn}) = -0.0029 * [\%Mn] - \frac{386}{T} + 0.891 \quad (2.17)$$

Moreover, the first order Wagner interaction parameter was determined to be -0.0029 in the proposed temperature range. Equation (2.18) exemplifies this statement.

First order Wagner interaction parameter for the activity of P in a Fe-Mn-C_{sat} alloy [34]

$$log(f_P^{Mn}) = e_P^{Mn} * [\%Cr] \quad (2.18)$$

Other researchers like Ban-Ya et. al. report values of -0.032 ± 0.005 at a temperature of 1673 K, which is in good agreement with the reported value by Shim et. al. [35]

Investigating the influence of the Mn content on the C solubility, a similar effect to the Fe-C_{sat}-Cr-P system can be identified. Figure 18 shows this correlation.

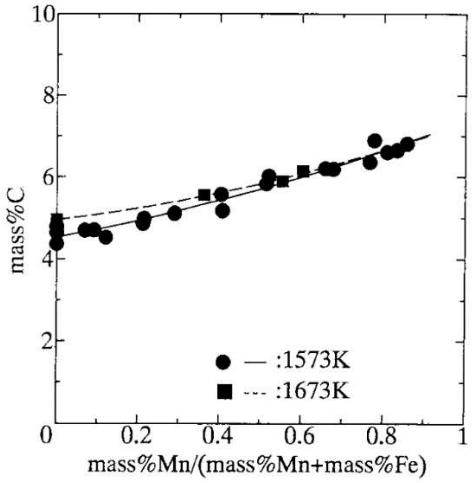

Figure 18: Influence of the Mn content on the C content in a Fe-Mn-C_{sat} system in the temperature range from 1573 K to 1673 K [34]

Increasing Mn contents slightly raise the C solubility in which a temperature change from 1573 K to 1673 K had no remarkable influence. The Cr content has a higher impact on the C solubility in the Fe-C_{sat}-Cr-P melt than the Mn content in the Fe-C_{sat}-Mn melt. [32, 34]

Insights into the Mn-P melt also show the decreasing trend of the P activity with increasing Mn contents reflecting a weak interaction between the Fe and P atoms and a strong interaction between the Mn and P atoms in the considered system. [32, 36]

To further understand the tendency of possible formation reactions in the considered temperature range, the following chapter 2.5.4 overviews possible phosphide reactions and compares their individual driving forces with regard to the temperature. Additionally, the stoichiometric values of the reaction agents will also be analyzed.

2.5.4 A Benchmark of the Driving Forces of Possible Phosphides

The novel suggested treatment route of BOFS resulted in high Cr, Mn and P slags, which are reduced in the InduMelt plant. Thereby, a Cr-rich alloy, pure gaseous P and standard product slag will be produced. Previous experiments regarding the treatment of these kind of slags showed a worse PRD than reducing high FeO slags. The formation of phosphides is a crucial point considering the P gasification rate, which is why the Gibbs free energies of potential phosphide formations in the considered temperature range are analyzed. Schlesinger et. al. provides up-to-date data of phosphide formation reactions. Figure 19 represents the temperature dependency of the Gibbs free energies of formation of various phosphides. In regard to Table 1 only phosphides with elements that can be found in BOFS are considered. [29]

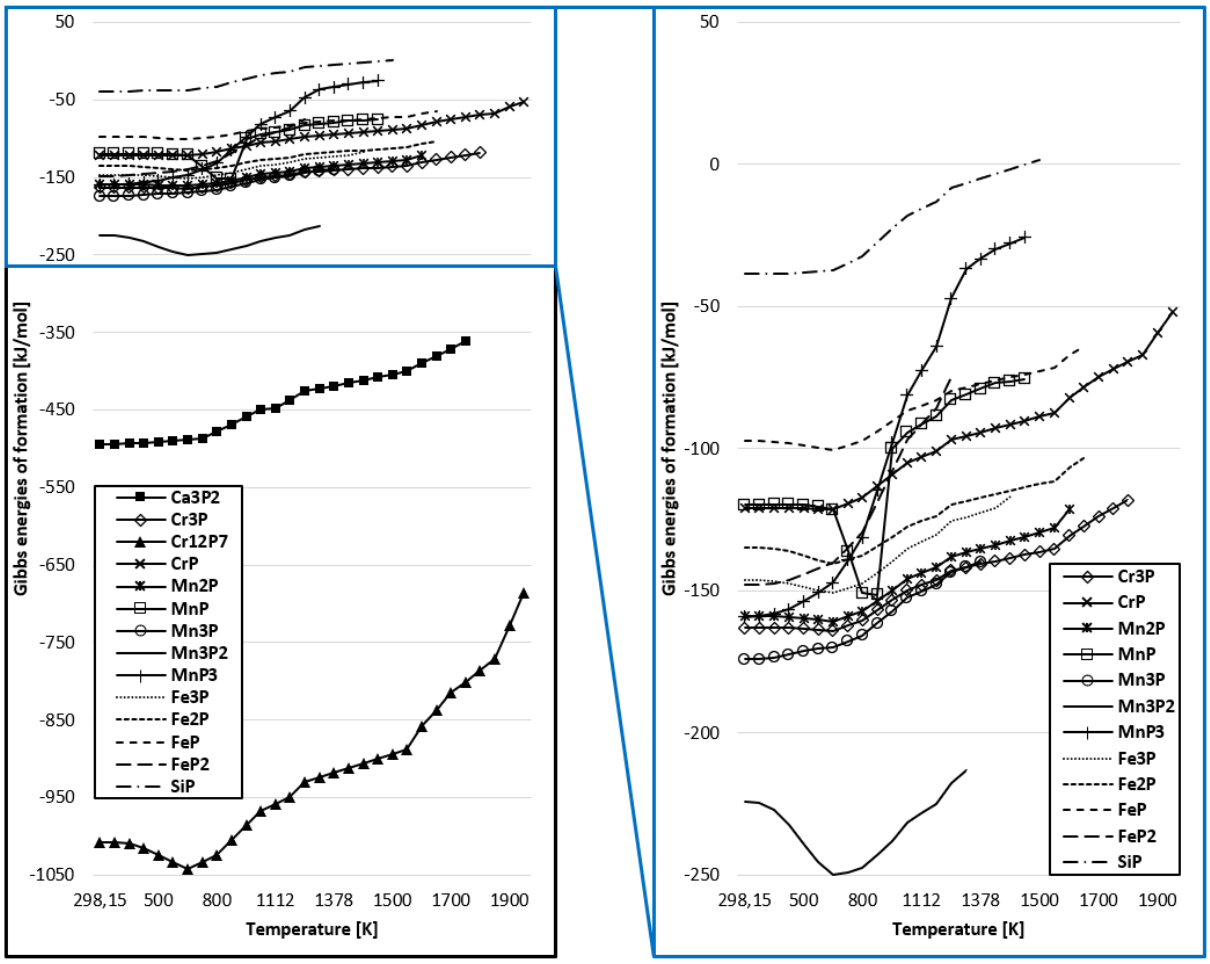

Figure 19: Gibbs energies of various phosphides in the temperature range from 298.15 K to 1900 K (data gathered from [29])

In Figure 19 a strong temperature dependency of the free Gibbs energies of potential phosphides can be identified. Some specific phosphides like $Cr_{12}P_7$ or CrP have gotten a lot of research attention in the past, which is the reason why these phosphides are more precisely analyzed and the Gibbs free energies of them can be determined for a wider temperature range. In general, the driving forces of all phosphides, which can be described as by the Gibbs free energy ΔG of a particular reaction, decrease with increasing temperature. Negative values of ΔG indicate that a reaction can proceed under the analyzed conditions spontaneously and without external forces, as explained in chapter 2.4.1. To understand potential formation processes of phosphides with regard to the proposed BOFS treatment method using the InduMelt plant in the following Table 3, the phosphide reactions at 1900 K, which is the maximum operating temperature of the plant, are benchmarked. Since not all Gibbs free energy values at the considered temperature have been currently measured by researchers, the values for ΔG are extrapolated based on the known measured trend.

Table 3: Ranked potential phosphide formation processes at 1900 K (data gathered from [29])

Rank Nr.	$\Delta G\ \left[\frac{kJ}{mol}\right]$ (at 1900 K)	Formation reaction	Equation
1	-727	$\frac{8}{3}Cr_3P + P_2(g) \rightarrow \frac{2}{3}\boldsymbol{Cr_{12}P_7}$	(2.19)
2	-333 (extrapolated)	$Ca_3(PO_4)_2 + 8C \rightarrow \boldsymbol{Ca_3P_2} + 8CO$	(2.20)
3	-155 (extrapolated)	$3Mn(g) + P_2(g) \rightarrow \boldsymbol{Mn_3P_2}$	(2.21)
4	-119 (extrapolated)	$3Mn(g) + \frac{1}{2}P_2(g) \rightarrow \boldsymbol{Mn_3P}$	(2.22)
5	-113 (extrapolated)	$3Cr(c) + \frac{1}{2}P_2(g) \rightarrow \boldsymbol{Cr_3P}$	(2.23)
6	-88 (extrapolated)	$2Fe(\gamma) + \frac{1}{2}P_2(g) \rightarrow \boldsymbol{Fe_2P}$	(2.24)
7	-82 (extrapolated)	$4Mn(g) + P_2(g) \rightarrow 2\boldsymbol{Mn_2P}(s)$	(2.25)
8	-74 (extrapolated)	$3Fe(\gamma) + \frac{1}{2}P_2(g) \rightarrow \boldsymbol{Fe_3P}$	(2.26)
9	-69 (extrapolated)	$Mn(g) + \frac{1}{2}P_2(g) \rightarrow \boldsymbol{MnP}$	(2.27)
10	-59	$\frac{2}{5}Cr_{12}P_7 + P_2(g) \rightarrow \frac{24}{5}\boldsymbol{CrP}$	(2.28)
11	-49 (extrapolated)	$Fe_2P + \frac{1}{2}P_2(g) \rightarrow 2\boldsymbol{FeP}$	(2.29)
12	-7 (extrapolated)	$MnP + \frac{1}{2}P_4(g) \rightarrow \boldsymbol{MnP_3}$	(2.30)
13	15 (extrapolated)	$Si + \frac{1}{4}P_4(g) \rightarrow \boldsymbol{SiP}$	(2.31)
14	79 (extrapolated)	$FeP + \frac{1}{2}P_2(g) \rightarrow \boldsymbol{FeP_2}$	(2.32)

The formation processes of potential phosphides needs to be further discussed due to mutual dependence of some phosphide formations. Regarding the Gibbs free energy, the phosphide $Cr_{12}P_7$ seems to be most likely to be generated, however a stochiometric ratio $\frac{Cr}{P_2}$ of 3,4 is needed to form $Cr_{12}P_7$ and additionally, first Cr_3P regarding (2.23) needs to be generated which has an estimated driving force of -113 $\frac{kJ}{mol}$ and is therefore more unlikely to be generated. Regarding the high amounts of Cr needed to produce $Cr_{12}P_7$ and around 3 m.% of Cr_2O_2 and around 12 m.% of P_2O_5 in the high Cr and Mn BOFS it is unplausible that this phosphide will be generated in the considered plant and the considered slag system. For the formation of Ca_3P_2, as seen in (2.20), tricalcium phosphate ($Ca_3(PO_4)_2$ or $3CaO \cdot P_2O_5$) needs to be available, which can occur regarding equations (2.33) and (2.34):

Formation of tetracalcium phosphate [37]
$$4Ca(l) + P_2(g) + 4{,}5O_2(g) \rightarrow Ca_4(PO_4)_2O(s) \quad (2.33)$$

Formation of tricalcium phosphate [37]
$$2Ca_4(PO_4)_2O(s) + P_2(g) + 2{,}5O_2(g) \rightarrow 4Ca_3(PO_4)_2(s) \quad (2.34)$$

Hudon et.al. evaluated the $CaO - P_2O_5$ system and estimated the Gibbs free energy of the formation of tetracalcium phosphate at 1900 K as -2990 $\frac{kJ}{mol}$ and for the formation of tricalcium phosphate out of tetracalcium phosphate as -1250 $\frac{kJ}{mol}$. The formation of tricalcium phosphate directly out of Ca, P_2 and O_2 was estimated to be around -2550 $\frac{kJ}{mol}$. Also, the formation of $Ca_2P_2O_7$, as well es $Ca(P_3)_2$ out of Ca, P_2 and O_2 was reported, but the driving forces for these reactions were less than for the formation of tricalcium phosphate. A stochiometric ratio $\frac{Ca}{P_2}$ of 3.2 and $\frac{Ca}{O_2}$ of 0.78 is needed to generate $Ca_3(PO_4)_2$. Due to the high amounts of CaO (almost 32 m.%) compared to P_2O_5 (around 12 m.%) the formation of tricalcium phosphate is likely in the considered slag system. [37]

As can be seen in Figure 20 the driving force of $Ca_3(PO_4)_2$ is very strong and also sinks with increasing temperature.

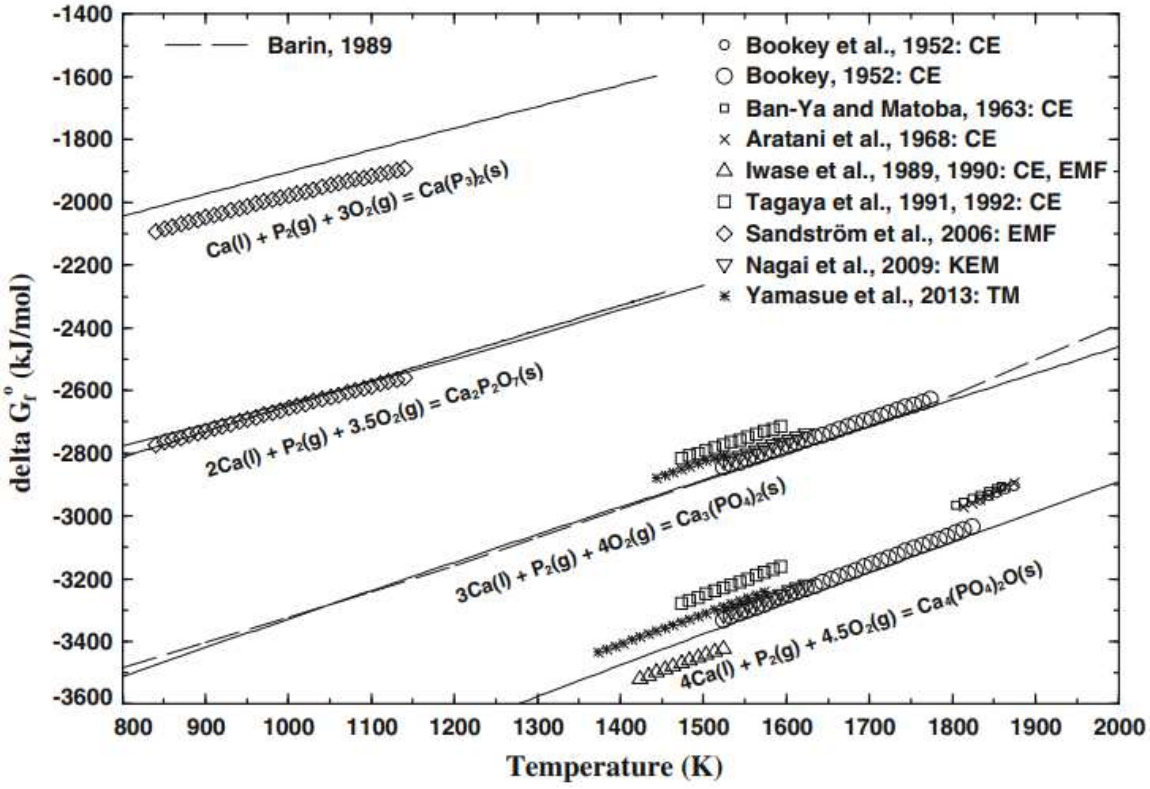

Figure 20: Trend of the driving force for the formation of various calcium phosphides [37]

The formation of tetracalcium phosphate, as well as tricalcium phosphate, is plausible in the considered BOFS due to their strong negative Gibbs free energies and the realistic stochiometric ratio of the needed elements in BOFS. As a result, Ca_3P_2 can also be transformed out of $Ca_3(PO_4)_2$ but high amounts of C are required for that formation process.

In terms of the formation of Mn phosphides, Mn_3P_2 is most likely to be formed considering the Gibbs free energy, followed by Mn_3P and Mn_2P. The formation of the Mn phosphide MnP regarding (2.27) needs relatively high amounts of P and hence its formation would be unusual, since the amounts of MnO and P_2O_5 are both around 12 m.% in the proposed BOFS. The generation of Mn (II) phosphide, Mn_3P_2, on the one hand has the highest driving force of all Mn phosphate reactions, but a stoichiometric ratio $\frac{Mn}{P_2}$ of 3 is needed for the reaction to take place regarding (2.21). The formation of Mn_3P regarding (2.22) has a slightly lower driving force than Mn_3P_2 and a stoichiometric ratio $\frac{Mn}{P_2}$ of 6 is necessary for its occurrence. Mn_2P with regard to (2.25) has a stoichiometric ratio $\frac{Mn}{P_2}$ of 4 and also a very low driving force. In case of potential Mn phosphide formations, the driving force for the formation of Mn_3P_2 out of gaseous Mn and gaseous P is most powerful, but around three times more Mn than gaseous P_2 are needed for this reaction.

With a view on the Cr phosphides, $Cr_{12}P_7$ has the highest driving force but unplausible high amounts of Cr are needed, which is why this formation process would be unlikely in the considered slag system. The emergence of Cr_3P out of Cr and gaseous P_2 like (2.23) needs a stoichiometric ratio $\frac{Cr}{P_2}$ of 6. As described in chapter 2.4.2.1, the considered BOFS has only around 3 m.% of Cr_2O_3, but around 12 m.% of P_2O_5, so generating Cr_3P seems to be unlikely. The formation of CrP as seen in (2.28) needs $Cr_{12}P_7$ as one of its reacting agents. As described above, generating $Cr_{12}P_7$ is unrealistic in the considered slag system making the occurrence of CrP also unplausible.

Regarding the emergence of Fe phosphides, Fe_2P, as well as Fe_3P, are most likely to be formed due to their high driving forces and their plausible needed stoichiometric ratio $\frac{Fe}{P_2}$ of 4 regarding Fe_2P and of 6 regarding Fe_3P. Generating FeP is supposed to be unrealistic due to its lower driving force than Fe_2P and Fe_3P and, on the other hand, Fe_2P is needed as an reaction agent regarding (2.29). Additionally, only two times more Fe_2P than gaseous P_2 is needed for this reaction making the formation of FeP unlikely.

2.6 Theoretical Predictions

The treatment of high Cr, Mn and P BOFS raises a lot of challenges in terms of the interaction of its containing elements. Previous experiments state that treating BOFS, which has high amounts of Cr, Mn and P, led to a minor PRD. Moreover, high amounts of P are accumulated

to the metal phase making the efficiency of the proposed treatment process highly dependent of its input BOFS composition. Therefore, the influence of Cr and Mn on the P activity in liquid Fe has been analyzed and the following findings can be elaborated:

1. The Cr amount has no significant impact on the P activity in a Fe-C_{sat}-Cr-P melt.
2. Increasing Cr content leads to an also rising C content in the Fe-C_{sat}-Cr-P system.
3. The variation of the holding temperature between 1623 K and 1723 K has neither significant influence on the C solubility nor on the P activity in the Fe-C_{sat}-Cr-P melt.
4. Increasing Mn contents in a Fe-Mn-C_{sat} alloy leads to slightly decreasing P activity. The decreasing P activity reflects a stronger interaction between Mn and P than between Fe and P.
5. High amounts of Mn slightly increase the C solubility of the Fe-Mn-C_{sat} alloy.
6. Changing the holding temperature from 1573 K to 1673 K had no remarkable influence both on the P activity and on the C solubility in the considered Fe-Mn-C_{sat} alloy.

To further understand the phosphide reaction probabilities in the considered BOFS, the driving forces as well as the needed stoichiometric values of potential formation reactions are benchmarked, whereby the following results can be elaborated:

1. Considering the formation of Mn phosphides, Mn_3P_2 is most likely to be formed due to its high driving force and relatively low required amounts of Mn compared to the formation of Mn_3P and Mn_2P.
2. Generating Cr phosphides generally seems to be unlikely in the considered slag system. $Cr_{12}P_7$ has the highest driving force but unrealistic high amounts of Cr are needed for its formation. This issue is also true for the formation of Cr_3P. Generating CrP is also unlikely because $Cr_{12}P_7$ is needed as a reaction agent for its formation.
3. In terms of potential Fe phosphides, Fe_2P and Fe_3P are most likely to occur due to their high driving forces on the one hand as well as plausible needed composition of Fe and P on the other hand. The formation of FeP is supposed to be unlikely because of its relatively low driving force and high needed amounts of Fe_2P.
4. In addition, insights into the Ca-P system indicate a possibility of forming Ca_3P_2 due to its high driving force and plausible composition of the reaction agents. $Ca_3(PO_4)_2$ is needed to form Ca_3P_2, which is certainly generated due to its high driving force and its realistic required stoichiometric ratio of calcium and P.

The reaction processes by carbo-thermal treatment of high-Cr, Mn and P BOFS are complex and various coactions occur. To estimate the influence of parameters like slag composition or reduction temperature on the efficiency of the proposed BOFS treatment process, and

specifically the influence on the PRD, in the following chapter 3 this thermodynamic process is simulated using the thermochemical simulation software FactSage™.

3 Thermodynamic Simulation using FactSage™

FactSage is a thermochemical simulation software, which is commonly used in the field of thermodynamics and chemical engineering to model the behavior of solutions. The abbreviation “FACT” represents “Facility for the Analysis of Chemical Thermodynamics”. This simulation software also accesses extensive up-to-date databases making it one of the most powerful tools in the area of chemical thermodynamics. For the following simulations in this master’s thesis the FactSage Equilib module is used to simulate the proposed BOFS treatment process and analyze the effect of changing input parameters as well as varying process conditions. This module calculates the concentrations of the specific species when the input compounds react, or partially react, to reach a chemical equilibrium. Therefore, the value of the Gibbs free energy is used to indicate which species tends to be formed. To achieve an accurate calculation, the specific selection of the databases and the preciseness of the input parameters is of highest importance. The goal of the conducted simulations is to better understand the behavior of P in the estimated slag composition after refining the metal phase from the EAF, as explained previously in chapter 2.4.2.1. Therefore, a total of three simulation series, each with different specific goals, were conducted.

1. Simulation series A: Treatment of the estimated slag composition after refining the metal phase from the EAF with a basicity of 1.5.
    a. Goals: Understand the temperature dependency on the accumulated compositions and on the mixture of the generated slag, metal and gas phase.
2. Simulation series B: Treatment of the estimated slag composition after refining the metal phase from the EAF with a changing Cr and Mn amount in the input mixture at 1900 K.

   a. Goals: Understand the influence of Cr and Mn on the distribution of the emerging phases. Analyze the effect of varying Cr and Mn contents in the input slag mixture on the P activity coefficient and the P inclusion in the accruing metal phase.
3. Simulation series C: Treatment of the same slag mixture from Simulation A, but with a basicity varying from 1.0 to 1.5.
   a. Goal: Analyze if the phosphide formation process is influenced by the basicity of the input slag mixture.

Simulation series A and B are of highest importance for this master's thesis because they directly analyze the estimated emerging slag composition, which will be generated by the novel treatment process. Hence, the temperature dependency of simulation series A will also be analyzed and mass balances of the emerging phases as well as P balances at 1900 K will be carried out. As explained previously in chapter 2.3, the operating temperature of the InduMelt plant is 1900 K, which is why this specific temperature will be considered for the mass and P balances. In simulation series B, the effect of altering Cr and Mn contents on the P distribution between the emerging phases will be analyzed. By changing these input conditions, the influence of the slag composition on the efficiency of the proposed treatment process will be better understood. The PRD can also be calculated, which is a value that indicates the effectiveness of treating this slag mixture. By comparing the PRD of the changing input slag mixture the most efficient slag system can be identified.

Simulation series C has the aim to depict the impact of a changing basicity on the P distribution. For that matter, the temperature dependency on the emergence of the phosphide compounds will further be analyzed and mass balances will be used to illustrate the P distribution between the phases.

To understand the development of these simulations, the used framework generally, as well as assumptions and restrictions will be explained in chapter 3.1. The input data of the three simulation series will also be overviewed and differences in these input values will be elucidated.

3.1 Framework of the Simulation

To conduct successful simulations in the FactSage Equilib module, some adjustments must be done, which are listed below:

- In the “View Data” module of the Database setting, the following elements are selected: Fe-O-Cr-Mn-P-Si-Ca-Al-Mg-Ti-S-C. The compounds of the input slag mixture consist only of these specific elements. Consequently, the generated phases and compounds also include only these elements.
- In the “Reactants” tab of the Equilib module the following units for the general calculation are defined: temperature in kelvin, pressure in atmospheres, energy in joules, quantity in grams and volume in litres. The input as well as the calculated output values will be represented with these units. However, in the “Results” module of the manipulate setting, FactSage also can calculate the outcome values with other units by internal conversion.
- The temperature of the input phases at the beginning of the simulation is set to be 300 K in the “Reactants” tab of the Equilib module because this is a good representation of the ambient temperature.
- The phases of the various specific input species at 300 K are suggested by FactSage and the pressure of each simulation is set to a value of 1 atm.
- Regarding the selection of the specific databases Mr. Moritz to Baben from GTT Technologies, which is the company that sells FactSage, recommended to use the databases “Fact Pure Substances” and “Fact Solutions”, which were selected in the “Data Search” module of the Reactants tab in the Equilib module. [38]
- In the “Last system” tab of the Equilib module the generated product compounds were selected to be gas, liquid or solid.
- The selection of the solution phases is also very important for an accurate simulation because these phases are supposed to be formed during the simulation. Previous research experiments at the InduMelt plant show that a liquid slag phase, a molten metal phase as well as a gaseous phase are formed. Based on that knowledge, the base-phases FSstel-Liqu, FToxid-SLAGA, FToxid-SPINB and FToxid-C2SP are chosen. The base-phase FSstel-Liqu represents a liquid steel phase, FToxid-SLAGA represents a liquid slag phase, FT-oxidSPINB represents a spinel phase and FToxid-C2SP represents the specific compounds C_2S and C_3P. Here it can be said that the conducted simulations show no emergence of the spinel phase. Previous experiments show that C_2S and C_3P may occur in the considered slag system, which is why these phases are also taken into account. The gaseous phase does not specifically need to be chosen in the selection of the solution phases.
- To achieve a running simulation without errors, it is important to suppress duplicate values, which can be done in the compound selection within the “Products” tab. By suppressing duplicate elements and duplicate compounds FactSage chooses the

compounds and elements, which are most likely to be generated based on the thermodynamic data of the databases. This is an important step if more than one database is selected.

3.1.1 General Assumptions and Restrictions

In the course of this master's thesis, the Equilib module, which is the most common application of FactSage, is used to simulate the dephosphorization process of BOFS. This module calculates the concentrations of the occurring species when the compounds react, or partially react, to a state of chemical equilibrium. In a practical operation of the InduMelt plant, this chemical equilibrium state does not exist because the output metal, slag and gaseous phases are separated and discharged continuously in order to further treat and use them. This continuous operation of the plant does not allow the emergence of chemical equilibria, but the results of the FactSage simulations are a good estimation of the actual practical treatment method because the amounts of the occurring slag, metal and gas phase at the considered temperature range are coherent with previously conducted experiments. However, at these previous experiments a slightly different input slag composition was analyzed.

Another factor that is neglected in the simulations is the changing concentration of the BOFS mixture over the height of the reactor. Due to the continuous separation of the slag, metal and gaseous phase, the concentration inside the reactor changes with the duration of the treatment. This behavior cannot perfectly be simulated in FactSage due to the manifold dependencies of changing the slag mixture during operation. However, a changing input slag composition can be simulated and illustrated perfectly, which is needed for analyzing the effect of changing the Cr and Mn amount of the input slag on the behavior of P in the product phases.

In addition, the input slag mixture is based on analyzing the composition of BOFS and by calculations. The accuracy of these previous measurements and calculations is also a parameter that defines the input parameters of the simulation.

The most important constraint of the whole simulation is that it strongly depends on the correctness of the data of the FactSage databases. GTT technologies therefore makes an enormous effort to keep the data correct and up to date, which is why FactSage is widespread by researchers in the field of engineering.

3.1.2 Input Parameters Simulation Series A

To conduct a simulation using the Equilib module, the input values need to be selected in the "Reactants" section. Based on the estimated slag composition figured in Table 2, the values for the input compounds are selected. To achieve the highest possible accuracy of the simulation, additional compounds and elements are added to the slag system:

- A total of 0.3 m.% of TiO_2, 0.11 m.% MnS and 0.1 m.% sulfur were added because these compounds have been detected in BOFS by prior analyses conducted by the Austrian-based steel company voestalpine AG and the University of Leoben. [19]
- 50 grams of C are added to the mixture to achieve a complete reduction of the oxides. This C represents the added C powder in the practical experiments of the InduMelt plant. It is important that enough C is available for the total reduction because otherwise the proposed treatment process would not comply its purpose. In all simulations elementary C can also be found in the product values, which indicates that the reduction is complete and enough C is available.

The basicity of the slag mixture stays constant with B_2=1.5 and the added TiO_2, MnS and S are evenly distributed in regard to the previous slag compounds. Consequently, the total mass of the input values adds up to 100 g of the slag mixture and 50 g of the added C. In Table 4 below, the input parameters of simulation series A are listed.

Table 4: Input values of simulation series A (T=1000 K – 2000 K)

Species	Phase (recommended by FactSage)	Quantity [g]	Quantity [m.%] (Without C)
FeO	solid-FactPS Wustite	11.50	11.50
Cr_2O_3	solid-FToxid	3.01	3.01
MnO	solid-FToxid	11.57	11.57
P_2O_5	solid-1-FToxid P2O5-H	12.32	12.32
SiO_2	solid-1-FactPS Quartz(l)	21.32	21.32
CaO	solid-FactPS Lime	31.92	31.92
Al_2O_3	solid-1-FactPS gamma	2.94	2.94
MgO	solid-FactPS Periclase	4.94	4.94
TiO_2	solid-1-FactPS Rutile	0.30	0.30
MnS	solid-FactPS Alabandite	0.11	0.11

S	solid-1-FactPS alpha orthorhombic A16 oF128 (70) Fddd	0.10	0.10
C	solid-1-FactPS Graphite	50.00	-

To enable an accurate visualisation of the formation of the metal, slag and gaseous phase, the temperature for simulation series A was increased from 1000 K to 2000 K in 5 K steps. In this temperature window especially the formation of gaseous P takes place, which is a crucial indicator for the dephosphorization process of BOFS.

3.1.3 Input Parameters Simulation Series B

This simulation aims to better understand the influence of the Cr and Mn amounts in the input slag mixture on the P behaviour at 1900 K in regard to the carbo-thermal InduRed treatment process. Especially the P distribution between the slag, metal and gas phase and the P activity therefore will be analyzed in detail. To scientifically analyze the influence of Cr and Mn on the output phases and to enable a benchmark between the input Cr and Mn amount, these elementary input parameters are set to values between 0 and 15 m.% each. To understand the influence of Cr and Mn, these broad mass distributions are taken into account. Therefore, elementary balances of the input slag mixture were conducted, because to make a reasonable benchmark, the m.% of Cr and Mn as input elements and not as oxides (Cr_2O_3 and MnO) are considered. To simplify the input calculation, the minimal amounts of 0,11 m.% of MnS are neglected and to make comparisons of the simulation results possible, a maximum mass of 100 g slag has been calculated. In each simulation 50 g of C were added summing the input mixture up to 150 g, as in simulation A. A total of 16 simulations, each with unique input parameters, are conducted in the course of simulation series B. The m.% of Cr and Mn in the input mixture are increased in 5 m.% steps from 0 m.% up to 15 m.%. The proportion of the remaining slag mixture stays constant. In Table 5 the input slag mixture for these 16 simulations can be seen. The phases of the input species have been recommended by FactSage and are the same as in simulation series A.

Table 5: Input values of simulation series B (T=1900 K)

Species in [g] (equals [m.%] due to 100 g total)																
Simulation Nr.	**1**	**2**	**3**	**4**	**5**	**6**	**7**	**8**	**9**	**10**	**11**	**12**	**13**	**14**	**15**	**16**
FeO	13.48	12.49	11.51	10.52	12.61	11.62	10.64	9.65	11.74	10.75	9.77	8.78	10.87	9.88	8.90	7.91
Cr_2O_3	0.00	7.31	14.61	21.92	0.00	7.31	14.61	21.93	0.00	7.31	14.61	21.93	0.00	7.30	14.62	21.93

MnO	0.00	0.00	0.00	0.00	6.46	6.46	6.46	6.46	12.91	12.92	12.91	12.92	19.37	19.37	19.36	19.37
P_2O_5	14.44	13.38	12.33	11.27	13.50	12.45	11.39	10.34	12.57	11.52	10.46	9.41	11.64	10.59	9.53	8.47
SiO_2	24.98	23.16	21.33	19.51	23.37	21.54	19.72	17.89	21.76	19.93	18.11	16.28	20.14	18.32	16.49	14.67
CaO	37.40	34.67	31.94	29.20	34.99	32.26	29.52	26.79	32.57	29.84	27.11	24.37	30.16	27.43	24.69	21.96
Al_2O_3	3.45	3.19	2.94	2.69	3.22	2.97	2.72	2.47	3.00	2.75	2.50	2.24	2.78	2.53	2.27	2.02
MgO	5.79	5.37	4.94	4.52	5.41	4.99	4.57	4.15	5.04	4.62	4.20	3.77	4.67	4.24	3.82	3.40
TiO_2	0.35	0.33	0.30	0.27	0.33	0.30	0.28	0.25	0.31	0.28	0.25	0.23	0.28	0.26	0.23	0.21
S	0.12	0.11	0.10	0.09	0.11	0.10	0.09	0.08	0.10	0.09	0.08	0.08	0.09	0.09	0.08	0.07
total [g]	100.00	100.00	100.00	100.00	100.00	100.00	100.00	100.00	100.00	100.00	100.00	100.00	100.00	100.00	100.00	100.00
Fe	10.47	9.71	8.94	8.18	9.80	9.03	8.27	7.50	9.12	8.36	7.59	6.82	8.45	7.68	6.92	6.15
Cr	**0.00**	**5.00**	**10.00**	**15.00**	**0.00**	**5.00**	**10.00**	**15.00**	**0.00**	**5.00**	**10.00**	**15.00**	**0.00**	**5.00**	**10.00**	**15.00**
Mn	**0.00**	**0.00**	**0.00**	**0.00**	**5.00**	**5.00**	**5.00**	**5.00**	**10.00**	**10.00**	**10.00**	**10.00**	**15.00**	**15.00**	**15.00**	**15.00**
P	6.30	5.84	5.38	4.92	5.89	5.43	4.97	4.51	5.49	5.03	4.57	4.11	5.08	4.62	4.16	3.70
Si	11.68	10.82	9.97	9.12	10.92	10.07	9.22	8.36	10.17	9.32	8.46	7.61	9.42	8.56	7.71	6.86
Ca	26.73	24.78	22.83	20.87	25.01	23.05	21.10	19.14	23.28	21.32	19.38	17.42	21.55	19.60	17.65	15.69
Al	1.82	1.69	1.56	1.42	1.71	1.57	1.44	1.31	1.59	1.45	1.32	1.19	1.47	1.34	1.20	1.07
Mg	3.49	3.24	2.98	2.73	3.27	3.01	2.76	2.50	3.04	2.78	2.53	2.27	2.81	2.56	2.30	2.05
Ti	0.21	0.20	0.18	0.16	0.20	0.18	0.17	0.15	0.18	0.17	0.15	0.14	0.17	0.15	0.14	0.12
S	0.12	0.11	0.10	0.09	0.11	0.10	0.09	0.08	0.10	0.09	0.08	0.08	0.09	0.09	0.08	0.07
O	39.17	38.62	38.06	37.51	38.10	37.55	36.99	36.43	37.03	36.47	35.92	35.36	35.95	35.4	34.84	34.29
total [g]	100.00	100.00	100.00	100.00	100.00	100.00	100.00	100.00	100.00	100.00	100.00	100.00	100.00	100.00	100.00	100.00

Simulation series B aims to analyze changing Cr and Mn amounts, which is why the input Cr_2O_3 and MnO oxides are altered in a way that the elements Cr and Mn in this mixture reach the desired values. The elementary amounts of Cr and Mn are highlighted in Table 5 above. Based on the simulation results of simulation 1 to 16, the emerging phases, the P distribution and the P activity will be analyzed at 1900 K.

3.1.4 Input Parameters Simulation Series C

To understand the influence of the B_2 of the input slag mixture in the course of simulation series C a total of six simulations with changing B_2 from 1.0 to 1.5 in 0.1 steps have been conducted.

The basicity B_2 is defined as the ratio of m.% CaO to m.% SiO_2, as previously discussed in chapter 2.2.1. A total input slag mixture of 100 g has been calculated and 50 g of C were added in each simulation to guarantee that the reduction process can happen completely. All input compounds mentioned in simulation series A were considered and the phases of each compound were recommended by FactSage. By varying the input CaO and SiO_2 amounts, the B_2 was modified. An overview of the input values of simulations a to f in the course of simulation series C is illustrated in Table 6 below. The input slag amount stays constant with 100 g and in each simulation 50 g of C were added, which is not individually viewed in Table 6. The simulations will be conducted in the temperature range between 1000 K to 2000 K to also analyze possible temperature dependencies when analyzing various B_2. To minimalize the change in the remaining input amounts, the base value for B_2 is 1.50 with 31.92 m.% CaO and 21.32 m.% SiO_2. By altering both the m.% of CaO and SiO_2 equally, based on these specific values, the change of the remaining compounds is reduced. Therefore, the input m.% of CaO was reduced by a specific number and the input m.% of SiO_2 was increased by the same number iteratively changing the B_2 to the desired rate with having the remaining composition in a constant relation to each other.

Table 6: Input values of simulation series C (T=1000 - 2000 K)

Species in [g] (equals [m.%] due to 100 g total)						
Simulation Nr.	**a**	**b**	**c**	**d**	**e**	**f**
FeO	11.50	11.50	11.50	11.50	11.50	11.50
Cr_2O_3	3.01	3.01	3.01	3.01	3.01	3.01
MnO	11.57	11.57	11.57	11.57	11.57	11.57
P_2O_5	12.32	12.32	12.32	12.32	12.32	12.32
SiO_2	**26.61**	**25.34**	**24.18**	**23.13**	**22.17**	**21.32**
CaO	**26.61**	**27.88**	**29.04**	**30.09**	**31.05**	**31.92**
Al_2O_3	2.94	2.94	2.94	2.94	2.94	2.94
MgO	4.94	4.94	4.94	4.94	4.94	4.94
TiO_2	0.30	0.30	0.30	0.30	0.30	0.30
MnS	0.11	0.11	0.11	0.11	0.11	0.11
S	0.1	0.1	0.10	0.1	0.1	0.1
B_2	**1.00**	**1.10**	**1.20**	**1.30**	**1.40**	**1.50**
total [g]	100.00	100.00	100.00	100.00	100.00	100.00

In Table 6 the changing input values of SiO_2 and CaO, which lead to an alteration of the B_2, are highlighted. The aim of the conducted simulations a to f in the course of simulation series C is to examine if the B_2 influences the reduction process of the BOFS mixture and the P allocation between the occurring slag and metal phase. The results of the simulations are discussed in chapter 3.2.3 and the findings out of it are overviewed in chapter 3.3.3.

3.2 Simulation Results

This chapter overviews the results of the conducted simulations using the FactSage Equilib module. Throughout the work on this thesis plenty additional simulations have been conducted, but these three simulation series deliver the most critical insights, which is why these are accentuated and will be further discussed.

3.2.1 Results of Simulation Series A

Based on the previously mentioned input values and the adjusted process conditions, this simulation series was carried out successfully and without any error. The occurring phases at 1900 K are described below in chapter 3.2.1.1 and the formation process of these various phases in the temperature window between 1000 K and 2000 K in 5 K steps is visualized in chapter 3.2.1.2. To further understand the mass distribution of the occurring phases, a total of six mass balances between 1000 K and 2000 K are pictured in chapter 3.2.1.3. The behavior of P in the considered temperature window is highly interesting, which is why six elementary balances of P between 1000 K and 2000 K are represented in chapter 3.2.1.4. Simulations below a temperature of 1000 K can also be conducted, but for these simulations some solution phases in the “Last system” tab of the Equilib module need to be de-selected because not all of these phases can be formed at that low temperature. The maximum operating temperature of the InduRed treatment process is around 1900 K and especially the formation behavior of the input BOFS mixture after reaching 1000 K is of interest, which is why the focus lays on that temperature window.

3.2.1.1 Overview of the Emerging Phases at 1900 K

The maximum operating temperature of the InduMelt plant is 1900 K, which is why analyzing the occurring phases and compounds at this specific temperature is highly important. The resulting phases are a slag, metal and gaseous phase, which can be described by the mass balance of the occurring elements. In Table 5 below these phases are overviewed.

Table 7: Resulting phases and their compositions at 1900 K

Gaseous phase (g)			**Slag phase (l)**			**Metal phase (l)**	
Amount: 23.93 g			Amount: 43.22 g			Amount: 25.05 g	
species	**m.%**		**species**	**m.%**		**species**	**m.%**
CO	98.33		CaO	49.31		Fe	35.66
Mg	0.75		SiO_2	33.85		Mn	34.48
Mn	0.54		MgO	8.42		P	20.77
P_2	0.33		Al_2O_3	6.77		Cr	8.22
SiO	0.03		MnO	0.42		C	0.46
CO_2	0.004		Ti_2O_3	0.39		Si	0.39
total	99.98		total	99.16		total	99.99

In the gaseous phase also minimal amounts of, for example, SiS, Fe and Ca were calculated, which is why the total is not exactly 100 %. However, this gaseous phase almost entirely consists of CO. At the temperature of 1900 K a total of 132 litres with the weight of 23.93 g of gas are produced. The liquid slag phase mainly consists of CaO and SiO_2, but also amounts of MgO and Al_2O_3 can be found. In the slag phase also fractional amounts of, for example, TiO_2, SiS_2 and CaS were calculated and therefore again the total m.% does not exactly sum up to 100 %. The metal phase consists of mainly Fe, Mn, P and Cr, but also amounts of S or Al can be found and therefore the sum adds up to almost 100 m.%. The composition of the metal phase highlights again the key point of this master's thesis, which is the accumulation of the P into this metal phase. The proposed InduMelt treatment method is based on the gasification of P, but by treating these kinds of slags, almost all P accumulates into the metal phase. This topic will be further discussed in chapters 3.2.2 and 3.2.3.

In addition to the three occurring phases, which are listed in Table 5, also a total of 9.57 g of C_2S and C_3P consisting of 99.996 m.% of C_2S ($Ca_4Si_2O_8$) and 0.004 m.% of C_3P ($Ca_3P_2O_8$) emerge. If these compositions were bound in the slag mixture, the total weight of this slag at 1900 K would be around 33.5 g. For further analyzations the compounds C_2S and C_3P are considered separately.

The simulation also has generated 8.36 g of a special solid composition, $O_8Ca_3Si_2Mg$ (s), which can also be described as $Ca_3Mg(SiO_4)_2$. It has no specific name in FactSage and is supposed to occur in the considered slag system due to the high amounts of Ca, Si and Mg. Especially the solid aggregate state of it at the temperature of 1900 K is very interesting, which is also why it is not bound in the resulting liquid slag or metal phases. In further mass balances this composition is also considered separately.

In the product phases also 39.87 g of C can be found, which indicates that enough C for a complete reduction process was available. As mentioned, the input value of C was set to be 50 g, which is an excessively high amount, but this ensures that the reduction process is entirely successful.

The mentioned phases and simulated compounds at a temperature of 1900 K are overviewed in Figure 21 in the form of a mass balance. The mass balance was generated by using the Software STAN 2.6, which is provided by the Institute for Water Quality and Resource Management of the Technical University of Vienna.

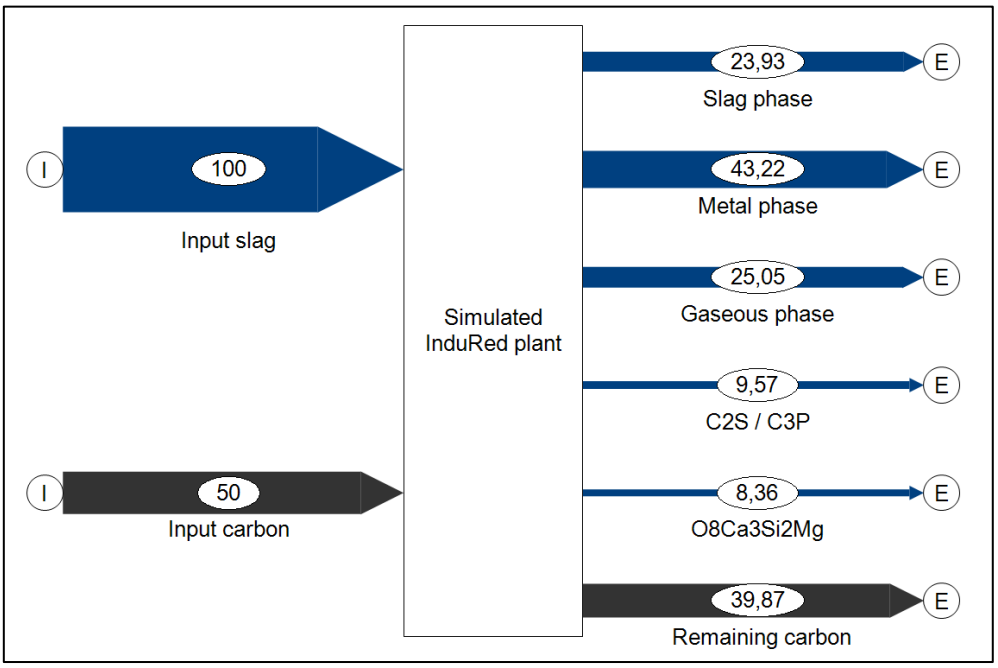

Figure 21: Mass balance in [g] of the emerging phases of Simulation series A (T=1900 K)

At 1900 K high amounts of the metal phase are generated, followed by the gaseous phase and the slag phase. To reduce the input slag mixture around 10.13 g of C are needed. The C_2S / C_3P phase consists of 9.56 g of C_2S and only roughly 0.01 g of C_3P.

To further understand the formation process of the different phases, in the following chapter 3.2.1.2 the most important species of the particular phases are visualized in dependency of the increasing temperature.

3.2.1.2 Temperature Influence on the Simulated Treatment Process

The reduction process of the input slag mixture needs a specific temperature to work properly. Therefore the temperature dependency of the agglomeration of the output compounds is analyzed in this chapter. Due to the emergence of various phases with different physical

conditions, these phases are analyzed separately. The gas, metal and slag phase were considered separately and, additionally, also the C_2S / C_3P phase and the interesting solid phase $O_8Ca_3Si_2Mg$, also known as $Ca_3Mg(SiO_4)_2$, were analyzed. The behavior of C in the simulated system is not of high interest and was therefore not considered in detail. In Figure 22 the formation of the gaseous phase is pictured between 1000 K and 2000 K.

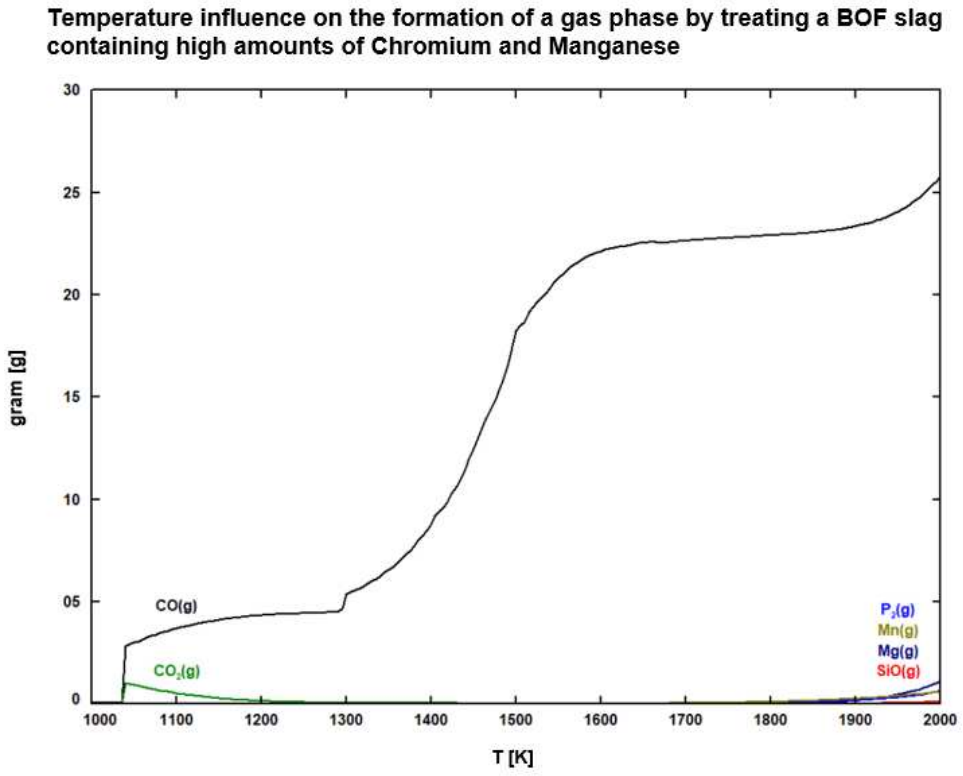

Figure 22: Emergence of the gaseous phase consisting of CO(g), Mg(g), CO_2(g), P_2(g), Mn(g) and SiO(g) (T=1000 – 2000 K)

At a temperature of roughly 1030 K the gasification process begins and the compositions CO(g) and CO_2(g) are formed. Up to a temperature of 1800 K, CO(g) is almost the only occurring gaseous substance in the system, but at 1800 K the amount of Mg(g) and Mn(g) are starting to increase. This very interesting process is shown in detail below in Figure 23.

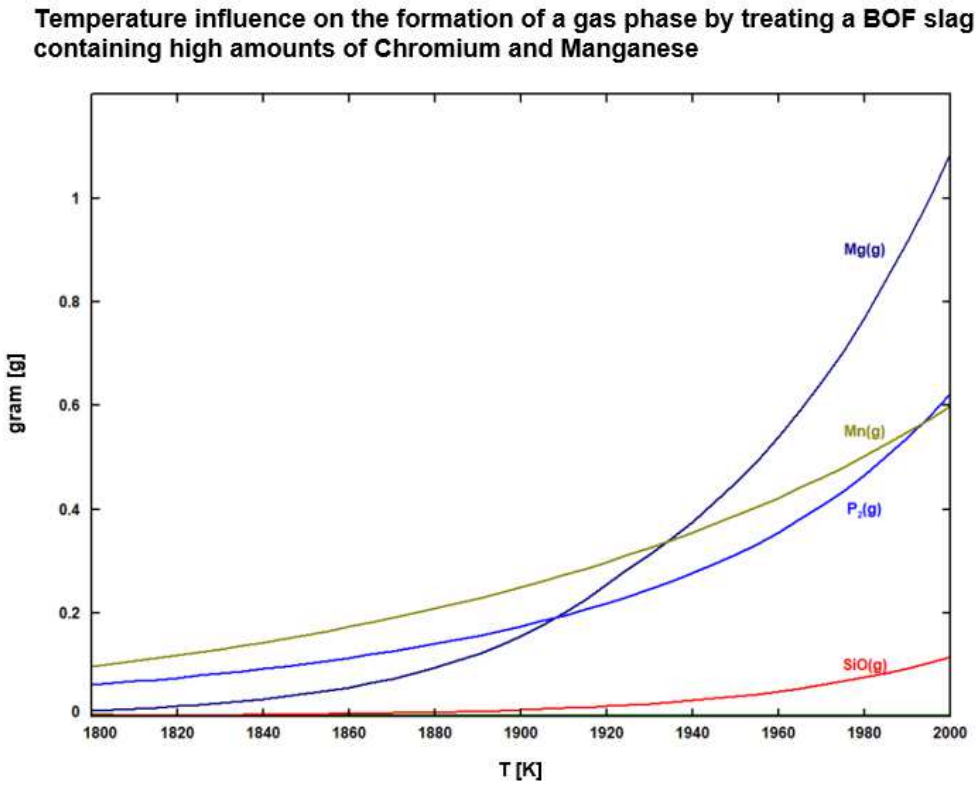

Figure 23: Emergence of CO(g), Mg(g), P_2(g), Mn(g) and SiO(g) (T=1800 - 2000 K)

At a temperature of 1900 K an exponential increase especially of the gaseous Mg can be seen. Also, the gaseous P and Mn rise with an increasing temperature higher than 1800 K. Considering that the input slag mixture included around 12.32 g of P_2O_5, which equals 5.38 g of P and 6.94 g of O, the 0.1745 g of gaseous P, which can be found at 1900 K are only 3.25 % of the input P, which is bound in P_2O_5. The specific analysis of the P distribution will be done in chapter 3.2.1.4, where various P balances will be calculated.

To further understand the occurrence of the different phases, the emerging slag phase in particular is further analyzed individually. By considering every phase and its formation separately, a better understanding also of the whole output system is expected. In Figure 24 the formation of the species of this phase in the temperature window between 1000 and 2000 K is pictured.

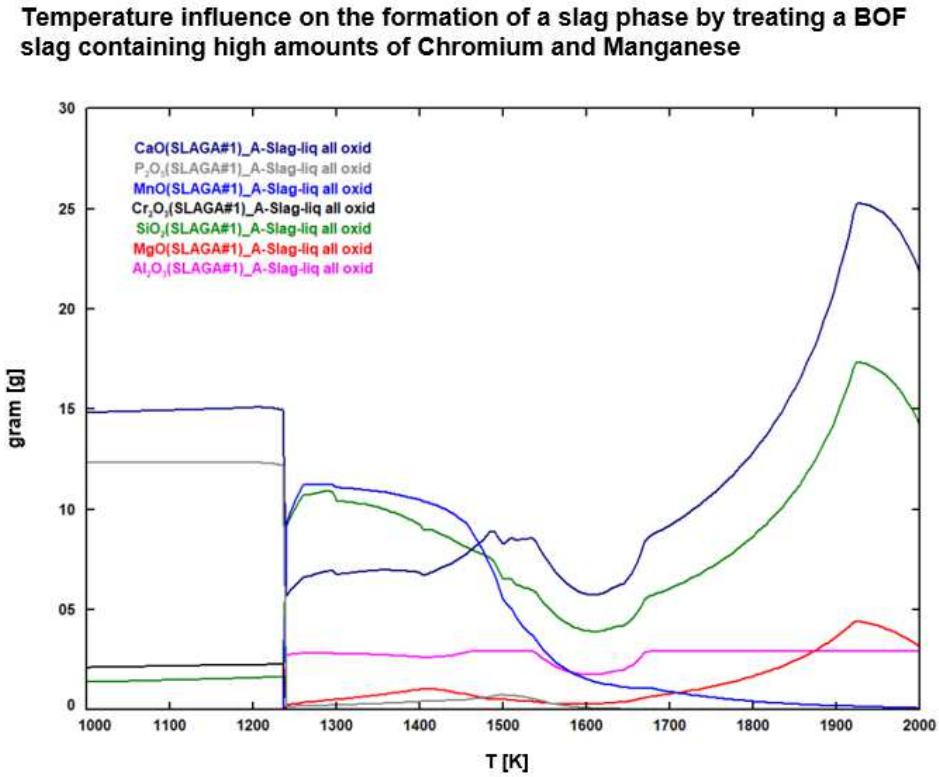

Figure 24: Emergence of the slag phase consisting of CaO, SiO_2, P_2O_5, MnO, MgO, Al_2O_3 and Cr_2O_3 (T=1000 – 2000 K)

The slag phase at 1900 K consists mainly of CaO, SiO_2, Al_2O_3 and MgO and considering the formation of these phases, particularly the temperature of 1238 K seems to be very interesting, which is why the formation of these species in a narrower temperature range is visualized in Figure 25. To increase the visibility of this formation process, the temperature steps of this specific temperature window were reduced to be 1 K.

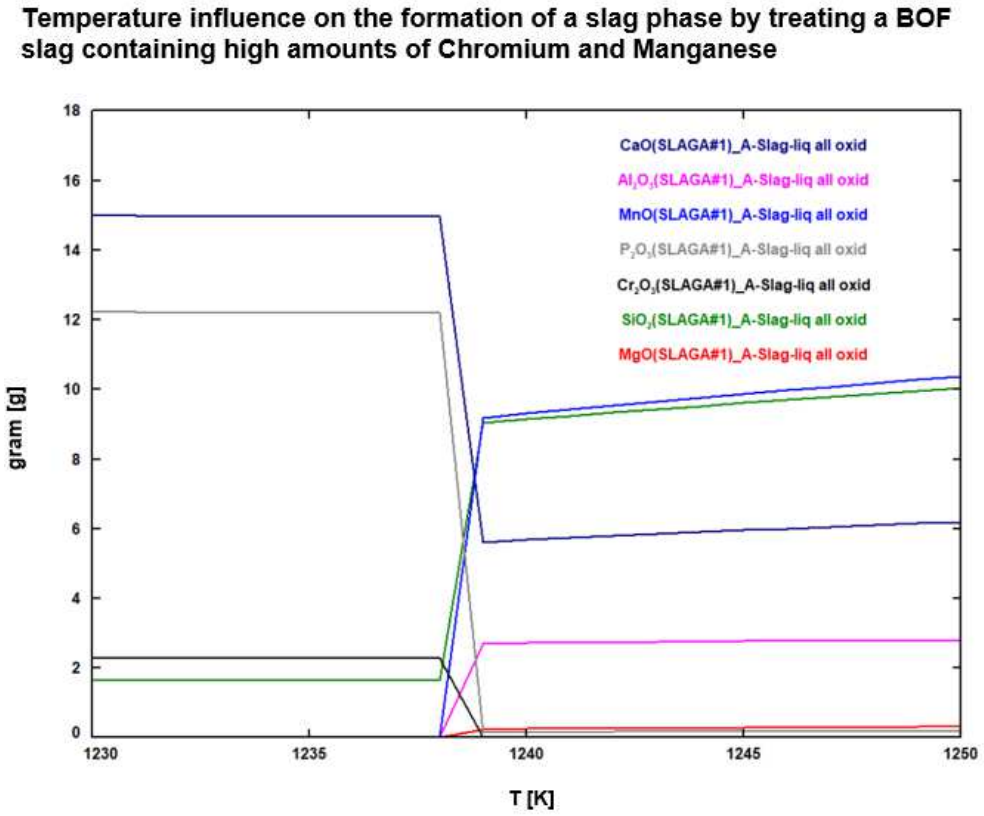

Figure 25: Behavior of the most important species of the slag phase (T=1230 - 1250 K)

In a temperature step of only 1 K, between 1238 K and 1239 K, the slag composition changes from a relatively high P_2O_5 and low SiO_2 slag to a high Si and low P slag. Moreover, in that small temperature window also the amounts of Cr_2O_3 are reduced and the amounts of Al_2O_3 are increased resulting in a typical slag composition consisting mainly of CaO and SiO_2. By conducting further mass- and P balances this transformation point will be highlighted to better understand the path of the specific elements in this system.

The formation of the species, which are constituent parts of the metal phase, is visualized in Figure 26 below. At a temperature of 1900 K, 43.22 g of this liquid metal phase consisting mainly of Fe, Mn, P and Cr occurs binding around 5.2 g of P, which is roughly 96.6 m.% of the input P, which is bound in the form of P_2O_5 in the initial slag mixture. This accumulation of P into the metal phase leads to a low PGD, which lowers the efficiency of the proposed BOFS treatment process and therefore needs to be further understood.

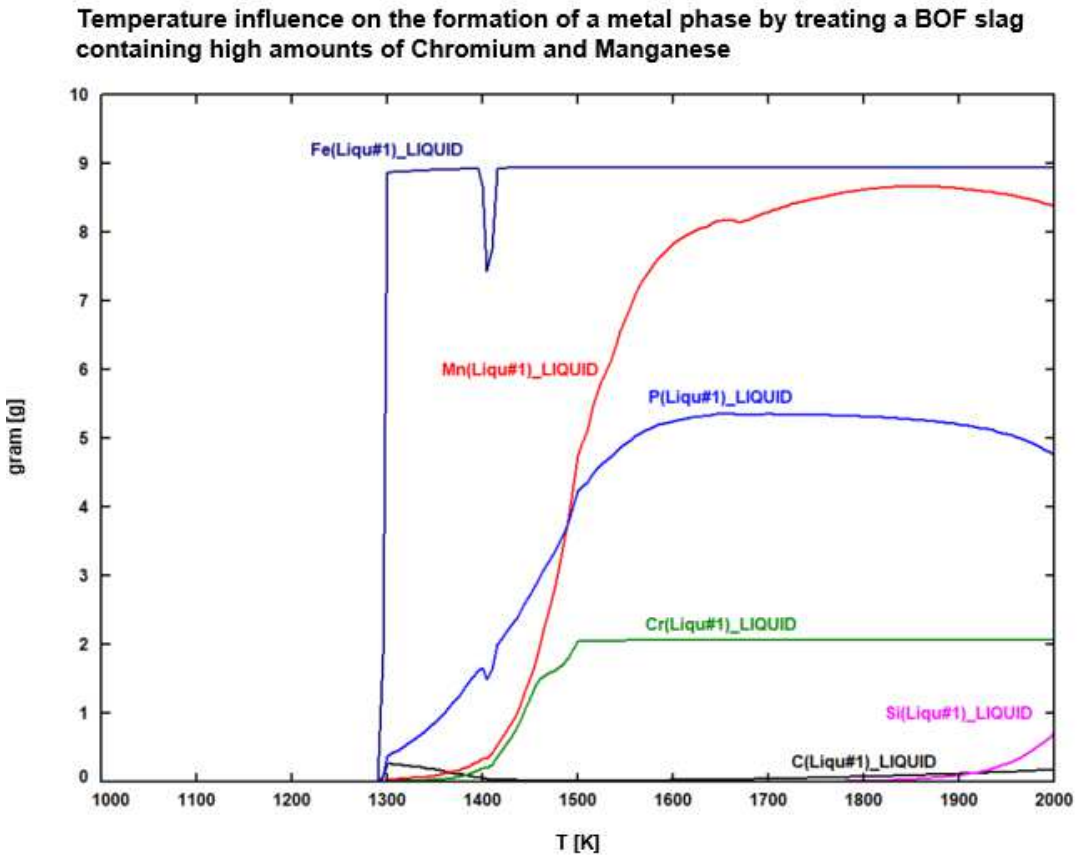

Figure 26: Emergence of the metal phase consisting of Fe(l), Mn(l), P(l), Cr(l) and Si(l) (T=1000 – 2000 K)

At around 1300 K the formation of the metal phase begins and especially an abrupt increase of the liquid Fe species can be identified. At this temperature also the amount of P in the metal phase increases, which stays constant at a temperature higher than 1600 K. At around 1800 K, a slight decrease of the intercalated P can be seen, which is highly interesting. As pictured in Figure 23 the P content in the gas phase starts to increase almost exponentially at 1800 K, which is why the coaction of this gaseous P(g) in the gas phase on the one hand and of the liquid P(l) in the liquid phase needs to be analyzed more precisely. In Figure 27 this decreasing P content in the liquid metal phase and the increasing P content in the gas phase are visualized. Almost no P can be found in any other phase, which is why only the coaction of these two phases is considered with more detail.

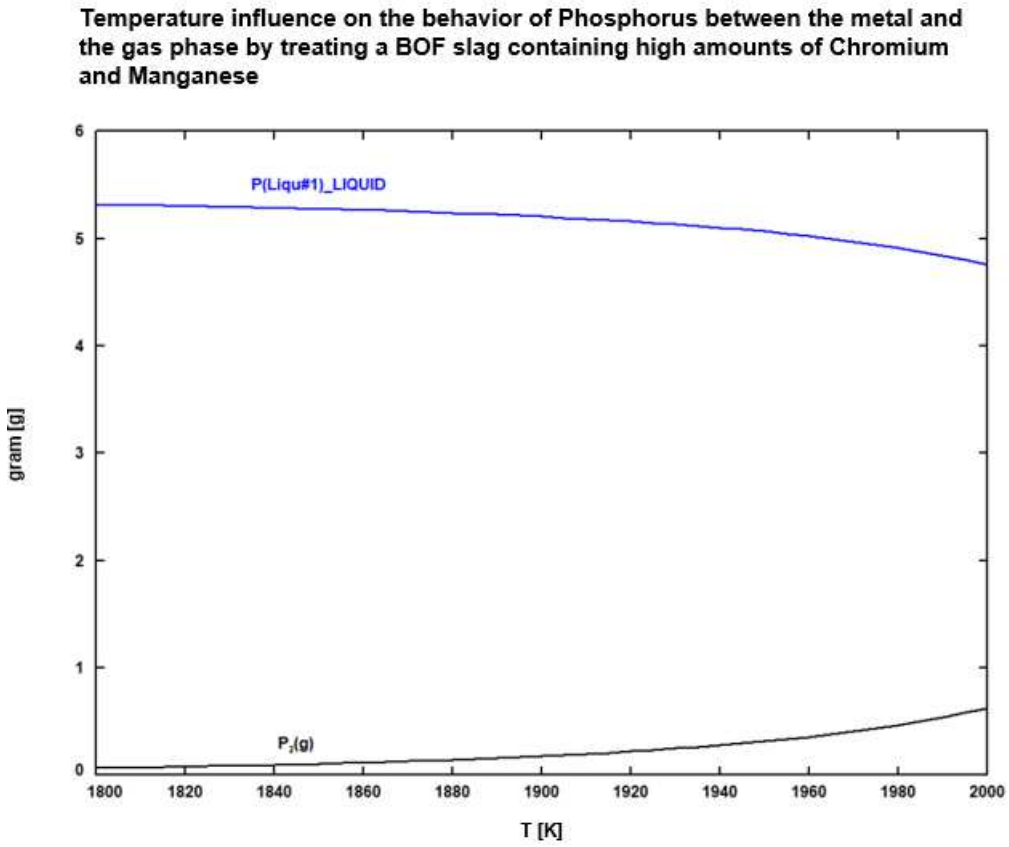

Figure 27: Coaction of the liquid P(l) in the metal phase and the gaseous P(g) in the gas phase (T=1800 - 2000 K)

This interrelation between the two different aggregate states of P is very crucial considering the dephosphorization process of BOFS. The P path with varying Cr and Mn values of the input slag system will be visualized and better understood in chapter 3.2.1.4.

As previously discussed and visualized in Figure 21, in addition to the slag, metal and gas phase also a C_2S / C_3P phase as well as another solid composition, $O_8Ca_3Si_2Mg$, also known as $Ca_3Mg(SiO_4)_2$, were detected in the calculated output species at 1900 K. To further understand the formation process of these phases, their including species in the temperature window between 1000 K and 2000 K are pictured in Figure 28.

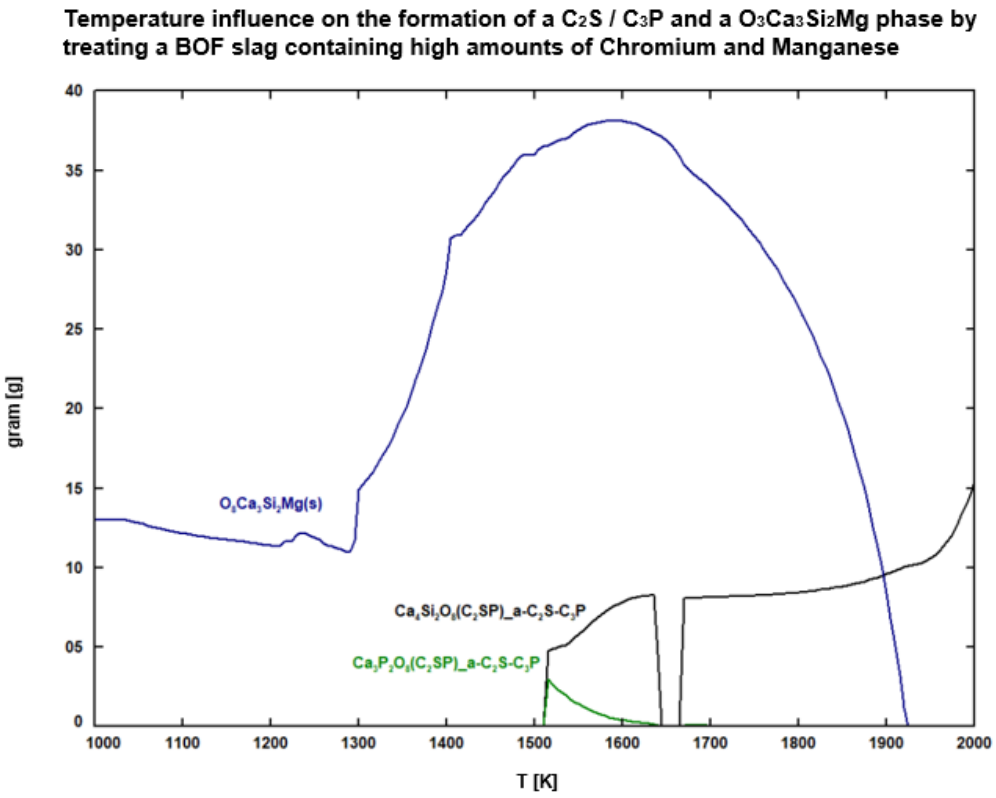

Figure 28: Emergence of the C_2S / C_3P phase and the solid composition $O_8Ca_3Si_2Mg$ (T=1000 – 2000 K)

At around 1500 K the C_2S and C_3P phases start to form. The solid composition $O_8Ca_3Si_2Mg$ ($Ca_3Mg(SiO_4)_2$) was already found below a temperature of 1000 K and this compound increases to a temperature of 1600 K and, after that, its formation starts to decrease. At a temperature higher than 1920 K this phase cannot be detected in the considered system. In addition to this interesting solid composition, also various other compositions like $O_7Ca_2Si_2Mg(s)$,$Mn_2SiO_4(s)$, $O_4CaSiMg(s)$, $CaSiO_3(s)$, $OFe(s)$, $Fe_3C(s)$, $Ca_7P_2Si_2O_{16}(s)$ or $Ca_2SiO_4(s)$, to name a few for example, can be found between the temperature of 1000 K and 2000 K, but these compositions do not occur at the operating temperature of the InduMelt plant (1900 K) and therefore are not further analyzed separately.

In the following chapter 3.2.1.3 various mass balances in the temperature window of 1000 K to 2000 K of the emerging phases are conducted. Thereby, the formation of the respective phases will be better understood and temperature influences will be illustrated. Especially the changing amount of the generated gas phase by altering the temperature will be highlighted.

3.2.1.3 Mass Balances of the Emerging Phases between 1000 K and 2000 K

In total, six mass balances in the temperature range between 1000 K and 2000 K were calculated with temperature steps of 200 K each. The central point of the mass balances is to better understand the temperature influence on the mass distribution of the output phases. The input parameters always stay constant with 100 g of input slag mixture and 50 g of C to ensure a complete reduction, as listed in Table 4, the only changing variable being temperature. Due to the consistency of the input parameters, these are not specifically taken into account when representing the mass balance results. The results of all six mass balances are viewed in Figure 29.

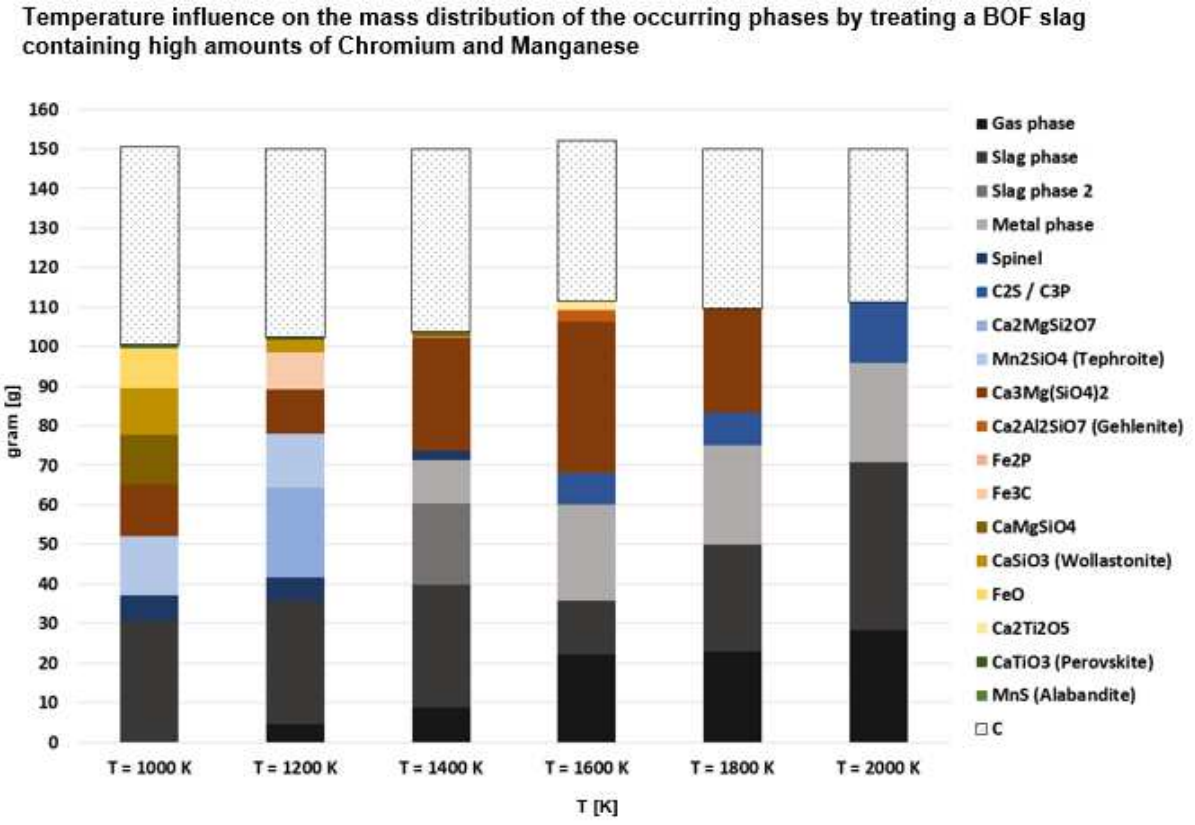

Figure 29: Results of the conducted mass balances on the output side (T=1000 - 2000 K)

This figure gives insights into the development of the composition of the output phases while treating the input slag mixture in the InduMelt plant. The formation of a gaseous phase starts between 1000 K and 1200 K and at 1200 K around 4.5 g of gas consisting only of CO(g) and CO_2(g) has been generated. At a temperature around 1400 K an additional slag phase consisting mostly of 48.6 m.% CaO, 38.8 m.% P_2O_5, 6.7 m.% Cr_2O_3 and 5.5 m.% SiO_2 occurs, which is detached from the initial slag phase. Between 1000 K and 1800 K various solids are formed and dissociated, like $Ca_3Mg(SiO_4)_2$, $CaMgSiO_4$ or $Ca_2MgSi_2O_7$. The previously

mentioned solid compound $O_8Ca_3Si_2Mg$ can also be expressed as $Ca_3Mg(SiO_4)_2$. The amount of generated gas and the formed metal phase increase with increasing temperature. High amounts of the solid compound $Ca_3Mg(SiO_4)_2$ are formed between 1400 K and 1800 K, which reduces the amount of the generated metal phase in this temperature range. Further discussions regarding the influence of the temperature on the composition of the resulting output phases will be done in chapter 4. This Figure 29 underlines the importance of treating the considered system with high temperatures. Thereby, a low formation of the solid compounds and high amounts of gaseous phase emerge.

The behavior of P during carbo-thermal treatment is one of the main areas, which will be analyzed in this thesis. On the one hand, the influence of the temperature on the P distribution between the phases and solid compositions needs to be further understood and on the other hand, the influence of varying input slag compositions like varying Cr and Mn amounts on the P distribution has to be analyzed. In chapter 3.2.1.4 the results of six P balances in the temperature range between 1000 K and 2000 K are revealed, which give a better understanding of how P could behave during this proposed treatment process.

3.2.1.4 Phosphorus Balances of the System between 1000 K and 2000 K

The key element of interest, which is the main parameter for the efficiency of the InduRed treatment process, is P. To better understand its potential occurring phases, formations and inclusions into other compounds, in Figure 30, results of six conducted P balances are overviewed. The input values always stay the same, which is why only the calculated output values are pictured. P can be found in the input slag mixture as a present element of the composition P_2O_5. This composition is a component of the high Cr, Mn and P slag mixture, which arises during the described novel BOFS treatment approach. 12.32 g of P_2O_5 can be found in the input slag mixture, which equals 5.38 g of P and 6.94 g of O. Therefore, the input P amount is 5.38 g, which stays the same in each calculation of simulation A.

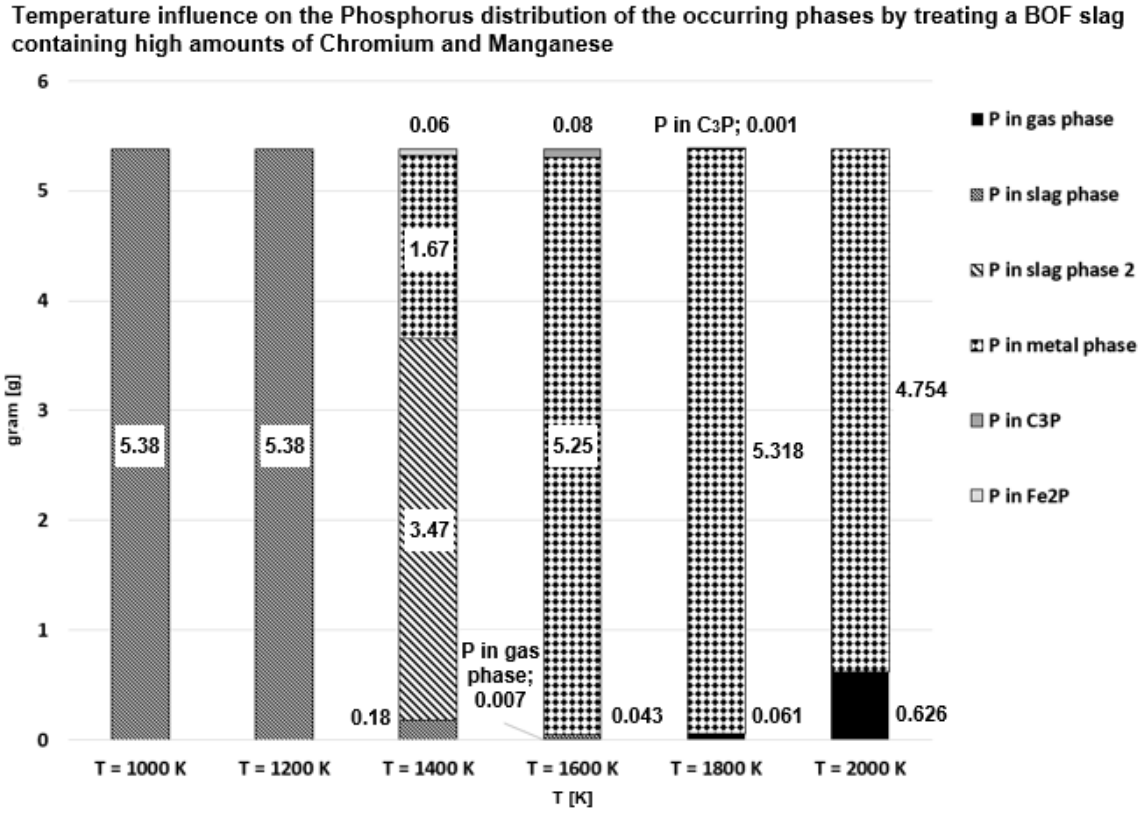

Figure 30: Results of the conducted P balances on the output side (T=1000 - 2000 K)

In Figure 30 it can be seen that between 1200 K and 1400 K the P is starting to be accumulated in the metal phase. At 1600 K minimal amounts of gaseous P already can be identified and with increasing temperature this amount of gaseous P also starts to increase. The temperature strongly depends the behavior of P resulting in an accumulation of P in the metal phase at first and then in the P gasification at a very high temperature. However, the most part of the P can be found in the metal phase at temperatures higher than 1600 K leading to a low PGD, which limits the purpose of the InduRed treatment process. In the considered temperature range also minor P inclusions in the compounds C_3P and Fe_2P can be found, but at the operating temperature of the InduMelt plant (1900 K) these compounds already dissociate and the P is shared between the gaseous and the metal phase. Between 1800 K and 2000 K a strong increase of the gaseous P can be identified, which has already been pictured in Figure 23 and Figure 27.

The inclusion process of P into the metal phase is supposed to depend on the amounts of Cr and Mn in the input slag mixture, which is why in simulation series B these species are altered and their impact on the P distribution is further analyzed.

3.2.2 Results of Simulation Series B

This simulation has the goal to better understand the influence of the amounts of Cr and Mn, which can be found in the input slag mixture, on the proposed treatment process. Therefore, various analyses of the output results have been conducted and the most significant results are overviewed in this chapter. At first, the mass distribution of the emerging phases with changing Cr and Mn amounts is discussed. Then, the P behavior under these specific conditions will be better understood by visualizing the P distribution between the slag, metal and gas phase. Finally, the P activity in dependence of the input slag mixture will be analyzed. The conducted simulations show very interesting results and their findings make for the main points of this thesis. In Figure 31, the influence of Cr and Mn on the distribution of the emerging phases at 1900 K is overviewed.

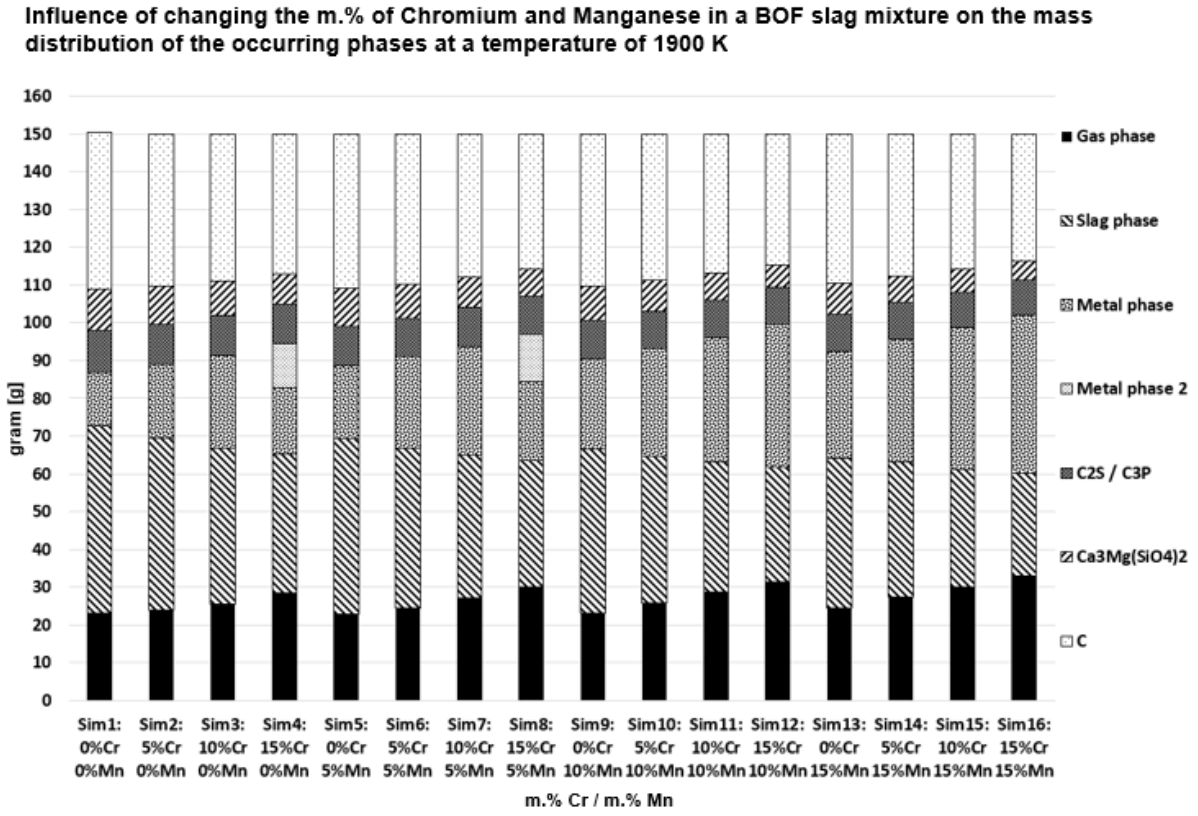

Figure 31: Mass distribution of the emerging phases of simulations 1 to 16 (T=1900 K)

The conducted simulations 1 to 16 have very different input Cr and Mn amounts, which also influences the mass distribution of the phases that occur at a temperature of 1900 K. Considering the gas phase, higher Cr and Mn amounts both increase the formation of gas and also result in a decrease of the occurring slag phase and an increase of the occurring metal phase. In simulation 4 and 8 an additional metal phase occurs, probably due to the high Cr

and low Mn amounts. In simulation 4 the ratio of $\frac{m.\%\ Cr}{m.\%\ Mn}$ is very high with $\frac{15}{0}$ and in simulation 8 this ratio is also quite high with the value 3. This emerging second metal phase in simulation 4 consists of 60.7 m.% Cr, 21.9 m.% Fe, 9.7 m.% P and 6.6 m.% C while the initial metal phase is formed out of 45.3 m.% Cr, 32.3 m.% Fe, 21.0 m.% P and only 0.6 m.% C. Therefore, the novel resulting metal phase in simulation 4 especially tends to bind more C and less P. However, higher Mn amounts, like in simulation 8, lead to another composition of these two metal phases. Here the initial metal phase binds more C and less P and consists of 47.1 m.% Cr, only 21.5 m.% Fe, 13.7 m.% Mn, 11.3 m.% P and 5.3 m.% C while the novel metal phase consists of 40.9 m.% Cr, 23.8 m.% Fe, 15.2 m.% Mn, 16.4 m.% P and 2.9 m.% C.

The interesting behavior of these novel input slag mixtures at 1900 K needs to be further understood and therefore will be analyzed and discussed in chapter 3.3.2.

Due to the changing input masses of Cr and Mn in the course of simulations 1 to 16, also the input amount of P, which is bound in P_2O_5, changes. In simulation 1 the input elementary P is at its highest value with 6.3 g, while in simulation 16 the amount of input P is only 3.7 g. To understand the behavior of P at 1900 K with varying Cr and Mn amounts, mass balances of the P distribution between the metal 1, metal 2 and gas phase have been conducted. The results of these mass balances are visualized in Figure 32. Due to the varying input P amounts, Figure 32 was pictured as specific percentages of the input P.

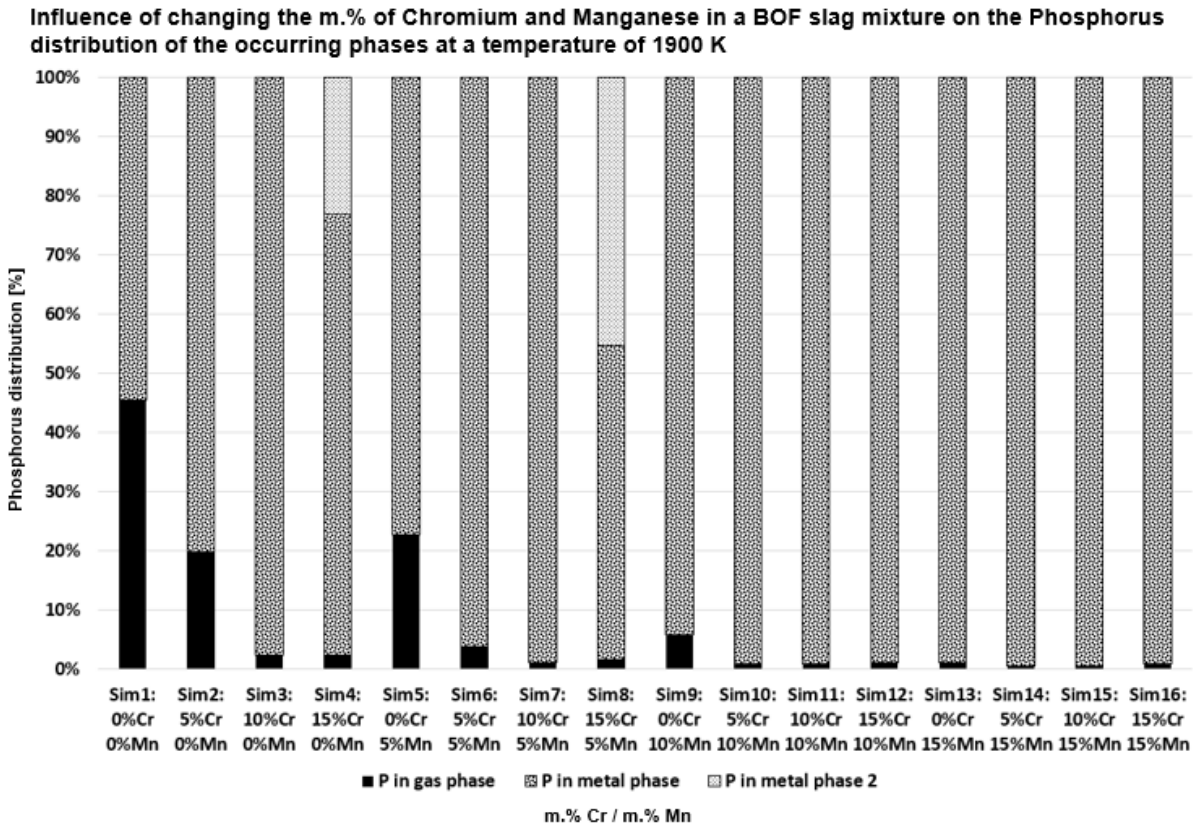

Figure 32: P distribution of simulations 1 to 16 (T=1900 K)

A high influence of Cr and Mn on the P distribution of the gas and metal phase can be seen. Minimal amounts of P below 0.000001 m.% were also found in the C_3P and in the slag phase at 1900 K, but these fractions have no remarkable influence on the mass distribution, which is why they are neglected. In general, lower Cr and Mn amounts lead to a higher PGD, which is supposed to be due to the tendency of Cr and Mn phosphide formation. By comparing simulation 2 with simulation 5 it can be seen that Mn has a higher influence to increase the PGD than Cr. This behavior can also be identified by comparing simulation 3 with simulation 9. Also, by increasing the Cr or the Mn amount in the input mixture from 5 m.% to 10 m.%, the PGD is strongly reduced. By analyzing the findings depicted in Figure 32, which are of interest in the course of this thesis, significant deductions can be made. Further analyzations of the P behavior with changing Cr and Mn amounts will be carried out in chapter 3.3.2.

The tendency of P to be intercalated in the emerging metal phase strongly depends on the effective P activity under the specific process conditions. An analyzation of the P activity in the liquid metal phase in dependency of the input Cr and Mn amounts is expected to result in novel interesting outcomes. In Figure 33 this P activity at a temperature of 1900 K is pictured with varying input elementary Cr and Mn amounts. This analysis of the P activity is crucial for better

understanding the P behavior in the proposed carbo-thermal treatment process regarding the high amounts of P, which is embedded in the metal phase, as described in Figure 32.

Influence of changing the m.% of Chromium and Manganese in a BOF slag mixture on the Phosphorus activity in the occurring liquid metal phase at a temperature of 1900 K

m.% Cr / m. % Mn	0 m.% Mn	5 m.% Mn	10 m.% Mn	15 m.% Mn
0 m.% Cr	Sim 1 0.023047	Sim 5 0.01562	Sim 9 0.0074478	Sim 13 0.0030873
5 m.% Cr	Sim 2 0.014105	Sim 6 0.0058418	Sim 10 0.0026971	Sim 14 0.0019688
10 m.% Cr	Sim 3 0.0045011	Sim 7 0.0028456	Sim 11 0.002324	Sim 15 0.0018749
15 m.% Cr	Sim 4 0.0040699	Sim 8 0.0031877	Sim 12 0.0024858	Sim 16 0.0019605

Figure 33: P activity heat map of the conducted simulations. The values are the activity of P in the liquid metal phase. (T=1900 K)

The P activity heat map shows an increasing P activity in the liquid metal phase with reducing the m.% of Cr and Mn in the input slag. In simulations 4 and 8, two different metal phases occur, but the P activity for both phases was the same in each simulation. The highest P activity was identified in the course of simulation 1 with 0 m.% Cr and 0 m.% Mn. As seen in Figure 32, simulation 1, 2 and 5 have a high PGD, which also correlates with a high P activity in the metal phase, as pictured in Figure 33. By analyzing the exact numbers of the P activity in the liquid metal phase at 1900 K, Mn increases the P activity more than Cr. To justify the theory that Mn has a higher influence on the P activity in the liquid metal phase, which results in a higher PGD, the PGD as well as the P activity in the metal phase are benchmarked in Table 7 and Table 8.

Table 8: Benchmark of the PGD with altering the Cr and Mn amounts in the input slag mixture (T=1900 K)

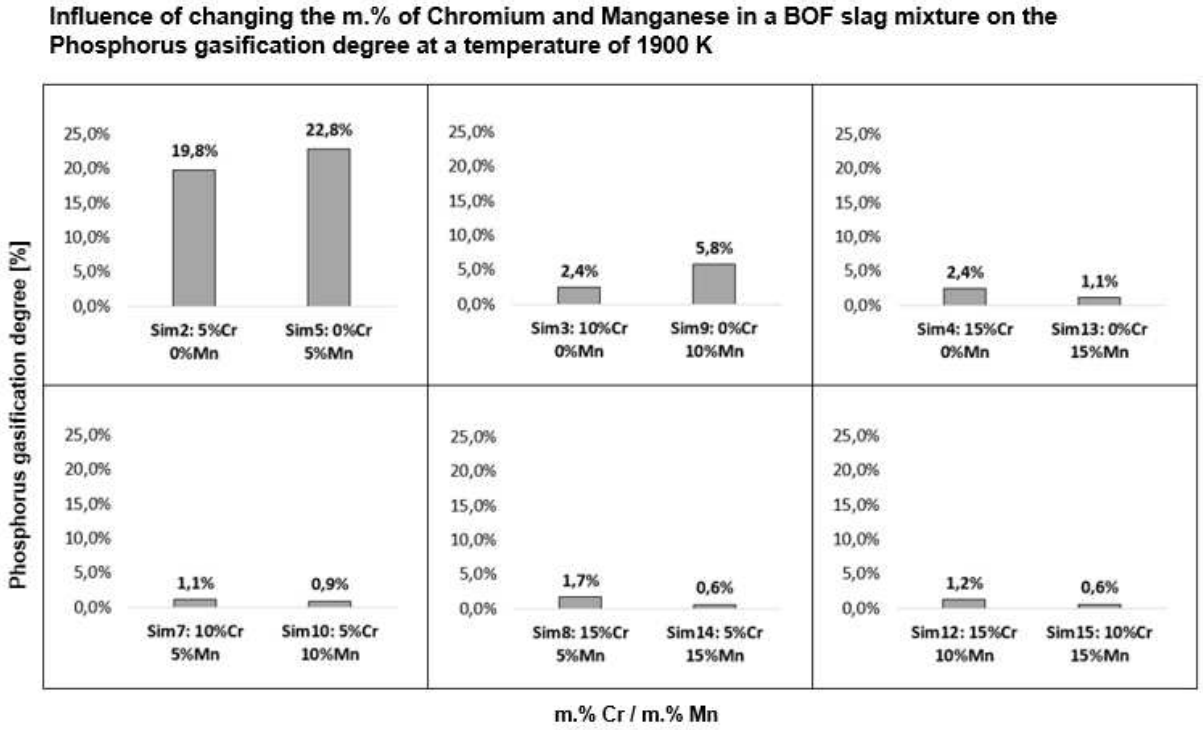

Table 9: Benchmark of the P activity in the emerging liquid metal phase with altering the Cr and Mn amounts in the input slag mixture (T=1900 K)

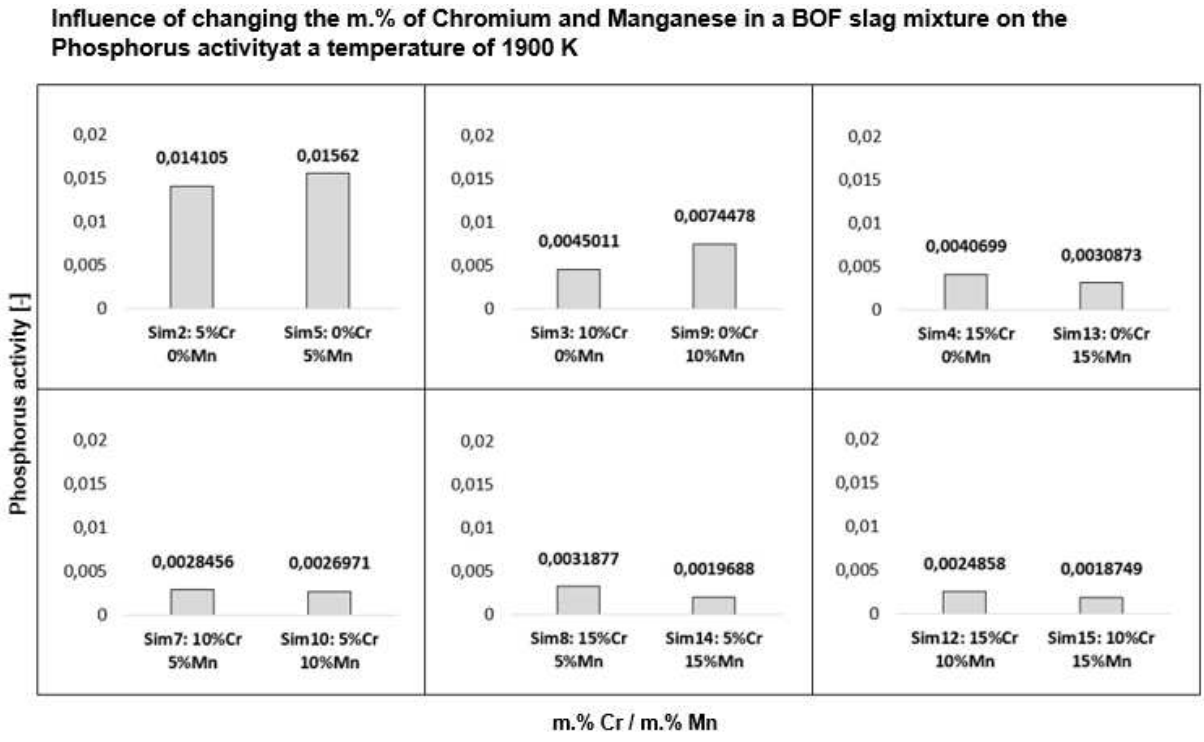

In the course of this benchmark, the input Cr and Mn amounts were compared exclusively, which overviews if rather Cr or Mn have a higher influence on the PGD and the P activity in

the metal phase at 1900 K. The outcomes of this benchmark are overviewed in chapter 3.3.2. Especially in the range of 0 m.% to 10 m.% of the input Cr and Mn amounts, a higher impact of Mn on both the PGD and the P activity in the metal phase can be seen. A change of this behavior occurs at higher Mn amounts than 10 m.%. Also, a strong reduction of the PGD and the P activity in the metal phase can be identified with very high Cr and Mn amounts.

In addition to the key issue of this thesis, which has been analyzed in simulation series B, the basicity of the input slag mixture is supposed to also influence the P distribution and the P activity. This subject will be discussed in simulation series C. The outcome of that analysis is overviewed in the following chapter 3.2.3.

3.2.3 Results of Simulation Series C

In the course of simulation series C in total six simulations with a changing B_2 from 1.0 to 1.5 in 0.1 steps were conducted. Within these simulations a to f, the influence of B_2 on the composition of the accruing phases at the operating temperature of the InduMelt plant (1900 K) will be analyzed. Furthermore, the P distribution at 1900 K in dependency of the changing basicity will be overviewed. Additionally, the emerging P amount in the gas phase and the incorporating P amount in the liquid metal phase by altering the B_2 in the temperature range between 1800 K and 2000 K will be examined. The mass distribution of the occurring phases at 1900 K is viewed in Figure 34.

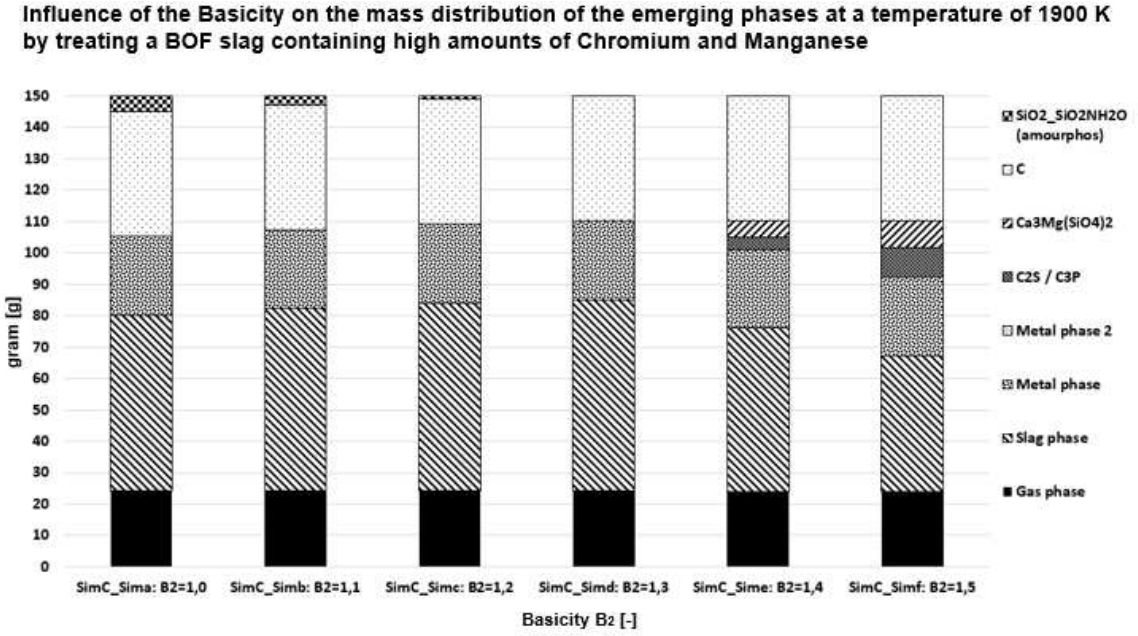

Figure 34: Mass distribution of the emerging phases of simulations a to f (T=1900 K)

Changing the basicity has an influence on the emerging phases at 1900 K, but not specifically on the amount of the formed gas phase. The second metal phase is formed only fractionally with minimal amounts and therefore cannot be identified in Figure 34.

From a B_2 from 1.0 to 1.2 the phase SiO_2_SiO_2nH_2O occurs and from a B_2 above 1.4 a C_2S/C_3P and a $Ca_3Mg(SiO_4)_2$ phase appears, which strongly impacts the amount of the produced slag phase. In the course of the conducted simulations the amount of produced gas and metal phases almost stays constant. The compositions SiO_2_SiO_2nH_2O, C_2S/C_3P and $Ca_3Mg(SiO_4)_2$ seem to mostly arise out of the slag phase. The phase SiO_2_SiO_2nH_2O mostly consists of Si and O and by considering that in this simulation the amount of input SiO_2 was the highest with 26.61 m.% this relatively high SiO_2 amount could lead to the formation of the incubation of H_2O in the input SiO_2 resulting in the phase SiO_2_SiO_2nH_2O. In simulation f the emerging C_2S/C_3P phase consists of 99.99 m.% C_2S ($Ca_4Si_2O_8$), which could be formed due to the high input amounts of CaO in relation to SiO_2. This C_2S phase consists of two times more Ca than Si and therefore higher basicity increases this $\frac{Ca}{Si}$ relation, which could be the main driver for the formation of C_2S.

The analysis of the occurring phases with changing B_2 at 1900 K gives an interesting first insight into the dependency of Ca and Si on the output composition. However, to understand the behavior of P in subject to the B_2, the distribution of that element specifically is analyzed in Figure 35 below. Analyzing each element separately increases the understanding of the formation process in general resulting in potential findings to raise the efficiency of this treatment process.

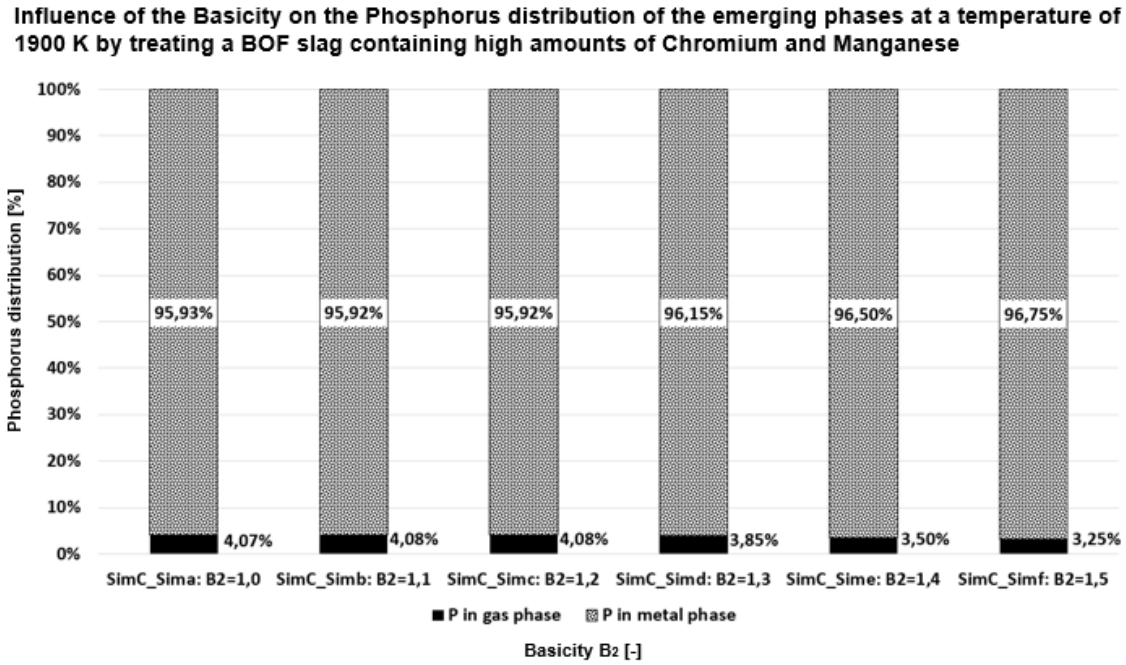

Figure 35: P distribution of simulations a to f (T=1900 K)

In each simulation, 12.32 m.% P_2O_5 was chosen as an input value resulting in 5.38 g of input P, respectively. Basically, the B_2 has no high influence on the P behavior in the analyzed system. Though, a relatively low B_2 tends to a reduced incubation of P in the metal phase, which results in a slight increase of the PGD. In simulation f, which has the highest B_2 with the value 1.5, only 0.1745 g of P were gasified and in simulation a, which has the lowest B_2 with the value 1.0, around 0.21897 g of gaseous P emerged at 1900 K. In a manner of speaking, by reducing the B_2 from 1.5 to 1.0 an increase of 0.82 % of the P gasification rate is supposed to be achieved.

An analysis of the P distribution between the emerging phases at 1900 K shows that the P is only shared between the gas and the metal phase. A reduction in B_2 therefore leads to a minimal increase of the formation of gaseous P. As previously discussed in chapter 3.2.1, the PGD highly depends of the temperature and specifically temperatures above 1800 K lead to a higher amount of gasified P. This finding leads to pose the question if by increasing the B_2 and the temperature also more P will be gasified. To analyze this hypothesis, in Figure 36 the coaction between the gaseous P and the P, which is embedded in the metal phase, is pictured.

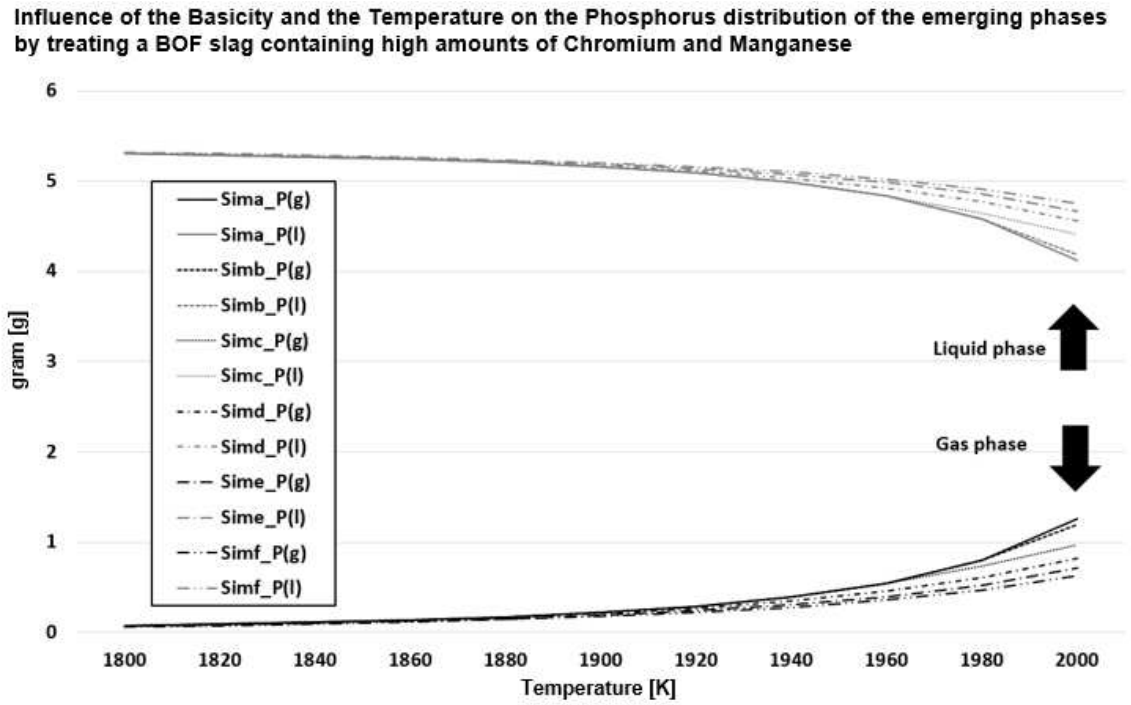

Figure 36: Coaction of the liquid P(l) in the metal phase and the gaseous P(g) in the gas phase (T=1800 - 2000 K)

In Figure 36 the input amount of P in each simulation was 5.38 g and by analyzing the output figure, the hypothesis, that the temperature increases the PGD can be confirmed. Increasing temperature leads to also a raise in the generated gaseous P and a reduction in the P in the metal phase, as also mentioned in the course of simulation A. In addition, the trend that a low B_2 increases the PGD is also shown by increasing the temperature. In every analyzed temperature step, the input slag mixture with a low B_2 shows higher amounts of gasified P than the mixture with a high B_2.

The results of the six conducted simulations a to f within simulation series C show interesting results in the area of treating various slags with specifically different CaO and SiO_2 amounts.

First results have been slightly discussed and further analyzations of the output results will be carried out in chapter 3.3.3.

3.3 Summary of the Simulation Findings

This chapter overviews and analyzes the most important findings, which can be derived based on the evaluated results of simulation series A, B and C. The simulations all have been carried out in the equilib module of FactSage. No simulation errors under the analyzed conditions were

spotted. Mass balances and P balances show that the input mass amounts can also be found in the output phases, which is an indicator regarding the trueness of the simulation. However, to measure the accuracy of any kind of simulation, a comparison with real measured experimental data is needed. The simulations conducted in the course of this master's thesis will be compared in the near future with experimental data, which gives an insight into the precision of the simulation input parameters and the simulation results. Based on previous experiments with the InduMelt plant and based on current knowledge regarding the dephosphorization process of BOFS the results of the simulations seem to be plausible. The following chapters 3.3.1, 3.3.2 and 3.3.3 examine the findings of each simulation.

3.3.1 Findings of Simulation Series A

The goal of simulation series A is to understand the temperature dependency on the carbo-thermal treatment of the novel emerging slag mixture in the InduMelt plant. With a B_2 of 1.5 in this slag mixture the amount of CaO in m.% is very high with 31.92 g. In total 100 g of slag mixture and 50 g of pure C were used as input values in the course of this simulation series A. In chapter 3.2.1 the results of this simulation are overviewed and first findings are shortly discussed. The temperature of 1900 K is crucial in each simulation because this is the maximum of the practically used temperature of the InduMelt plant.

In Table 7 the resulting phases at 1900 K are overviewed, which gives a better understanding of the behavior of the elements during the InduMelt treatment method. In total, three phases can be identified, a CO-rich gas phase, a CaO- and SiO_2-rich slag phase and a Fe-, Cr-, Mn- and P-rich metal phase. At this temperature a strong intercalation of P into the metal phase resulting in a low P gasification rate of only 3.25 % can be identified. The efficiency of the InduMelt treatment process is based on the gaseous detachment of P out of the system and a low P gasification questions the purpose of this treatment method. Therefore, the P behavior in this slag system has gotten a lot of attention in this thesis and is analyzed in regard to a changing temperature, a changing input slag mixture and a changing B_2 of the slag system. A mass balance of the input and output phases shows that additionally, at 1900 K, a C_2S / C_3P phase and another solid composition consisting mainly of Ca and Si and low amounts of Mg can be identified. A detailed investigation of the C_2S / C_3P phase shows, that this phase consists of 99.996 m.% C_2S, which is why the C_3P phase and the P intercalation in that phase are negligible. The solid composition $O_8Ca_3Si_2Mg$, also described as $Ca_3Mg(SiO_4)_2$, has a mass of 8.36 g, which is around 5.57 m.% of the input mixture. No specific name for that composition can be found in FactSage, but by further literature research the name "Merwinite"

for this composition can be found, which is also consistent with the analyzations by Ponak et.al. [19, 29]

Merwinite needs around 35.5 m.% of SiO_2, 49.96 m.% of CaO and 11.62 m.% of MgO to be formed and it can be found in the analyzed slag system also below a temperature of 1000 K and up to a temperature of 1920 K. It is a solid composition and it is possible, that this composition can be found scattered in the output slag mixture due to its density of 3.14 $\frac{g}{ml}$ at 1900 K. The most important species of the emerging slag at 1900 K have a density between 3.35 $\frac{g}{ml}$ (CaO) and 2.65 $\frac{g}{ml}$ (SiO_2), which is why Merwinite could be integrated into this slag mixture at 1900 K.

The emerging C_2S phase weighs 9.57 g at 1900 K, which is 6.38 m.% of the input slag mixture. C_2S is also known as $Ca_4Si_2O_8$ and by looking at that chemical formula, around two times more Ca than Si are needed so that C_2S can be formed. A higher B_2 also indicates a higher relation of CaO in regard to SiO_2, which could promote the formation of C_2S. The density of this specific phase strongly depends on the particular phase of C_2S, but at a temperature of 1900 K the $\propto -hexagonal$ phase of C_2S is existent. FactSage does not give a specific insight into the density of C_2S, but in recent literature a density of $\propto -C_2S$ of around 2.97 $\frac{g}{ml}$ can be found. The behavior of C_2S during heating and cooling processes is not perfectly illustrated by current researchers and especially the volume change of C_2S between 763 K and 1450 K is an area that needs further experiments and simulations to be scientifically understood. This master's thesis however does not focus on the C_2S phase, which is why this phase is not further analyzed in detail. [19, 29]

Considering that the density of the output slag mixture at 1900 K is between 2.65 and 3.35 $\frac{g}{ml}$, the enclosure of Merwinite with a density of 3.14 $\frac{g}{ml}$ and C_2S with a density of 2.97 $\frac{g}{ml}$ is very likely. By treating this input BOFS mixture in the InduMelt plant in total three phases, a gas phase, a liquid metal phase and a liquid slag phase with partly scattered pieces of solid C_2S and solid Merwinite could potentially be found.

To better understand the influence of the temperature on the formation of the gas, metal, slag and the remaining solid phases, in Figure 22 the emergence of the gas phase, in Figure 24 the formation of the slag phase and in Figure 26 the occurrence of the metal phase, are pictured. A strong temperature dependency in the considered temperature window between 1000 K and 2000 K of all phases can be identified. Figure 22 states, that at a temperature of 1030 K the gasification process begins with the first emergence of gaseous CO and CO_2. Due to the Boudouard reaction between the gaseous CO and CO_2 phase, increasing temperature leads

to the occurrence of predominantly CO(g). The Boudouard reaction is described in formula (3.1) below.

Boudouard reaction $$CO_2(g) + C(s) \leftrightarrow 2\,CO(g) \quad (3.1)$$

An increasing temperature reduces the formation of CO_2(g) and increases the formation of CO(g), which takes place in the analyzed system in the temperature range between 1030 K and 1400 K resulting in the strong enrichment of CO(g) in the output gas phase.

In Figure 22 the gasification process of P_2(g), Mn(g), Mg(g) and SiO(g) tends to take place at very high temperatures above 1800 K, which is why this specific gasification of P, Mn, Mg and SiO is exclusively visualized in Figure 23. The gaseous phases of Mg, Mn, P_2 and SiO almost exponentially increase by raising the temperature from 1800 K to 2000 K. As viewed in Table 7, most of the P can be found in the metal phase and only minimal amounts of P were gasified. By taking into consideration that the input value of P is 5.38 g and only 0.17 g of P were gasified at 1900 K, the gasification degree is only 3.25 % at 1900 K. However, due to the consistent input P amounts, the increase in gaseous P has to lead to a decrease of P in another phase. By analyzing the coaction between the P, which is embedded in the metal phase, and the gaseous P, the increasing gasification of P leads to a reduction of the P in the metal phase. As pictured in Figure 27, P is only distributed between the gas and the metal phase and an increasing temperature above 1800 K leads to a higher PGD by removing P from the metal phase. FactSage does not show a specific Fe-P phase that occurs due to the inclusion of P in the metal phase at this temperature, but research conducted by Matinde et.al. states, that an Fe-P alloy is formed by reducing sewage sludge, which contains amounts of Fe oxide. [41]

As analyzed by Ponak et.al., during carbo-thermal treatment of BOFS the formation of Fe-P phases is supposed to take place at the time when the liquid Fe from the metal phase and the gaseous P convene. Therefore, this P inclusion process can be described by the following reactions (3.2), (3.3) and (3.4).

Dissolution of gaseous P into liquid Fe $$P_2(g) \leftrightarrow 2\,P(l) \quad (3.2)$$

Formation of the Fe phosphide out of P(l) $$x * Fe(l) + y * P(l) \leftrightarrow Fe_xP_y(l) \quad (3.3)$$

Formation of the Fe phosphide out of P_2(g) $$x * Fe(l) + y * P_2(g) \leftrightarrow Fe_xP_{2y}(l) \quad (3.4)$$

This formation process of Fe phosphides out of gaseous P also explains the influence of the Fe amount on the development of Fe phosphides, as discussed by Nakase et.al. [30]

In addition to the metal and gas phase, also the emergence of the slag phase shows an interesting behavior especially at the temperature difference from 1238 K to 1239 K. As pictured in Figure 25 in only a minimal temperature difference of 1 K the slag composition

enormously changes from a CaO- and P_2O_5-rich slag to a MnO- and SiO_2-rich slag. This also comes along with a change in every phase, as viewed in Figure 29, where between 1200 K and 1400 K another slag phase, which encloses the P_2O_5 from the initial slag phase, is formed. This also explains why the amount of gasified P and P, which is embedded in the metal phase, do not change dramatically. To sum this up, between 1238 K and 1239 K the initial slag phase is split into two separate slag phases, as can be described in Figure 37 below.

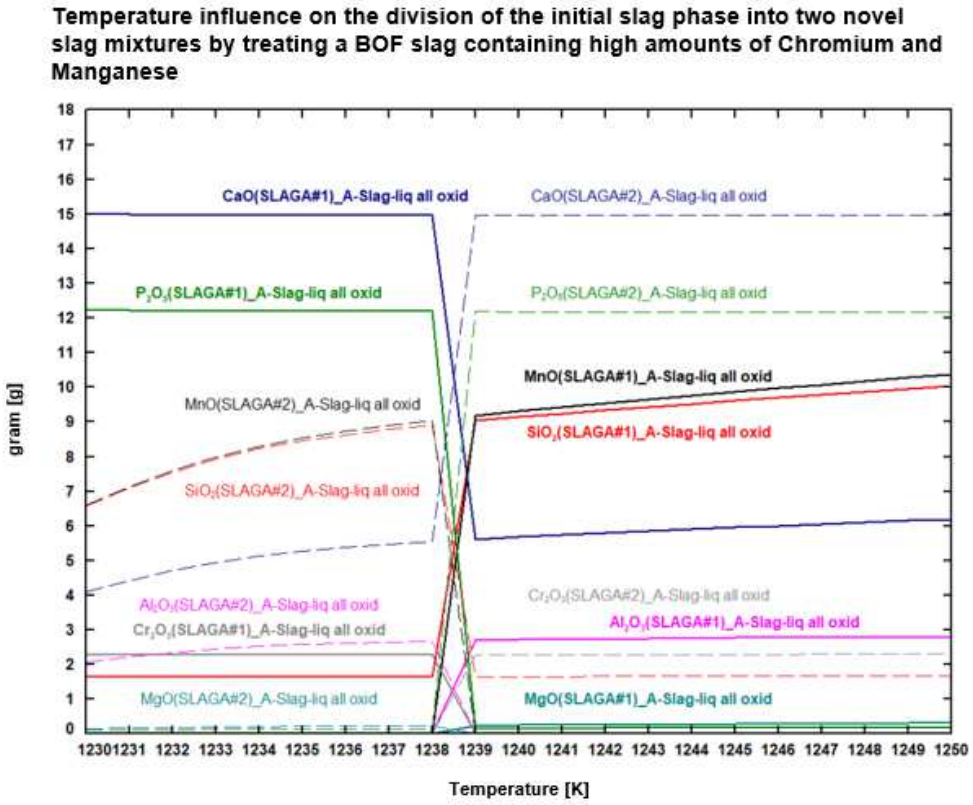

Figure 37: Emergence of a second slag phase (T=1230 - 1250 K)

The slag system changes between 1238 K and 1239 K resulting in the formation of two slags with different compositions. The initial CaO-, P_2O_5-, Cr_2O_3-, and SiO_2-rich slag changes into a MnO-, SiO_2-, CaO- and Al_2O_3-rich slag and the novel second slag system binds the remaining amount of CaO, P_2O_5 and Cr_2O_3. However, these two slag phases consist of the same compositions and between this minimal temperature difference also the density of these compositions does not change, which is why the slag system after 1239 K could be a mixture of these two slag phases.

In addition to the slag and gas phase, also the emerging metal phase is described in Figure 26. The melting point of Fe is around 1295 K and simultaneously with the emergence of the liquid metal phase, which consists mainly of Fe, also the amount of P in this metal phase increases. To further understand the P path during the heating process, in Figure 30 the P

distribution between the gas phase, both slag phases, the metal phase and the C_3P and Fe_2P phase is shown. With the emergence of the liquid Fe phase at 1295 K the amount of P from the slag phase is reduced and more P is accumulated into the liquid metal melt. At 1400 K relatively high amounts of 0.18 g of P can also be found in the C_3P phase and also the formation of a Fe_2P phase can be identified. With an increasing temperature more P occurs in the metal phase, but at 1800 K the gasification process of P begins, which reduces the amount of P in the metal melt and increases the amount of gasified P. Again, the big increase in the gasified P at temperatures higher than 1800 K has to be accentuated.

Due to the relatively high amounts of Cr and Mn in the initial BOFS system an alteration of these elementary amounts on the PGD and the P activity in the liquid metal phase has been conducted within simulation series B. Sixteen simulations with varying Cr- and Mn-amounts in the input slag system have been conducted, as stated in Table 5. These simulations lead to interesting findings in the treatment of Cr- and Mn-rich slags and the most important outcomes are discussed in the following chapter 3.3.2.

3.3.2 Findings of Simulation Series B

The key area of this master`s thesis is to better understand the impact of changing Cr and Mn amounts in the input slag mixture on the efficiency of the proposed carbo-thermal treatment process. Recent literature research conducted in chapter 2.5 states that by increasing the Cr amount, the activity of P almost stays constant, as pictured in Figure 14 and Figure 16 and by increasing the Mn amount the activity of P minimally decreases, as viewed in Figure 17. In general, both increasing Cr and Mn amounts lead to either no change, or a slight decrease, in the P activity in a liquid Fe melt. To understand this hypothesis for the proposed slag mixture, which is discussed in this thesis, in total 16 simulations, each with a different amount of Cr and Mn in the input mixture, in the range between 0 m.% and 15 m.% in 5 m.% steps have been carried out. The results of these simulations are overviewed in chapter 3.2.2 and the most important findings derived out of them will be investigated in this chapter.

The mass distribution of the occurring phases at 1900 K, as seen in Figure 31, gives a first insight into the impact of Cr and Mn on the output phase system. A dependency of the amount of Cr and Mn especially on the amount of generated gas, slag and metal can be identified. In simulation 1 with 0 m.% Cr and 0 m.% Mn a low amount of gas and metal and a high amount of slag occurs at 1900 K and in simulation 16 with 15 m.% Cr and 15 m.% Mn relatively high amounts of gas and metal are generated which reduces the mass of generated slag. The C_2S / C_3P phase and the $Ca_3Mg(SiO_4)_2$ phase are not particularly influenced by the amount of

Cr and Mn. As viewed in Figure 31, simulations 4 and 8 show the emergence of a second metal phase at 1900 K. The initial metal phases of simulation 4 and 8 and the additionally emerging metal phases are overviewed in Table 10.

Table 10: Composition of both metal phases in simulations 4 and 8 (T=1900 K)

Species	**Simulation 4: 15 m.% Cr / 0 m.% Mn**		**Simulation 8: 15 m.% Cr / 5 m.% Mn**	
[-]	**Initial metal phase [m.%]**	**Additional metal phase [m.%]**	**Initial metal phase [m.%]**	**Additional metal phase [m.%]**
Fe	32.30	21.89	21.55	23.86
Cr	45.32	60.76	47.12	40.94
Mn	0.00	0.00	13.78	15.21
P	21.09	9.70	11.38	16.41
C	0.60	6.61	5.00	2.00
total	99.31	98.96	98.83	98.42

By analyzing the density of the components of the metal phases, no density difference in the initial and the additional metal phase can be identified, which could also lead to the development of a holistic metal phase system consisting of a mixture of both phases. The additional metal phase indeed consists of the same elements, but the mass distribution in relation to the initial metal phase of these elements changes. Especially the amount of P in the second metal phase is only half that of the initial metal phase in the course of simulation 4. Moreover, the C and the Cr amount in the novel metal melt are higher than in the previous metal phase. Simulation 8 shows a different behavior because the extra metal melt consists of more P and more Mn. The amounts of Cr and of C are reduced in comparison to the previous metal phase. To conclude, a very high ratio of $\frac{m.\%\ Cr}{m.\%\ Mn}$, as analyzed in simulation 4, leads to the formation of a P-, Cr- and Fe-rich alloy with only minimal amounts of C and an additional Cr-, Fe-rich alloy with lower amounts of P and around 6.6 m.% more C. By increasing the Mn amount in the input slag mixture, two metal phases, one consisting mostly of Cr, Fe, Mn and P, and another one with lower Cr and C, but higher P and Mn amounts are developed at 1900 K. Most of the P in the analyzed system is shared between these two metal phases.

As P being the element, which is of highest interest in this thesis, a P balance at 1900 K of simulations 1 to 16 shows highly interesting results regarding the P distribution between the gas and the metal phases. In Figure 32 a strong influence of the slag composition on the P

distribution can be seen. Especially in case of minimal Cr and Mn amounts in the input slag system, like in simulation 1 with 0 m.% Cr and 0 m.% Mn, almost half of the input P is gasified already at 1900 K. On the other hand, in simulation 16, with very high amounts of Cr and Mn, only a fraction of P is gasified resulting in a high P metal alloy. To better compare the influences of Cr and Mn on the PGD, in Table 8 a benchmark with particular amounts of input Cr and Mn give a better understanding, which of these two elements has a higher impact on the behavior of P. In terms of minimal amounts of up to 5 m.%, Mn reduces the PGD to 22.8 %, while Cr lowers the P gasification rate to only 19.8 %. By increasing the input m.% of Cr or Mn up to 10 m.%, Mn still leads to a higher PGD and Cr reduces the P gasification down to only 2.4%, which is less than half of the PGD by adding only Mn. However, considering very high amounts of Cr and Mn, like 15 m.% in simulation 4 and 13, Cr leads to a higher PGD. By analyzing both the addition of Cr and Mn in the input slag mixture on the P behavior, all simulations with over 10 m.% of one of these elements show a PGD below 2%. However, the PGD of the conducted simulations are lower than in previously conducted experiments in treating a similar high Cr and Mn BOFS by Ponak et.al. To further understand the behavior of this treatment method, also considering kinetic effects is recommended to be taken into account.

In a nutshell two findings can be exemplified:

- The lower the amounts of both Cr and Mn in the input slag mixture, the higher the PGD.
- In a case of very low amounts of up to 5 m.% of Cr or Mn, Mn tends to lead to a higher PGD stating a stronger interaction between P and Cr than between P and Mn.

To better understand the phosphide formation process in the liquid metal phase, the P activity in that phase is an indicator for the equilibrium constant for the Fe phosphide formation, which was previously mentioned in equation (3.3). For this equation, the equilibrium constant can be described as the ratio of the activities of Fe_xP_y, Fe and P, as viewed in equation (3.5).

Equilibrium constant for the formation of Fe phosphide

$$K = \frac{a(Fe_xP_y(l))}{a\left(P(l)\right)^y * a(Fe(l))^x} \tag{3.5}$$

By analyzing equation (3.5), a strong influence of the activities of the liquid Fe and the P in the metal phase on the formation of Fe phosphides can be seen. Higher activities of Fe and P in the liquid melt lead to a lower equilibrium constant of reaction (3.3), which shifts the favored composition on the right side of the equation resulting in a stronger formation of the product Fe phosphide phase. FactSage, unfortunately, does not give a clear insight into the exact chemical compounds of the liquid metal phase in the analyzed temperature window and only shows the main existing elements in this liquid metal phase, which is why the compounds Fe_xP_y cannot be found in the output mixture of the metal phase.

However, the P activity in the liquid metal phase indicates where the equilibrium of equation (3.5) could tend to be, which is why the activities of P in the liquid metal melt with changing Cr and Mn amounts are benchmarked in Figure 33. An increasing P activity in the liquid metal melt with reducing Cr and Mn amounts can be detected. Also, Mn tends to have a slightly higher influence on the P(l) activity until the m.% of Mn are increased over 10 m.%. The lowest P activity can be found in simulation 16 with the highest m.% of Cr and Mn.

In general, simulation B results in interesting findings regarding the interaction between P, Mn and Cr in the analyzed output phases and the influence of a changing input slag mixture on the P distribution and, especially the PGD. In addition to analyzing the impact of changing Cr and Mn on the simulated output phases, also a varying B_2 from 1.0 to 1.5 of the initial input slag mixture was analyzed in the course of simulation series C. The findings derived are described in chapter 3.3.3.

3.3.3 Findings of Simulation Series C

The goal of this simulation series is to analyze, if the basicity, B_2, of the input slag mixture influences the distribution of the emerging phases at 1900 K and the P distribution between the occurring liquid metal phase and the gaseous phase. Therefore, the B_2 of the initial input slag mixture was altered from 1.0 up to 1.5 in 0.1 steps resulting in a total of six simulations.

By examining the mass distribution of the emerging phases at 1900 K, as pictured in Figure 34, a basicity above 1.4 leads to a reduction of the slag phase and the formation of a solid C_2S / C_3P phase and a solid $Ca_3Mg(SiO_4)_2$ phase (also known as Merwinite). The emergence of these two phases has been studied in chapter 3.3.1. The formation of these two phases is supposed to be mainly influenced by the higher ratio of Ca to Si due to the increasing B_2. The C_2S / C_3P phase consists of more than 99.99 m.% of C_2S ($Ca_4Si_2O_8$) and this composition tends to be formed by a minimal ratio of $\frac{Ca}{Si}$ of $\frac{2}{1}$ and so a higher B_2 is potentially the main driver for the emergence of that compound. For the formation of merwinite the ratio of $\frac{Ca}{Si}$ only needs to be $\frac{3}{2}$, which can also be reached with a lower basicity of around 1.4. Therefore, at B_2=1.4 the relation of $\frac{Merwinite}{C_2S}$ is also slightly higher than at B_2=1.5. In Figure 34 no strong influence of the basicity on the emerging gas phase is identified resulting in the thought that the basicity also has no noticeable impact on the PGD. To look at the P distribution at 1900 K in more detail, in Figure 35 the P appearance at 1900 K can be identified. At the temperature of 1900 K and the considered input mixture a relatively low PGD between 3.25 m.% and 4.08 m.% by changing the basicity between 1.0 to 1.5 can be seen. Basically,

increasing the B_2 leads to a slightly lower PGD, which results in a higher P inclusion in the liquid metal phase. Due to the previously discussed finding, that an increasing temperature leads to a higher PGD, in Figure 36 the temperature influence on the P share between the gas and metal phase in the temperature range between 1800 K and 2000 K is pictured. A huge increase in the amount of generated gaseous P and a decrease in the P, which was enclaved in the metal phase, is stated. A reducing B_2 value also leads to a higher PGD.

Based on the mentioned findings out of the conducted simulations, the results of the literature research and these simulations are compared in the following chapter 4. Additionally, previously conducted practical experiments treating a similar BOFS composition by Ponak et.al. are also considered and benchmarked with the simulation results. The most important findings and critical trends are underlined in chapter 4.2.

4 Interpretation and Conclusions

This chapter has the goal to overview again the most important outcomes of the conducted simulations. A benchmark of the P activities gained from literature research and the P activities simulated using FactSage™ should give a tendency of the possible impact of Cr and Mn on the P behavior in a BOF slag system. Moreover, results from prior experiments using a similar BOFS treatment approach and a related input BOFS composition should indicate if the simulation results are in a good harmony with practical results.

In the beginning of this chapter, the two comparisons are discussed and critical findings are highlighted. That followed, the most relevant conclusions out of this master`s thesis are overviewed. Afterwards, a summary gives an overview of the whole approach of this thesis and states, how the results were reached. At the end, potential topics for further research in this area are overviewed and their possible impact is illustrated.

4.1 Comparison between the Simulation Results, Findings of the Literature Research and previously Conducted Experiments

The conducted simulations using the equilib module in FactSage™ give a first insight of how a high Cr and high Mn BOFS could behave during a carbo-thermal treatment. In the course of this thesis especially the influence of changing Mn and Cr contents in the input slag mixture on the P activity in the emerging liquid metal phase is of high interest. In chapter 2.5 the results of a conducted literature research with focus on the impact of Cr and Mn amounts in a slag mixture on the P activity in an occurring liquid metal phase are described. In Figure 38 below,

the P activities in a liquid metal phase in dependency of the input Cr amount are pictured. In this figure the results from the literature research and the results from the conducted simulations are benchmarked.

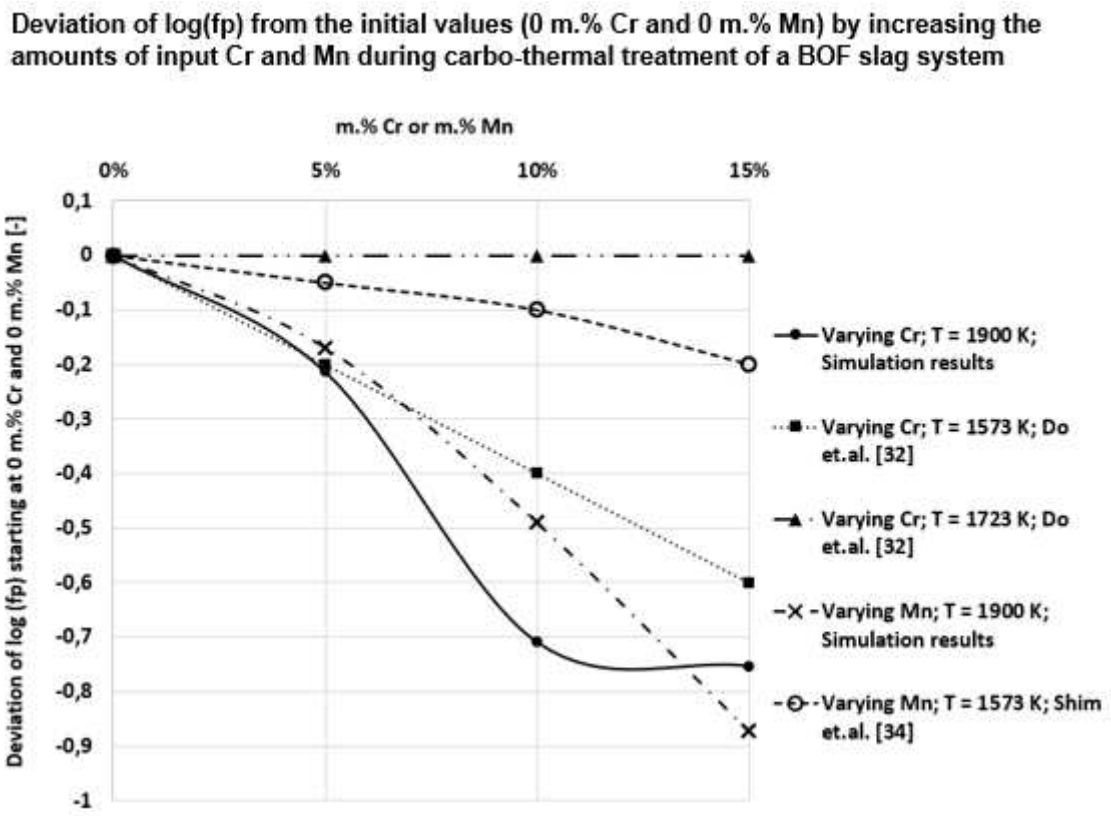

Figure 38: Influence of Cr and Mn on the deviation of the P activity

To better compare the simulation results with the results from other researchers, the deviation of the initial logarithmic P activity with increasing rather the input Cr or Mn amount from the initial input mixture having 0 m.% Cr and 0 m.% Mn is considered.

It can be seen that both increasing Cr or Mn leads to a decrease of the P activity in the conducted simulations. This falling trend of the P activity with increasing the m.% of Cr or Mn is also in good agreement with conducted experiments by Do et.al. In the considered temperature window the influence of the temperature on the P activity is proven to be very low by Do. et.al., Ichise et.al. and Shim et.al. [34]

The simulations show a stronger influence of Mn on the P activity than results by Shim et.al., but also the input composition of Shim et.al. derivates from the input BOFS mixture, which was analyzed in the course of this thesis.

At 5 m.% Cr the simulation results and the practical results carried out by Do et.al. are in good harmony with having a simulated deviation of -0,21 and a practically analyzed deviation of -0,20.

The input mixture of the experiments from Do et.al. and Shim et.al. differs from the analyzed BOFS mixture in this thesis, which is why the benchmark of these findings in regard to the P activity can only be used to estimate a potential trend of how log(fp) depends on the amounts of Cr and Mn. To achieve an approximate estimation of the accuracy of the undertaken simulations, the simulation outcomes and results from prior experiments using a similar BOFS treatment approach with a similar input BOFS mixture are compared in Table 11 below. The initial composition of the conducted simulations in this thesis and the results of practical experiments carried out by Ponak et.al. using a standard carbo-thermal reduction is almost the same. Only minimal amounts of added TiO_2, MnS and S in the course of the simulations lead to a slight discrepancy. The amounts of TiO_2, MnS and S only account for 0.51 m.% of the slag mixture, which is why the influence of these compositions on the distribution of the emerging phases is supposed to be neglected. [19]

Table 11: Benchmark of the product streams of the simulation outcomes and results from practical experiments conducted by Ponak et.al.

Product stream	**Amount analyzed by standard carbo-thermal reduction (T = 1873.15 K – 1923.15 K) [19]**	**Amount simulated using FactSage™ (T = 1900 K)**
slag	66.47 m.%	55.54 m.%
metal	22.44 m.%	22.74 m.%
gas	11.09 m.%	21.72 m.%
total	100.00 m.%	100.00 m.%

Generally, a good agreement of the amount of formed slag and metal phase can be identified. The amount of the emerging simulated metal phase only differs 1.3 % of the experimental results. Considering the slag and especially to the gas phase, those phases have a higher discrepancy with 16.44 % regarding the slag and up to 95.85 % regarding the gas phase. The slag phase of the simulation results also includes amounts of C_2S / C_3P and $Ca_3Mg(SiO_4)_2$.

P is the element of interest in this thesis, which is why the P distribution between the slag, metal and gas phase of the simulation and the prior practical experiments is compared in the following Table 12.

Table 12: Benchmark of the P distribution of the simulation outcomes and results from practical experiments conducted by Ponak et.al.

P destination	Amount analyzed by standard carbo-thermal reduction (T = 1873.15 K – 1923.15 K) [19]	Amount simulated using FactSage™ (T = 1900 K)
P to slag	15.62 m.%	0.00 m.%
P to metal	73.49 m.%	96.75 m.%
P to gas	10.89 m.%	3.25 m.%
total	100.00 m.%	100.00 m.%

The PRD of the practical experiments using the standard carbo-thermal reduction is 84.38 % and the simulation results show a PRD at 1900 K of 100 % resulting in a P free output slag mixture, a high P inclusion in the metal phase and a relatively low PGD. However, higher temperatures exponentially increase the PGD. At 2000 K the PGD of the simulation is already at 11.63 %, which is also a value that is more similar to the experimental results.

To give an overview of all results of the experiments and benchmarks conducted in this thesis, the following chapter gives a list of the analyzed areas and, out of that, states the derived critical findings and trends considering the dephosphorization process of high Cr and Mn containing BOF slag systems.

4.2 Conclusions

The conducted literature research and executed simulations give a better understanding of the dephosphorization process of Cr- and Mn-rich BOF slags. Especially the temperature dependency, the influence of changing input Cr and Mn amounts and the impact of a changing B_2 on the output results was analyzed in detail. In Table 13 the individual simulations series, their specific characteristics and the findings out of that are overviewed.

Table 13: Overview of the conducted simulations and the derived findings

Simulation designation	**Specific characteristics of the simulation**	**Critical findings and identified trends**
Simulation series A	Treatment of the initial slag mixture with B_2 = 1.5 between 1000 K and 2000 K	• Strong increase in the gas phase at temperatures higher than 1900 K • Emergence of a second slag phase at 1238 K • Higher Temperature leads to an increase in P_2(g) and a decrease of the embedded P in the metal phase • The formation of a metal phase at 1300 K embeds most of the P • Reduced formation of $Ca_3Mg(SiO_4)_2$ after 1600 K and increased formation of C_2S after 1900 K • Strong increase in the PGD from 1800 K to 2000 K
Simulation series B	Treatment of the initial slag mixture, mutually changing the input Cr and Mn amounts between 0 m.% and 15 m.% at 1900 K	• Lower Cr and Mn amounts lead to a higher PGD • Lower Cr and Mn amounts lead to a higher P activity in the liquid metal phase • Mn increases the PGD more than Cr considering 5 m.% and 10 m.% Mn in the input mixture • Cr increases the PGD more than Mn considering 15 m.% Cr in the input mixture • Mn increases the P activity more in the liquid metal phase than Cr considering 5 m.% and 10 m.% Mn in the input mixture • Cr increases the P activity more in the liquid metal phase than Mn considering 15 m.% Cr in the input mixture
Simulation series C	Treatment of the initial slag mixture, changing the B_2 between 1.0 and 1.5 at 1900 K	• The B_2 has no remarkable influence on the PGD at 1900 K • A low B_2 with 1.0, 1.1 and 1.2 leads to the formation of $SiO_2 \cdot nH_2O$ (Silica) • A high B_2 with 1.4 and 1.5 leads to the formation of $Ca_3Mg(SiO_4)_2$ and C_2S • Lower B_2 leads to a slightly higher PGD at 2000 K resulting in a lower P intercalation into the metal phase

The conducted simulation series give a better understanding of the proposed treatment process of high Cr and Mn BOF slags and lead to first triggers to optimize this treatment approach. Especially a higher reduction Temperature and an adjusted input slag mixture could potentially lead to an increase in the PGD resulting in an advanced efficiency of this carbo-thermal reduction process.

4.3 Summary

In the course of this master's thesis the dephosphorization process during carbo-thermal treatment of BOF slag, which consists of high amounts of Cr and Mn, has been analyzed. An analyzation of the experimental results of other researchers states, that both Cr and Mn tend to reduce the P activity in the liquid metal phase, which is a crucial parameter considering the P distribution between the gas and the Fe melt. This trend also was seen by conducting simulations using the thermochemical software FactSage™. Additional simulations give insights on how the treatment of those kind of slag systems could be influenced by variables like the temperature or the input slag composition. By comparing the results of the conducted simulations with analyzed parameters of previously undertaken experiments using a similar slag composition, a good agreement of the mass distribution of the emerging phases in the considered temperature range can be seen. Though, this benchmark shows aberrations considering the P distribution between the slag, metal and gas phase at a temperature of 1900 K, but at 2000 K the simulated P distribution better matches the experimental results.

In total three simulation series consisting of 23 simulations with varying input compositions in detail have been undertaken. This results in a total of 223 specific simulation scenarios, which have been analyzed. The most important findings which could lead to an increase in the PGD are enumerated below:

- An increase in temperature higher than 1800 K results in a higher PGD and a less inclusion of P into the metal phase.
- Lower amounts of both Cr and Mn lead to a higher PGD.
- In a case of low amounts of up to 10 m.% of Cr or Mn, Mn tends to lead to a higher PGD stating a stronger interaction between P and Cr than between P and Mn.
- At high temperatures above 1900 K a lower B_2 results in a higher PGD relocating the P distribution from the metal phase more to the gas phase.

As mentioned in chapter 1.2 the previously expressed research questions are aimed to give a quick overview of relevant novel findings. Based on the overview of the outcome results of this master`s thesis, as can be seen in Table 13, answers to these research questions can be found below:

1. How does the activity coefficient of P depend on the amount of Cr and Mn in Fe-P-Mn-Cr alloys?

- A lower amount of Cr and Mn of the input slag mixture leads to a higher P activity in the liquid iron alloy. Mn stronger increases the P activity in the liquid iron alloy than Cr considering 5 m.% and 10 m.% Mn in the input mixture.

2. How does the amount of Cr and Mn in BOFS affect the inclusion of P in the metal phase?
    - Lower Cr and Mn amounts lead to a higher PGD resulting in a stronger tendency to develop a P gas phase and a reduced tendency to incorporate P into the metal phase. Due to the stronger interaction between Cr and P than between Mn and P considering low amounts of Mn or Cr in the input mixture, Mn has a slightly stronger impact on the PGD than Cr.
3. Which composition of BOFS could lead to high P gasification rates and simultaneously low P accumulation in the metal phase?
    - The input system should be low in Cr and Mn because high amounts of these elements restrict the formation of a P gas phase. Moreover, a lower B_2 leads to a slight increase of the PGD at very high temperatures, which is why an increase of SiO_2 and a reduction of CaO could also lead to an increased efficiency of the P gasification process. In addition to considering the BOFS input composition, the maximum treatment temperature strongly influences the emergence of a P gas phase, which is why treating the input BOFS with very high temperatures higher than 1800 K is recommended.

4.4 Research Prospects

The simulations conducted in this thesis show interesting theoretical results in regard to a carbo-thermal treatment of BOF slags. By comparing these results with findings from other researchers and with prior conducted experiments treating a similar BOFS composition, in general a reasonable agreement of the results was obtained. Therefore, it is of high importance to conduct future experiments using especially various input BOFS compositions, which can be specifically benchmarked to the simulation outcomes. The goal of this specific consideration is to analyze the entire accuracy of the simulation and to deviate optimizations resulting in changing the adjustments of the simulation parameters.

To further achieve a better reproduction of the carbo-thermal treatment of high Cr and Mn BOF slags, some specific phenomena, which are listed below, need to be precisely analyzed:

- Analyzation of the kinetic behavior especially considering the low PRD of the simulations compared to the experimental results.
- Simulation of the continuous operation of the InduMelt plant with an uninterrupted discharge of the metal, slag and gas phase without allowing the emergence of an ideal chemical equilibrium.
- Simulating the changing concentration of the BOFS mixture over the height of the reactor, which occurs due to the continuous separation of the emerging output phases.

To conclude, the conducted simulations and the executed literature research in the course of this thesis led to a better understanding of the behavior of high Cr and Mn BOF slags during a carbo-thermal reduction treatment. Based on the derived findings impulses for further optimizations of this treatment approach were expressed.

5 Bibliography

[1] World Steel Association (2019): Fact Sheet: Steel and raw materials. Edited by World Steel Association. Available online at https://www.worldsteel.org/en/dam/jcr:16ad9bcd-dbf5-449f-b42c-b220952767bf/fact_raw%2520materials_2019.pdf, checked on 1/16/2021.

[2] World Steel Association (2018): Fact Sheet: Steel industry co-products. Edited by World Steel Association. Available online at https://www.worldsteel.org/en/dam/jcr:1b916a6d-06fd-4e84-b35d-c1d911d18df4/Fact_By-products_2018.pdf, checked on 1/16/2021.

[3] Guo, Jianlong; Bao, Yanping; Wang, Min (2018): Steel slag in China: Treatment, recycling, and management. In Waste management (New York, N.Y.) 78, pp. 318–330. DOI: 10.1016/j.wasman.2018.04.045.

[4] World Steel Association (2020): World Steel in Figures. With assistance of Dr Edwin Basson. Edited by World Steel Association. Available online at https://www.worldsteel.org/en/dam/jcr:f7982217-cfde-4fdc-8ba0-795ed807f513/World%2520Steel%2520in%2520Figures%25202020i.pdf, checked on 1/16/2021.

[5] voestalpine AG (2014): LD-Schlacke. Daten und Fakten. Edited by voestalpine AG. Available online at https://www.voestalpine.com/group/static/sites/group/.downloads/de/konzern/2013-weissbuch-ld-schlacke.pdf, checked on 1/16/2021.

[6] voestalpine AG (2014): Zwischenlager für Stahlwerksschlacken am Erzberg. With assistance of Mag. Christian Treml. Edited by VA Erzberg GmbH. Available online at

https://www.voestalpine.com/group/static/sites/group/.downloads/de/konzern/2014-06-zwischenlager-fuer-stahlwerksschlacken-am-erzberg.pdf, checked on 1/16/2021.

[7] Nikolas Martelaro (2016): Energy Use in US Steel Manufacturing. Edited by Stanford University. Stanford University. Available online at http://large.stanford.edu/courses/2016/ph240/martelaro1/, checked on 1/16/2021.

[8] Arcelor Mittal (2015): Annual review. Steel making process. Edited by Arcelor Mittal. Available online at https://annualreview2015.arcelormittal.com/fact-book/additional-information/steel-making-process, checked on 1/16/2021.

[9] U.S. Geological Survey (Ed.) (2012): USGS Minerals Yearbook. U.S. Geological Survey. Available online at https://pubs.er.usgs.gov/publication/70048194, checked on 1/16/2021.

[10] Manchisi, James; Matinde, Elias; Rowson, Neil A.; Simmons, Mark J. H.; Simate, Geoffrey S.; Ndlovu, Sehliselo; Mwewa, Brian (2020): Ironmaking and Steelmaking Slags as Sustainable Adsorbents for Industrial Effluents and Wastewater Treatment: A Critical Review of Properties, Performance, Challenges and Opportunities. In Sustainability 12 (5), p. 2118. DOI: 10.3390/su12052118.

[11] Fruehan, Richard J. (1998): Steelmaking and refining volume, 11. ed. Pittsburgh, Pa.: AISE Steel Foundation (The making, shaping and treating of steel / the AISE Steel Foundation, [2]).

[12] Naidu, Tamlyn Sasha; Sheridan, Craig Michael; van Dyk, Lizelle Doreen (2020): Basic oxygen furnace slag: Review of current and potential uses. In Minerals Engineering 149, p. 106234. DOI: 10.1016/j.mineng.2020.106234.

[13] Yildirim, Irem Zeynep; Prezzi, Monica (2011): Chemical, Mineralogical, and Morphological Properties of Steel Slag. In Advances in Civil Engineering 2011, pp. 1–13. DOI: 10.1155/2011/463638.

[14] Waligora, J.; Bulteel, D.; Degrugilliers, P.; Damidot, D.; Potdevin, J. L.; Measson, M. (2010): Chemical and mineralogical characterizations of LD converter steel slags: A multi-analytical techniques approach. In Materials Characterization 61 (1), pp. 39– 48. DOI: 10.1016/j.matchar.2009.10.004.

[15] Yi, Huang; Xu, Guoping; Cheng, Huigao; Wang, Junshi; Wan, Yinfeng; Chen, Hui (2012): An Overview of Utilization of Steel Slag. In Procedia Environmental Sciences 16, pp. 791–801. DOI: 10.1016/j.proenv.2012.10.108.

[16] Zheng, Guo-Hui; Kozinsk, Janusz A. (1996): Solid waste remediation in the metallurgical industry: Application and environmental impact. In Environ. Prog. 15 (4), pp. 283–292. DOI: 10.1002/ep.670150419.

[17] Das, B.; Prakash, S.; Reddy, P.S.R.; Misra, V. N. (2007): An overview of utilization of slag and sludge from steel industries. In Resources, Conservation and Recycling 50 (1), pp. 40–57. DOI: 10.1016/j.resconrec.2006.05.008.

[18] Shi, Caijun (2005): Steel Slag — Its Production, Processing, Characteristics, and Cementitious Properties. In ChemInform 36 (22). DOI: 10.1002/chin.200522249.

[19] Dr.mont. Christoph Ponak (2019): Carbo-thermal reduction of basic oxygen furnace slags with simultaneous removal of Phosphorus via the gas phase. Dissertation. University of Leoben, Leoben. Chair of Thermal Processing Technology.

[20] Branca, Teresa Annunziata; Colla, Valentina; Algermissen, David; Granbom, Hanna; Martini, Umberto; Morillon, Agnieszka et al. (2020): Reuse and Recycling of By-Products in the Steel Sector: Recent Achievements Paving the Way to Circular Economy and Industrial Symbiosis in Europe. In Metals 10 (3), p. 345. DOI: 10.3390/met10030345.

[21] European Union (2019): Removal of phosphorus from BOF-slag (PSP-BOF). Final report. With assistance of Directorate-General for Research and Innovation (European Commission). Edited by Publications Office of the European Union. Available online at https://op.europa.eu/en/publication-detail/-/publication/cd7e0571-22af-11e9-8d04-01aa75ed71a1, checked on 1/16/2021.

[22] Du, Chuan-ming; Gao, Xu; Ueda, Shigeru; Kitamura, Shin-ya (2018): Effect of Slag Composition on the Dissolution of Phosphorus from Steelmaking Slag by Selective Leaching. In ISIJ International 58 (9), pp. 1659–1668. DOI: 10.2355/isijinternational.ISIJINT2018-240.

[23] The Legal Information System of the Republic of Austria (2021): Entire legal regulation for recycling building materials regulation. Edited by The Legal Information System of the Republic of Austria. Available online at https://www.ris.bka.gv.at/GeltendeFassung.wxe?Abfrage=Bundesnormen&Gesetzesnummer=20009212, checked on 1/16/2021.

[24] Guo, Jianlong; Bao, Yanping; Wang, Min (2018): Steel slag in China: Treatment, recycling, and management. In Waste management (New York, N.Y.) 78, pp. 318–330. DOI: 10.1016/j.wasman.2018.04.045.

[25] Bureau of International Recycling (2020): World Steel Recycling in Figures 2015 - 2019. Steel Scrap - a Raw Material for Steelmaking. Edited by Bureau of International Recycling. Available online at https://www.bir.org/publications/factsfigures/download/643/175/36?method=view#:~:text=In%202019%2C%20there%20was%20an,for%2082%25%20of%20global%20steelmaking, checked on 1/16/2021.

[26] Baosteel Iron and Steel Co., Ltd. (2006): Status of Comprehensive Utilization of Steel Slag at Baosteel. With assistance of Zhang Geng. Edited by Baosteel Iron and Steel Co., Ltd. Available online at https://en.cnki.com.cn/Article_en/CJFDTotalBGJS200601005.htm, checked on 1/16/2020.

[27] Dr.mont. Christoph Ponak (2019): Phosphorus removal and metal recovery from BOF-slags. With assistance of Dr.mont. Christoph Ponak, Prof. Harald Raupenstrauch. Chair of Thermal Processing Technology, University of Leoben. Available online at https://www.ffg.at/sites/default/files/allgemeine_downloads/strukturprogramme/20180830_k1- met_successstory_en_stahlwerksschlacken.pdf, checked on 1/16/2021.

[28] Massachusetts Institute of Technology: Ellingham Diagrams. Edited by Massachusetts Institute of Technology, checked on 1/16/2021.

[29] Schlesinger, Mark E. (2002): The thermodynamic properties of phosphorus and solid binary phosphides. In Chemical reviews 102 (11), pp. 4267–4301. DOI: 10.1021/cr000039m.

[30] Nakase, Kenji; Matsui, Akitoshi; Kikuchi, Naoki; Miki, Yuji (2017): Effect of Slag Composition on Phosphorus Separation from Steelmaking Slag by Reduction. In ISIJ International 57 (7), pp. 1197–1204. DOI: 10.2355/isijinternational.ISIJINT-2017-071.

[31] Zaitsev, A. I.; Shelkova, N. E.; Litvina, A. D.; Mogutnov, B. M.; Dobrokhotova, Zh. V. (1998): Thermodynamic properties and phase equilibria in the Cr-P system. In JPE 19 (3), pp. 191–199. DOI: 10.1361/105497198770342201.

[32] Do, Kyung-Hyo; Nam, Hong-Sik; Jang, Jung-Mock; Kim, Dong-Sik; Pak, Jong-Jin (2017): Thermodynamic Interaction between Chromium and Phosphorus in High Cr Containing Liquid Iron. In ISIJ International 57 (8), pp. 1334–1339. DOI: 10.2355/isijinternational.ISIJINT-2016-646.

[33] ICHISE, Eiji; MORO-OKA, Akira (1988): Interaction parameter in liquid iron alloys. In ISIJ Int. 28 (3), pp. 153–163. DOI: 10.2355/isijinternational1966.28.153.

[34] Shim, Sang Chul; Morita, Kazuki; Sano, Nobuo (1994): Thermodynamics of phosphorus in carbon-saturated manganese-based alloys. In Steel Research 65 (12), pp. 523–527. DOI: 10.1002/srin.199401205.

[35] BAN-YA, Shiro; MARUYAMA, Nobutoshi; KAWASE, Yukio (1984): Effects of Ti, V, Cr, Mn, Co, Ni, Cu, Nb, Mo, and W on the Activity of Phosphorus in Liquid Iron. In Tetsu-to-Hagane 70 (1), pp. 65–72. DOI: 10.2355/tetsutohagane1955.70.1_65.

[36] Lee, Y. E. (1986): Thermodynamics of the Mn-P system. In MTB 17 (4), pp. 777–783. DOI: 10.1007/BF02657140.

[37] Hudon, Pierre; Jung, In-Ho (2015): Critical Evaluation and Thermodynamic Optimization of the CaO-P2O5 System. In MTB 46 (1), pp. 494–522. DOI: 10.1007/s11663-014-0193-x.

[38] Baben, Moritz (2020): FactSage full download. E-mail message to Felix Breuer and Claudia Wichmann. n.p., 8/17/2020.

[39] Mineral Data Publishing (2001): Merwinite Ca3Mg(SiO4)2. Edited by Mineral Data Publishing. Available online at https://rruff.info/doclib/hom/merwinite.pdf, checked on 1/16/2021.

[40] University of Aberdeen (2009): The Density of Cement Phases. With assistance of M. Balonis, F.P. Glasser. Department of Chemistry, Meston Building, University of Aberdeen. Available online at https://www.nanocem.org/uploads/Modules/MCMedias/1409057517897/the_densitiy_of_cement_phases_worksheets.pdf, checked on 1/16/2021.

[41] Matinde, Elias; Sasaki, Yasushi; Hino, Mitsutaka (2008): Phosphorus Gasification from Sewage Sludge during Carbothermic Reduction. In ISIJ International 48 (7), pp. 912–917. DOI: 10.2355/ISIJINTERNATIONAL.48.912.